# Sentinel-6A validation and cross calibration activities

## 2022 Annual Report

Reference : SALP-RP-MA-EA-23618-CLS
Issue : 1/ 2
Date : June 20, 2023

EUMETSAT
Eumetsat-Allee 1, D-64295 Darmstadt, Germany
Tel: +49 6151 807-7
Fax: +49 6151 807 555
http://www.eumetsat.int

| | |
|---|---|
| **Document Reference:** | SALP-RP-MA-EA-23618-CLS |
| **Date:** | June 20, 2023 |
| **Issue** | 1.2 |

| | | |
|---|---|---|
| **Project:** | MISSION PERFORMANCE SERVICE FOR SENTINEL-6 MISSION | |
| **Title:** | Sentinel-6A validation and cross calibration activities<br>2022 Annual Report | |
| | **Name** | **Company** |
| **Author(s):** | B. Courcol<br>E. Cadier | CLS<br>CLS |
| **Approved by:** | F. Bignalet-Cazalet | CNES |
| **Application authorized by :** | C. Martin-Puig | EUMETSAT |

# Change Log

| Version | Date | Changes |
|---|---|---|
| 1.0 | 31/03/2023 | First Draft |
| 1.1 | 11/04/2023 | CNES review taken into account |
| 1.2 | 19/06/2023 | EUMETSAT review taken into account |

# Acronyms

| | |
|---|---|
| **AMR** | Advanced Microwave Radiometer |
| **CLS** | Collecte Localisation Satellites |
| **CMEMS** | Copernicus Marine Service |
| **CNES** | Centre National d'Etudes Spatiales |
| **DUACS** | Data Unification and Altimeter Combination System |
| **DV** | Default Value |
| **ECMWF** | European Centre for Medium-range Weather Forecasting |
| **EUMETSAT** | European Organisation for the Exploitation of Meteorological Satellites |
| **ESA** | European Space Agency |
| **GIM** | Global Ionosphere Maps |
| **GDR** | Geophysical Data Record |
| **GMSL** | Global Mean Sea Level |
| **HR** | High Resolution Mode, also called Synthetic Aperture Radar (SAR) or Delay Doppler Altimetry (DDA) |
| **HRMR** | High Resolution Microwave Radiometer |
| **LR** | Low Resolution Mode (=LRM) |
| **MLE** | Maximum Likelyhood Estimator |
| **MQE** | Mean Quadratic Error |
| **MSS** | Mean Sea Surface |
| **NASA** | National Aeronautics and Space Administration |
| **NOAA** | National Oceanic and Atmospheric Administration |
| **NTC** | Non Time Critical |
| **PB** | Processing Baseline |
| **RMC** | Range Migration Correction |
| **SSH** | Sea Surface Height |
| **SSHA** | Sea Surface Height Anomaly(=SLA) |
| **SLA** | Sea Level Anomaly(=SSHA) |
| **SSB** | Sea State Bias |
| **STD** | Standard Deviation |
| **SWH** | Significant Wave Height |
| **WTC** | Wet troposphere Correction |

# Table of Content

# List of Figures

# List of Tables

# 1 Introduction

Sentinel-6 is a collaborative Copernicus mission, implemented and co-funded by the European Commission, ESA, EUMETSAT and the USA through NASA and NOAA.

EUMETSAT is responsible for the Sentinel-6 operations as part of the Copernicus component of the EU Space Programme. The Sentinel-6 Quality Assessment reports are generated by CNES in the frame of a EUMETSAT CNES agreement in the context of Copernicus.

This document presents the synthesis report concerning validation activities of Sentinel-6 data for the year 2022.

## 1.1. History

Sentinel-6 MF satellite was successfully launched on the 21th of November 2020. On November 30th, its Poseidon-4 altimeter was switched on, and since December 17th 2020, Sentinel-6 MF is on its operational orbit to continue the long term climate data record on the primary TOPEX, Jason-1, Jason-2 and Jason-3 ground track.

In order to calibrate both altimeters, POS4 was switched to its redundant side (POS4-B) on the 14th of September 2021. It remains in this configuration from this date onwards.

Until April 7th, 2022, Sentinel-6 MF and Jason-3 were in tandem flight, with only a 30 seconds delay, before Jason-3 was moved to the same interleaved orbit that was used by TOPEX from 2002 to 2005, Jason-1 from 2009 to 2012 and Jason-2 from 2016 to 2017.
After the tandem phase with Jason-3, Sentinel-6 MF has become the reference mission in DUACS system.

Over 2022, the main events for Sentinel-6 MF are :

- The end of the tandem phase with Jason-3 on April 7th, after which Sentinel-6 has become the reference mission in DUACS system.
- Processing baseline update to F06 (see section 2.4.), deployed on 2022-05-31. This baseline was used to perfomed the first Sentinel-6 full mission reprocessing, available to all users in July 2022 (see related Eumetsat news).
- Processing baseline update to F07 (see section 2.4.), deployed on 2022-09-15. NTC products are processed with PB F07 from 2022-08-15 sensing time.
- A calibration error in the microwave radiometer caused a drift of -2 mm per month of the radiometer wet tropospheric correction from 2022-10-01. From 2022-12-14 (NTC sensing time), calibration files have been updated, resulting in a jump of +5 mm back to previous level for the WTC (cf section 4.9.2.).

Since the beginning of the mission, Sentinel-6 data have been analyzed and monitored in order to assess the products quality. Cycle per cycle reports summarizing mission performance are generated and made available through Eumetsat website. Please note that analyses are done over ocean only, no assesment is

done over hydrological targets. This encompasses several points, which are either part of Cal/Val routine activities or following mission events:

- mono-mission validation and monitoring,
- accuracy and stability of SLA measurements check,
- specific studies and investigations.

## 1.2. Overview

The present document assesses Sentinel-6 MF data quality and performance over ocean. After an executive summary in the next page, dedicated sections of this report deal with:

- description of data processing,
- data coverage / availability,
- monitoring of rejected spurious data,
- analysis of relevant parameters derived from instrumental measurements and geophysical corrections,
- system performance via analyses at crossover points,
- system performance via along-track Sea Level Anomalies monitoring,
- GMSL analysis,
- compliance with system requirements.

Over all these parts, the document also focuses on Sentinel-6 MF/Jason-3 cross-calibration :

- During the tandem flight (November 21st 2020 to April 7th 2022) both satellites were on the same ground track, which was a unique opportunity to precisely assess parameter discrepancies between both missions and detect geographically correlated biases, jumps or drifts.
- But even after Jason-3 moved to interleaved orbit comparisons are still possible.

The difference at crossovers, SLA performance and consistency with Jason-3 are described.

## 1.3. Executive summary

By succeeding to TOPEX/Poseidon, Jason-1, Jason-2 and Jason-3 on their primary ground track, Sentinel-6 MF has extended the high-precision ocean altimetry data record.

Sentinel-6 MF was launched on November 21st 2020. Its onboard altimeter (POS4) operates simultaneously in two acquisition modes in a so-called **interleaved mode**. These modes are:

- Low Resolution Mode, hereafter "LR", which is the historical mode used by previous altimeters in the Topex/Jason satellites.
- High Resolution Mode, hereafter "HR", a.k.a. Synthetic Aperture Radar (SAR) or Delay Doppler Altimetry (DDA), already used on Cryosat-2 and on the Sentinel-3 satellites.

HR data can be telemetred on ground either on RAW mode, i.e. with the full range window of the HR waveform, or in RMC mode, that transmits a truncated waveform thanks to on-board processing, to cut data volume in half. More information on the different telemetry configurations can be found in the L1 Product Generation Specification[1].
Sentinel-6 MF POS4 operates in LR plus HR-RMC mode globally since cycle 32 (2021/09/21). This configuration is called LRMC. Before 2021/09/21, several configurations have been tested via predefined mode masks, mainly in order to validate to HR-RMC performance versus HR-RAW.

During Sentinel-6 MF tandem phase with Jason-3 (2020/12/17 to 2022/04/07), both satellites were on the same ground-track (with only 30 seconds delay), which was a unique opportunity to precisely assess parameter discrepancies between both missions and detect geographically correlated biases, jumps or drifts. In order to calibrate both altimeters, POS4 was switched to its redundant side (POS4-B) on 2021/09/14. It remains in this configuration from this date onwards.
Thanks to this tandem phase, Sentinel-6 MF has been precisely calibrated leading to a seamless transition between Jason-3 and Sentinel-6 MF LR as reference mission in the DUACS system.

In July 2022, the **first Sentinel-6 full mission reprocessing** was distributed. LR and HR data were reprocessed using **Processing Baseline F06** (see F06 product notice for details[2]). This reprocessing was the first opportunuity to assess Sentinel-6 MF performance with an homogenuous processing. This assessment is available in the associated reprocessing Cal/Val report[3].
The reprocessed period spanned from the beginning of the mission till 2022/04/28 (NTC sensor time). PB F06 has then been used to produce F06 data operationaly until 2022-08-15 (NTC sensor time). **Processing baseline F07** was then used see F06 product notice for details[4].

During each cycle, missing measurements were monitored, spurious data were edited and relevant parameters derived from instrumental measurements and geophysical corrections were analysed. Please note that analysis are done **over ocean** only, no assessment is done over hydrological targets.

[1] https://www.eumetsat.int/media/48261
[2] https://www.eumetsat.int/media/48237
[3] https://www-cdn.eumetsat.int/files/2022-10/S6A_F06_Reprocessing_Calval_Assesment_v2_draft4.pdf
[4] https://www.eumetsat.int/media/50079

# 1/ Data availability

Data availability over ocean is excellent for Sentinel-6 MF LR products, with 99.45% of available data over the complete mission lifetime. It is only impacted by few events, occuring during Sentinel-6 MF commissioning phase, represented with grey lines on figure 9 and listed below.

Sentinel-6 MF HR requirements on data availability are met, with a slightly reduced percentage of available data compared to LR at 97.9 %. From cycle 4 to 31 (i.e. from 2021/02/05 to 2021/09/21, in red on the figure), different mode masks were activated on POS-4. Over these cycles, HR data were not always available globally. From cycle 32, the average percentage of available HR data is of 99.1 %, which is still lower than LR. This difference is mainly due to a known anomaly impacting HR data recovery: the Fairbanks Ground Station key hole effect.

The following events impacts data availability in both LR and HR products:

- POS4 restart on 2021/01/26
- POS4 restart on 2021/02/25
- POS4 restart on 2021/04/22
- Satellite switch off for satellite software patch from 2021/04/27 03:35 to 2021/04/28 17:07
- POS4 restart on 2021/08/26
- Switch from POS4-A to POS4-B on 2021/09/14.

**No important event occured over 2022.**

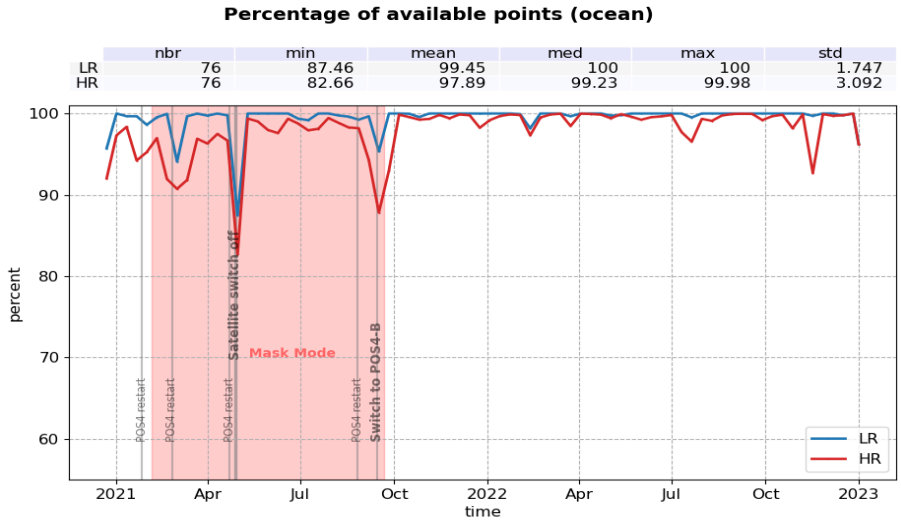


*Figure 1 – Percentage of available data over ocean for NTC Sentinel-6 MF LR (blue) and HR (red) per cycle.*

## 2/ Sea Level Anomalies

Sentinel-6 MF and Jason-3 SSHA follow identical seasonal cycles and variations, with mean value of 4.7 cm for Sentinel-6 MF LR, 3.5 cm for Sentinel-6 MF HR and 3.4 cm for Jason-3. The curves diverge from Jason-3 between october and december 2022. This is due to an anomaly in Sentinel-6 MF radiometer calibration, causing a drift of -2 mm/month of Sentinel-6 MF wet tropospheric correction. Sentinel-6 MF SSHA cyclic standard deviation is lower for Sentinel-6 MF LR and HR than Jason-3 by about 6mm up until the update to processing baseline F07 on 2022-08-15. With this update, ionospheric correction was made available over the Caspian Sea, enabling SSHA computation and subsequently increasing the standard deviation of the entire dataset to levels consistent with Jason-3. The drop in April 2022 in Jason-3 SSHA standard deviation is due to missing measurements during Jason-3 move to the interleaved orbit.

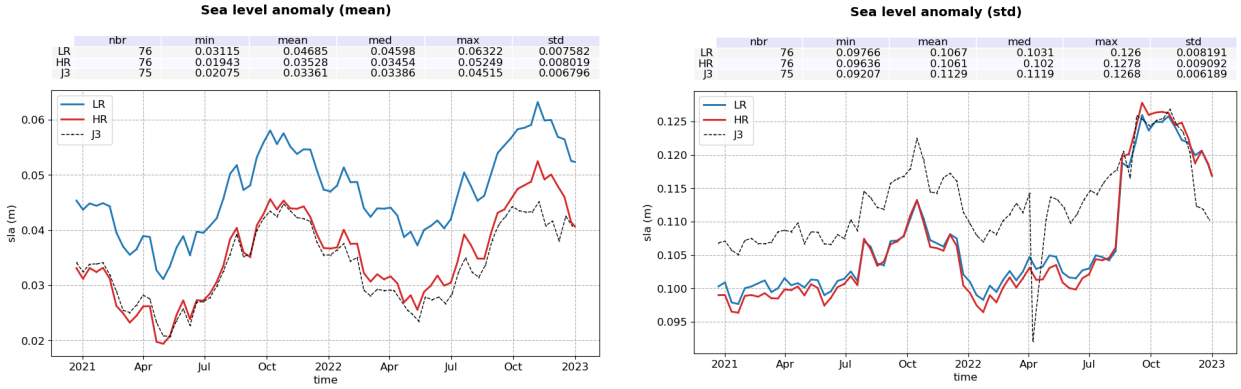


*Figure 2 – Mean (left) and standard deviation (right) SSHA by cycle for LR (red), HR (red) and Jason-3 (black).*

Over the tandem phase, the mean SLA differences between Sentinel-6 MF and Jason-3 per cycle is centred around 1.17 cm for Sentinel-6 MF LR and -0.05cm for Sentinel-6 MF HR. The time monitoring of this difference (figure 3) highlights two events of similar amplitudes in LR and HR:

- a jump of about +5 mm is visible after the satellite restart of 27-28 April 2021. This is partly caused by a strong variation in radiometer WTC.
- a jump of about +2.5 mm is visible around the 20 January 2022.

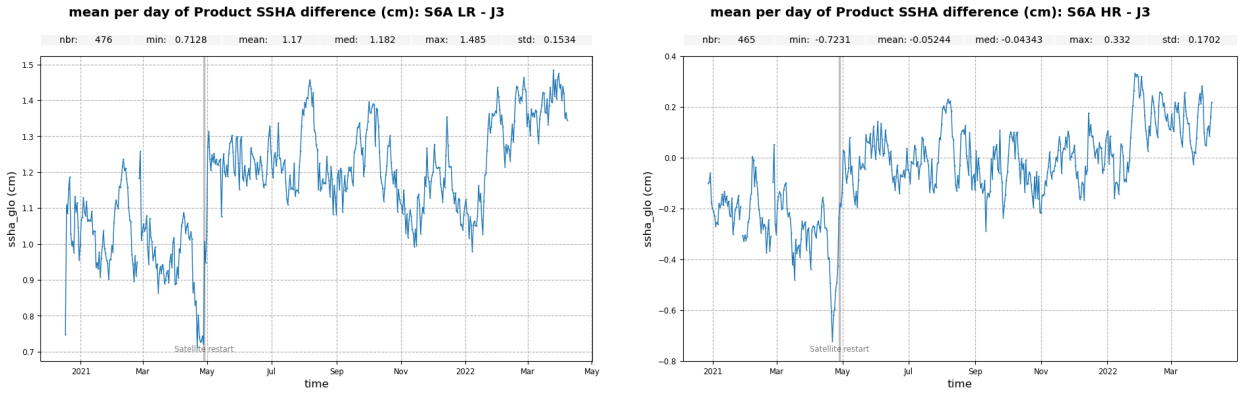


*Figure 3 – Time monitoring of product SSHA difference: Sentinel-6 MF LR (left) and HR (right) minus Jason-3. Mean per day computed over the complete tandem period.*

The map of the SSHA residuals between Sentinel-6 MF LR and Jason-3 (figure 4 left panel) highlights a clear correlation to SWH (+1.3 cm between 2 and 7 m wave). It is linked to range and ionosphere correction bias as well as pulse-to-pusle correlation effects, as Sentinel-6 MF uses a 9kHz PRF while Jason-3 uses a 2kHz PRF. LR numerical retracker implemented in PB F08 should improve this behavior.
In HR (figure 4 right panel), the map of SSHA differences highlights a strong correlation to sea state condi-

tion, mainly due to the usage of different skewness coefficient in the Jason-3 and Sentinel-6 HR retracking but also to the remaining impact of ocean vertical velocity on HR data [5]. Both should be corrected in PB F09 thanks to HR numerical retracking.
An equatorial band of 5 mm amplitude is visible on both maps. Investigations have shown that this behavior is most likely coming from Jason-3. The root cause is still to be identified.

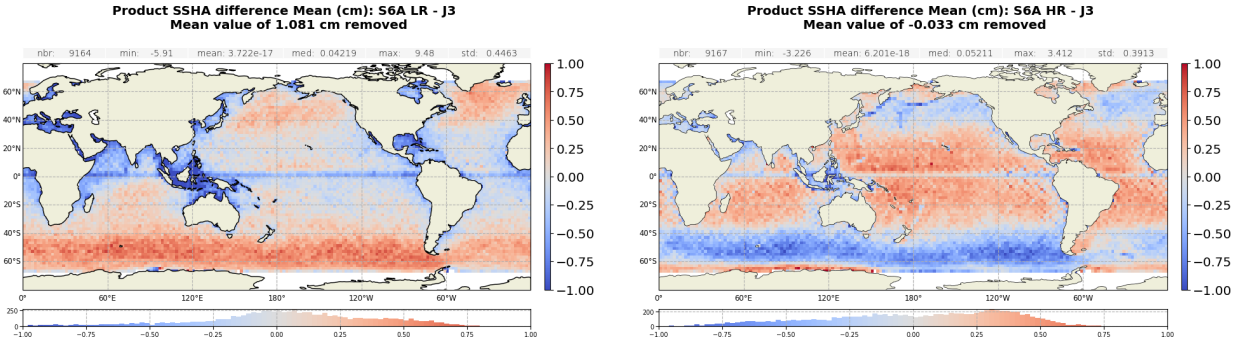


*Figure 4 – Gridded map of product SSHA difference: Sentinel-6 MF LR (left) and HR (right) minus Jason-3 computed over the complete tandem period. To better compare the results, the mean value (1.081cm for the left graph, -0.033cm for the right graph) between differences have been subtracted.*

## 3/ Performance at crossover points

Looking at SSH difference at mono-mission crossovers, mean values are well centred around 0 for both LR and HR data (figure 5 left panel). A small 120 day signal similar to Jason-3 is visible with amplitude below 1.5 cm. Prior Sentinel-6 MF launch, the origin of this signal was linked to Jason-3 platform. As the two satellites do not have the same platform, this hypothesis seems not to be the right one. Further investigations are required to fully understand this behavior.

Concerning SSH error at mono-mission crossovers ( $STD\ /\ \sqrt{2}$ ), Sentinel-6 MF shows very good and stable performance with an error of 3.32 cm for Sentinel-6 MF LR, which is in line with Jason-3 (3.28 cm) (figure 5 right panel). The error for Sentinel-6 MF HR SSH is even lower (3.18 cm).

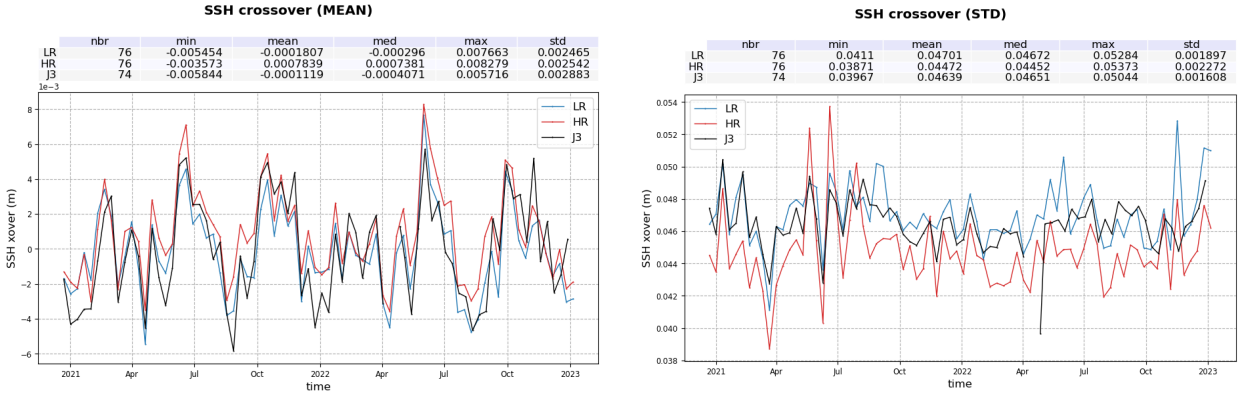


*Figure 5 – Monitoring of SSH difference at mono-mission crossover for Sentinel-6 MF LR (blue), Sentinel-6 MF HR (red) and Jason-3 (black), mean (left) and std (right) per cycle. Only data with |latitude| < 50 °, bathymetry < -1000m and low oceanic variability were selected.*

The mean SSH differences at Sentinel-6 MF/Jason-3 crossovers is following the same variations for LR and HR, with means of -1.3cm and 0.1cm respectively (figure 6 top panel). A downward drift is visible.

It might be caused by different PTR shape degradation between both satellites, and in HR mode by the omission of the range walk application in the baseline currently deployed in operation. Between October and December 2022, the Sentinel-6 MF/Jason-3 differences at crossover increase in absolute value. This is due to an anomaly in Sentinel-6 MF radiometer calibration, causing a drift of -2 mm/month of Sentinel-6 MF wet tropospheric correction from 2022/10/01 to 2022-12-14.
No significant regional pattern can be seen in the Sentinel-6 MF LR/Jason-3 SSH crossovers differences (figure 6 bottom panel). The map of Sentinel-6 MF HR/Jason-3 SSH differences at crossover highlight the absence of skewness parameter in the HR processing, leading to correlation to sea state conditions in the comparison to Jason-3.

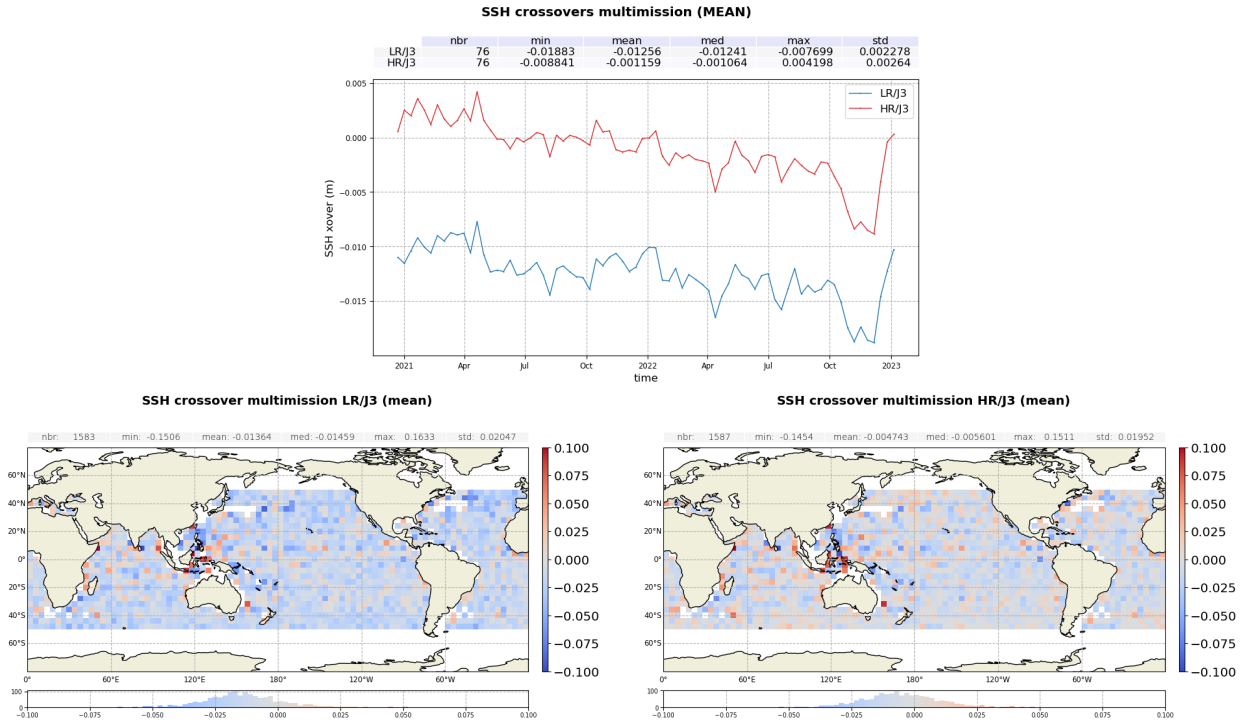


*Figure 6 – Cyclic monitoring of Sentinel-6 MF - Jason-3 SSH crossover differences mean (top) and maps over cycle 42 to 79 (bottom). Only data with |latitude| < 50 °, bathymetry < -1000m and low oceanic variability were selected.*

## 4/ Contribution to Global Mean Sea Level

Since April 2022 (Sentinel-6 MF cycle 52), Sentinel-6 MF is the reference altimetry mission to estimate the Global Mean Sea Level (GMSL), replacing Jason-3. Regional and global biases between missions have to be precisely estimated in order to ensure the quality of the reference GMSL serie as seen on Figure 113. For more precisions, see the dedicated section on AVISO+ website[5].

Sentinel-6 MF GMSL are impacted by three known effects:

- a -2 mm/month drift in the wet tropospheric correction between October and December 2022 follow by a +5 mm jump. This has been tracked to a calibration error in the radiometer. This drift will be corrected in the upcoming PDAP PB F08 upcoming update.
- the evolution of the PTR shape in the range direction. It impacts range and SWH estimates both in LR and HR. Numerical rectracker allows to account for the PTR shape evolution thanks to the use of true PTRs. Such retrackers will be implemented in the upcoming PDAP processing baseline : F08 for LR and F09 for HR.
- the evolution of the PTR shape in the azimuth direction, impacting the range variations within a burst, in HR only. It is corrected thanks to the range walk correction, that will be available in PB F09.

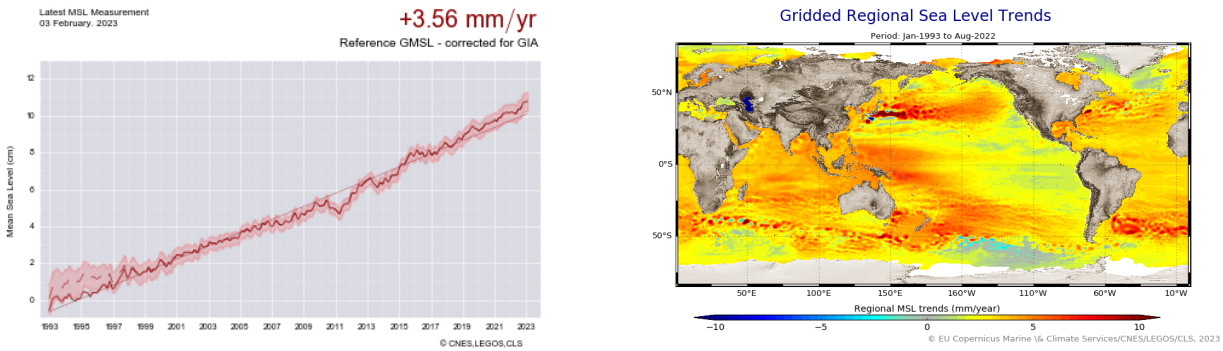


*Figure 7 – Global (left) and regional (right) MSL trends from 1993 onwards.*

[5] https://www.aviso.altimetry.fr/en/data/products/ocean-indicators-products/mean-sea-level.html

# 2 Processing Status

## 2.1. Data used

**Sentinel-6 MF**
Metrics provided in this document are based on Sentinel-6 MF dataset from cycle 4 pass 14 to cycle 79 for L2 NTC 1Hz products (corresponding to December 17th 2020 to December 31th 2022). Data before cycle 4 pass 14 are not included as Sentinel-6 MF was not yet on its definitive orbit.

From 2020-12-17 to 2022-08-15 (corresponding to cycle 65 pass 21), Sentinel-6 MF data were processed with the Processsing Baseline (PB) F06. No data with PB anterior to F06 is present in this report thanks to the 2022 F06 reprocessing. Data after 2022-08-15 were processed with the PB F07. See section 2.4. for more details on the processing baselines.

For LR and HR modes ”ocean” retrackers were used, being MLE4 and SAMOSA, respectively. A detailed description of the products can be found in the Sentinel-6 MF user handbook [1].

**Jason-3**
Comparison with Jason-3 uses L2 1 Hz GDR-F products on the same periods as Sentinel-6.

Sentinel-6 MF F06-F07 and Jason-3 GDR-F share the same standard in terms of geophysical corrections: same tide models, same mean surface height, etc. In particular :

- for the wind speed, Collard algorithm is used on both mission
- for the sea state bias, Sentinel-6 MF processing uses sea state bias parametrisation derived from Jason-3 GDR-F date, both in LR and in HR.

Note that after the end of the tandem phase on 07-04-2022, and until Jason-3 reached its current interleaved orbit on 25-04-2022, no data are available. Furthermore, cycles before and after the transition (cycles number 227 and 300) are truncated, lasting only 5h30 and 4 days respectively instead of the standard 10 days. This can lead to artefacts in cyclic monitoring involving Jason-3.

## 2.2. List of events

The following table shows the major events that occured over Sentinel-6 MF lifetime.

| Date start | Date end | Cycle | System | Event |
|---|---|---|---|---|
| 30/11/2020 | N/A | 1 | POSEIDON | POS4 switch on |
| 17/12/2020 19:38 | N/A | 4 | | Sentinel-6 MF on its final orbit |
| 18/01/2021 | N/A | 7 | STR | On-board star-tracker update |
| 25/01/2021 19:45 | 25/01/2021 19:45 | 7 | AMR-C | AMR deep sky calibration |
| 26/01/2021 12:17 | N/A | 8 | POSEIDON | POS4 restart |
| 04/02/2021 23:59 | N/A | 9 | POSEIDON | POS4 mode mask activated |
| 25/02/2021 | N/A | 11 | POSEIDON | POS4 restart |

| | | | | |
|---|---|---|---|---|
| 27/02/2021 00:43 | 27/02/2021 00:43 | 11 | AMR-C | AMR deep sky calibration |
| 11/03/2021 05:00 | 11/03/2021 05:00 | 12 | AMR-C | AMR-C Deep-sky Calibration Over Land-Ocean Boundary |
| 16/03/2021 21:53 | 16/03/2021 21:530 | 13 | AMR-C | AMR-C Deep sky calibration over Ocean |
| 17/03/2021 09:36 | 18/03/2021 09:38 | 13 | AMR-C | 24h Warm target Calibration |
| 23/03/2021 15:12 | 23/03/2021 15:27 | 13 | AMR-C | Deep Sky Calibration over the Ocean/Land Boundary |
| 15/04/2021 00:36 | 15/04/2021 00:36 | 15 | Platform | (+0.4) POS-4 Roll bias |
| 15/04/2021 12:56 | 15/04/2021 12:56 | 16 | Platform | (-0.4) POS-4 Roll Bias |
| 22/04/2021 13:24 | N/A | 16 | POSEIDON | POS4 restart |
| 25/04/2021 01:31 | 25/04/2021 01:31 | 16 | AMR-C | AMR deep sky calibration |
| 27/04/2021 03:35 | 28/04/2021 17:07 | 17 | Platform | Satellite switched off for satellite software patch. |
| 21/05/2021 20:20 | 21/05/2021 20:36 | 19 | AMR-C | AMR deep sky calibration |
| 24/05/2021 16:30 | 24/05/2021 16:30 | 19 | Platform | -0.4deg Roll |
| 25/05/2021 04:50 | 25/05/2021 04:50 | 20 | Platform | +0.4deg Roll |
| 18/06/2021 06:46 | 18/06/2021 06:46 | 22 | AMR-C | AMR deep sky calibration |
| 01/07/2021 13:08 | 01/07/2021 13:12 | 23 | Platform | Yaw flip maneuver |
| 05/07/2021 12:56 | 05/07/2021 13:00 | 24 | Platform | Yaw flip maneuver |
| 19/07/2021 19:59 | 19/07/2021 19:59 | 25 | AMR-C | AMR deep sky calibration |
| 18/08/2021 01:40 | 18/08/2021 01:40 | 28 | AMR-C | AMR deep sky calibration |
| 26/08/2021 10:00 | 26/08/2021 | 29 | POSEIDON | POS4 restart: POS4-A Application Software (ASW) 2.4 upload and activation |
| 01/09/2021 04:44 | 01/09/2021 05:18 | 29 | Platform | Yaw flip maneuver |
| 05/09/2021 06:11 | 05/09/2021 06:46 | 30 | Platform | Yaw flip maneuver |
| 14/09/2021 09:00 | 15/09/2021 09:00 | 31 | POSEIDON | Switch from POS-A to POS-B |
| 17/09/2021 20:02 | 17/09/2021 20:02 | 31 | AMR-C | AMR deep sky calibration |
| 21/09/2021 01:25:37 | N/A | 32 | POSEIDON | End of POS4 mode mask. LRMC-OL acquisition mode activated globally from cycle 32 onwards. |
| 20/10/2021 00:58 | 20/10/2021 00:58 | 34 | AMR-C | AMR deep sky calibration |
| 05/11/2021 16:26 | 05/11/2021 16:26 | 36 | Platform | Yaw flip maneuver |
| 09/11/2021 17:29 | 09/11/2021 17:29 | 37 | Platform | Yaw flip maneuver |
| 16/11/2021 14:37 | 16/11/2021 14:37 | 37 | AMR-C | AMR deep sky calibration |
| 19/11/2021 03:45:52 | 19/11/2021 03:45:52 | 37 | Platform | Yaw slew +90deg |
| 19/11/2021 04:03:45 | 19/11/2021 04:03:45 | 37 | Platform | Roll -0.4 deg |
| 19/11/2021 04:27:45 | 19/11/2021 04:27:45 | 37 | Platform | Roll +0.4 deg |
| 19/11/2021 04:38:20 | 19/11/2021 04:38:20 | 37 | Platform | Yaw slew -90deg |
| 19/11/2021 16:13:21 | 19/11/2021 16:13:21 | 38 | Platform | Yaw slew +90deg |
| 19/11/2021 16:24:25 | 19/11/2021 16:24:25 | 38 | Platform | Roll +0.4 deg |
| 19/11/2021 16:48:25 | 19/11/2021 16:48:25 | 38 | Platform | Roll -0.4 deg |
| 19/11/2021 16:59:00 | 19/11/2021 16:59:00 | 38 | Platform | Yaw slew -90deg |
| 19/11/2021 17:38:00 | 19/11/2021 17:38:00 | 38 | AMR-C | AMR deep sky calibration |
| 16/12/2021 01:42:00 | 16/12/2021 01:42:00 | 40 | AMR-C | AMR deep sky calibration |
| 17/07/2022 15:42:57 | 17/07/2022 15:42:57 | 62 | Platform | Yaw Slew +90deg |
| 17/07/2022 16:18:55 | 17/07/2022 16:18:55 | 62 | Platform | Yaw Back Slew -90deg |
| 18/01/2022 04:03:34 | 18/01/2022 04:03:34 | 44 | Platform | Yaw Slew -90deg |
| 18/01/2022 04:39:32 | 18/01/2022 04:39:32 | 44 | Platform | Yaw Back Slew +90deg |
| 12/02/2022 01:03:00 | 12/02/2022 01:03:00 | 46 | AMR-C | AMR deep sky calibration |
| 27/02/2022 15:54:35 | 27/02/2022 16:03:24 | 48 | Platform | Yaw flip maneuver |
| 03/03/2022 17:12:32 | 03/03/2022 17:21:21 | 48 | Platform | Yaw flip maneuver |
| 13/03/2022 15:30:00 | 13/03/2022 15:30:00 | 49 | AMR-C | AMR deep sky calibration |
| 11/04/2022 02:12:00 | 11/04/2022 02:12:00 | 52 | AMR-C | AMR deep sky calibration |
| 25/04/2022 16:45:10 | 25/04/2022 16:53:58 | 53 | Platform | Slew 180deg |
| 29/04/2022 16:36:20 | 29/04/2022 16:45:08 | 54 | Platform | Back Slew 180deg |

| | | | | |
|---|---|---|---|---|
| 10/05/2022 20:16:00 | 10/05/2022 20:16:00 | 55 | AMR-C | AMR deep sky calibration |
| 07/07/2022 19:29:00 | 07/07/2022 19:29:00 | 61 | AMR-C | AMR deep sky calibration |
| 08/07/2022 01:38:00 | 08/07/2022 01:38:00 | 61 | AMR-C | AMR deep sky calibration |
| 05/12/2022 10:25:05 | 05/12/2022 10:33:52 | 76 | Platform | Slew 180deg |
| 05/12/2022 10:44:46 | 05/12/2022 10:45:26 | 76 | Platform | Back Slew 180deg |
| 07/12/2022 00:28:00 | 07/12/2022 00:28:00 | 76 | AMR-C | AMR deep sky calibration |

*Table 1 – Events on Sentinel-6 MF.*

## 2.3. Tracking and acquisition mode

Sentinel-6 MF altimeter, Poseidon-4, always operates in interleaved mode, which enables simultaneous measurements in :

- Low Resolution Mode, hereafter "LR", which is the historical mode used by previous altimeters in the Topex/Jason satellites. Please note that while Topex/Jason altimeters were acquiring data with a 2kHz PRF, Sentinel-6 LR mode uses a 9kHz PRF.
- High Resolution Mode, hereafter "HR", commonly called Synthetic Aperture Radar (SAR) or Delay Doppler Altimetry (DDA), already used on Cryosat-2 and on the Sentinel-3 satellites.

HR mode can be downlinked in two ways :

- HR-RAW, which contains the entire waveform. This mode cannot be activated globally, as the volume of data is too large to be downlinked.
- HR-RMC (Range Migration Correction), which only transmits to the ground a lighter, truncated waveform computed after on-board RMC compensation. This mode enables global coverage, as the volume of data is only half of HR-RAW's.

Table 2 summarizes the acquisition modes under which POS-4 can operate. All these modes have been activated during Sentinel-6 MF Phase-E1.

| **Acquisition mode** | **Open Loop** | **Closed Loop** | **Data telemetered** |
|---|---|---|---|
| LRM | X | X | Only LR data |
| LX | X | X | LR + HR-RAW data |
| LX2 | | X | LR + HR-RAW + HR-RMC data |
| LRMC | X | X | LR + HR-RMC data |
| TRANSPONDER | | | LR + HR-RAW + HR-RMC data (fixed Gain and H0) |

*Table 2 – POS-4 acquisition modes*

In order to validate HR-RMC versus HR-RAW modes, a masking mode has been activated on the 05/02/2021 (start of cycle 9) and lasted until the 21/09/2021 (end of cycle 31). Over this period, POS-4 operated :

- in LRM only over land,
- in LX over coastal areas
- in LRMC over open ocean except over the masks where it operates in LX.

Several masks have been used, covering different areas of interest (ocean with strong geoid slopes or dynamic regions, ice zones, Amazon for hydrology, etc.).
Switching from LRMC to LX over open ocean allows to verify the continuity between HR-RMC and HR-RAW data. Furthermore, an on-ground convertor allowed to convert HR-RAW data to HR-RMC. It enables direct comparison between the two retrievals.
After the complete validation of the HR-RMC mode, POS4 mode mask ended and the acquisition mode has been set to LRMC-OL globally from cycle 32 (21/09/2021).

The LR and HR modes use separate retrackers (MLE4 and SAMOSA respectively) and the resulting data are available in distinct products.
Please note that while LR products contain both Ku and C bands, because of data volume constrains, the telemetry of HR does not include C band data, and therefore HR products contain only the Ku band.

## 2.4. Processing versions

HR and LR NTC products are available in Processing Baseline version F06 until 2022-08-15 (cycle 65 track 20). Thanks to the 2022 reprocessing campain, PB prior to F06 are no longer present in the datasets.

In PB F06, HR processing has been updated : the number of Doppler beams (a.k.a. looks) incoherently integrated within the stack to generate the multi-looked L1B power waveforms has been reduced, from 448 originally, to now 322 looks. This allows for not accounting undesired Doppler ambiguity effects within the stack. This also allows for HR SWH bias reduction as outer beams are the most affected by vertical velocity effects (full correction foreseen in F09). With the reduced number of looks in the stack, SWH differences between HR and LR are considerably reduced, and range differences between LR and HR are less dependent on SWH.

More details on the PB F06 can be found in the associated product notice [2].
The 2022 PB F06 reprocessing campaign was the first opportunity to assess Sentinel-6 MF performance with an homogenuous processing. The F06 reprocessing Cal/VAL assessment is available online [3].

From 2022-08-15 (cycle 65 track 21), Sentinel-6 MF NTC data are processed using a new processing baseline : PB F07. The main changes brought by this PB are :

- The availability of High Resolution Microwave Radiometer (HRMR) data in all radiometer products. All variables within the Level 2 altimeter products derived from the radiometer result from the combination of AMR-C and HRMR data (ex: WTC).
- The usage of ECHO CAL as main source of CAL1.
- An update of the ionospheric correction filtering method. With this update, the filtered ionospheric correction became available over the Caspian Sea in the products, enabling SLA computation in this region.

Mode details on the PB F07 can be found in the associated product notice [4].

# 3 Data coverage and edited measurements

## 3.1. Missing measurements

### 3.1.1. Over land and ocean

Determination of missing measurements relative to the theoretically expected orbit ground pattern is an essential tool to detect missing telemetry or satellite events.

Figure 8 shows the percentage of available measurements for Sentinel-6 MF LR and HR modes for all surfaces observed. In average LR mode provides 98.5% of measurements over 75 cycles.

HR mode provides in average less measurements (91.1%) on the same time-period. From cycle 4 to 31 (in red on the figure), different mode masks were activated on POS-4. Over these cycles, HR data were not always available globally. It was the case only on cycles where the LRMC acquisition mode is activated everywhere (cycles 14, 22, 28 and from cycle 32 onwards).
From cycle 32, the average percentage of available HR data is of 98.3%, which is still lower than LR. This difference is mainly due to a known anomaly: Fairbanks Ground Station key hole effect.

Other events, such as POS4 restarts or the switch from POS4-A to POS4B, impact data availability during Sentinel-6 MF first year (see grey lines on the figure).

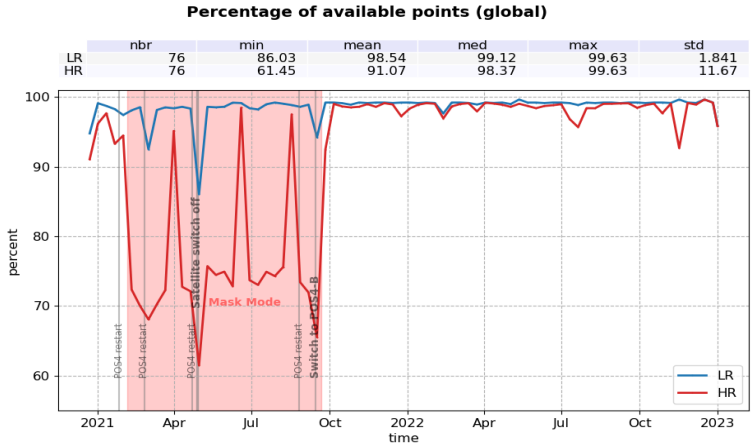


*Figure 8 – Percentage of available data over all surfaces for both LR (blue) and HR (red) per cycle.*

Table 3 and 4 give the list of fully missing passes for LR and HR respectively, along with related events.

| Cycle | Pass | Date | Comment |
|---|---|---|---|
| 4 | 15 | 2020-12-17 23:13:55 to 2020-12-18 00:10:08 | |
| | 26 | 2020-12-18 09:32:15 to 2020-12-18 10:28:29 | |
| | 88 | 2020-12-20 19:25:52 to 2020-12-20 21:21:40 | |

| | | | |
|---|---|---|---|
| | 152 | 2020-12-23 07:25:51 to 2020-12-23 09:22:07 | |
| | 216 | 2020-12-25 19:22:58 to 2020-12-25 21:18:53 | POS4 restart |
| | 232 | 2020-12-26 10:32:29 to 2020-12-26 11:28:43 | |
| 8 | 126 to 128 | 2021-01-30 23:04:03 to 2021-01-31 02:49:31 | |
| 10 | 1 | 2021-02-24 19:56:33 to 2021-02-24 20:52:47 | |
| 11 | 207 to 221 | 2021-03-04 20:47:15 to 2021-03-05 11:13:52 | |
| 17 | 52 to 79 | 2021-04-27 07:28:16 to 2021-04-28 09:56:12 | Satellite switched off for satellite software patch |
| | 83 to 86 | 2021-04-28 11:43:02 to 2021-04-28 17:07:49 | |
| 23 | 230 | 2021-07-02 18:06:02 to 2021-07-02 20:01:59 | |
| 24 | 230 | 2021-07-12 16:04:34 to 2021-07-12 18:00:31 | |
| 31 | 84 to 85 | 2021-09-14 08:58:51 to 2021-09-14 11:45:01 | |
| | 88 to 90 | 2021-09-14 12:42:06 to 2021-09-14 16:39:47 | Switch from POS4-A to POS4-B |
| | 110 | 2021-09-15 09:18:54 to 2021-09-15 11:13:23 | |
| | 112 to 114 | 2021-09-15 11:13:35 to 2021-09-15 15:07:45 | |
| 46 | 22 | 2022-02-07 16:31:06 to 2022-02-07 18:26:45 | |
| | 98 | 2022-02-10 15:43:12 to 2022-02-10 17:38:39 | |
| 74 | 35 | 2022-11-12 20:14:59 to 2022-11-12 21:11:12 | |
| | 68 | 2022-11-14 03:10:04 to 2022-11-14 04:06:17 | |

*Table 3 – List of missing passes in LR*

| Date | Cycle | Pass | Comment |
|---|---|---|---|
| 4 | 15 | 2020-12-17 23:13:55 to 2020-12-18 00:10:08 | |
| | 26 | 2020-12-18 09:32:15 to 2020-12-18 10:28:29 | |
| | 82 to 84 | 2020-12-20 13:37:34 to 2020-12-20 17:19:22 | |
| | 88 | 2020-12-20 19:25:52 to 2020-12-20 21:21:40 | |
| | 152 | 2020-12-23 07:25:51 to 2020-12-23 09:22:07 | |
| | 198 | 2020-12-25 02:23:06 to 2020-12-25 04:19:34 | |
| | 216 | 2020-12-25 19:15:12 to 2020-12-25 21:18:53 | POS4 restart |
| | 226 | 2020-12-26 04:41:52 to 2020-12-26 06:37:48 | |
| | 249 | 2020-12-27 02:28:08 to 2020-12-27 03:24:22 | |
| 5 | 32 | 2020-12-28 12:16:13 to 2020-12-28 14:09:25 | |
| | 76 | 2020-12-30 06:12:27 to 2020-12-30 07:52:28 | |
| | 78 | 2020-12-30 08:08:40 to 2020-12-30 09:58:41 | |
| | 226 | 2021-01-05 02:40:24 to 2021-01-05 04:36:20 | |
| 6 | 224 | 2021-01-14 22:45:17 to 2021-01-15 00:38:57 | |
| | 232 | 2021-01-15 06:27:01 to 2021-01-15 07:32:58 | |
| 7 | 104 | 2021-01-20 04:32:35 to 2021-01-20 05:28:49 | |
| | 126 | 2021-01-21 01:09:18 to 2021-01-21 02:05:32 | |
| | 150 | 2021-01-21 23:38:28 to 2021-01-22 00:34:41 | |
| | 154 | 2021-01-22 03:23:19 to 2021-01-22 04:19:33 | |
| | 176 | 2021-01-23 00:00:03 to 2021-01-23 00:56:16 | |
| | 204 | 2021-01-24 02:14:03 to 2021-01-24 03:10:17 | |
| | 206 | 2021-01-24 04:06:29 to 2021-01-24 05:02:43 | |
| | 226 | 2021-01-24 22:37:27 to 2021-01-25 00:33:23 | |
| | 229 to 230 | 2021-01-25 00:53:22 to 2021-01-25 03:47:04 | |
| | 234 | 2021-01-25 06:03:49 to 2021-01-25 07:33:31 | |
| 8 | 22 | 2021-01-26 21:41:30 to 2021-01-26 22:37:44 | |
| | 24 | 2021-01-26 23:33:56 to 2021-01-27 00:30:10 | |
| | 30 | 2021-01-27 04:18:50 to 2021-01-27 06:11:57 | |

| | | | |
|---|---|---|---|
| | 46 | 2021-01-27 19:56:11 to 2021-01-27 21:49:31 | |
| | 126 to 129 | 2021-01-30 22:57:13 to 2021-01-31 02:52:42 | |
| | 226 | 2021-02-03 20:35:58 to 2021-02-03 22:31:54 | |
| 9 | 102 to 103 | 2021-02-08 22:27:28 to 2021-02-09 00:30:02 | |
| | 178 to 179 | 2021-02-11 21:36:30 to 2021-02-11 23:41:59 | |
| | 204 to 205 | 2021-02-12 21:59:32 to 2021-02-13 00:04:35 | |
| | 254 | 2021-02-14 20:51:49 to 2021-02-14 22:55:02 | |
| 10 | 42 | 2021-02-16 12:19:05 to 2021-02-16 14:11:54 | |
| | 98 | 2021-02-18 16:34:04 to 2021-02-18 18:29:51 | |
| | 128 to 129 | 2021-02-19 20:46:54 to 2021-02-19 22:51:07 | |
| | 150 | 2021-02-20 17:13:47 to 2021-02-20 19:17:01 | |
| | 178 to 179 | 2021-02-21 19:33:41 to 2021-02-21 21:40:30 | |
| | 226 | 2021-02-23 16:16:48 to 2021-02-23 18:28:56 | |
| | 252 to 253 | 2021-02-24 16:47:09 to 2021-02-24 20:52:26 | |
| | 1 | 2021-02-24 20:52:41 to 2021-02-24 20:53:33 | |
| 11 | 16 | 2021-02-25 09:59:47 to 2021-02-25 10:56:00 | |
| | 26 to 27 | 2021-02-25 19:12:30 to 2021-02-25 21:15:05 | |
| | 102 to 103 | 2021-02-28 18:25:12 to 2021-02-28 20:27:05 | |
| | 128 to 129 | 2021-03-01 18:48:34 to 2021-03-01 20:49:39 | |
| | 178 to 179 | 2021-03-03 17:33:58 to 2021-03-03 19:39:02 | |
| | 207 to 221 | 2021-03-04 20:47:14 to 2021-03-05 11:13:52 | |
| 12 | 26 to 27 | 2021-03-07 17:11:56 to 2021-03-07 19:13:37 | |
| | 48 | 2021-03-08 13:27:54 to 2021-03-08 15:39:02 | |
| | 64 | 2021-03-09 04:56:37 to 2021-03-09 05:52:50 | |
| | 124 | 2021-03-11 12:42:51 to 2021-03-11 14:44:38 | |
| | 128 to 129 | 2021-03-11 16:46:24 to 2021-03-11 18:48:11 | |
| | 156 | 2021-03-12 18:59:31 to 2021-03-12 20:04:36 | |
| | 178 to 180 | 2021-03-13 15:33:46 to 2021-03-13 18:33:45 | |
| | 204 to 206 | 2021-03-14 15:54:47 to 2021-03-14 18:55:20 | |
| | 226 | 2021-03-15 12:21:13 to 2021-03-15 14:26:00 | |
| | 232 | 2021-03-15 18:00:07 to 2021-03-15 19:16:55 | |
| | 254 | 2021-03-16 14:48:36 to 2021-03-16 16:49:30 | |
| 13 | 26 to 27 | 2021-03-17 15:08:14 to 2021-03-17 17:12:08 | |
| | 70 | 2021-03-19 08:16:37 to 2021-03-19 10:10:15 | |
| | 178 to 179 | 2021-03-23 13:32:15 to 2021-03-23 15:36:05 | |
| | 254 | 2021-03-26 12:47:06 to 2021-03-26 14:43:27 | |
| 14 | 48 | 2021-03-28 09:40:38 to 2021-03-28 11:36:28 | |
| | 118 | 2021-03-31 03:25:12 to 2021-03-31 05:11:13 | |
| | 146 | 2021-04-01 05:30:01 to 2021-04-01 07:21:09 | |
| | 226 | 2021-04-04 08:27:07 to 2021-04-04 10:23:03 | |
| 15 | 172 | 2021-04-12 03:39:20 to 2021-04-12 05:41:18 | |
| 16 | 120 | 2021-04-20 01:18:27 to 2021-04-20 02:14:58 | |
| | 200 to 205 | 2021-04-23 04:01:49 to 2021-04-23 09:54:15 | |
| 17 | 48 to 86 | 2021-04-27 03:36:11 to 2021-04-28 17:07:49 | Satellite switched off for satellite software patch |
| | 88 to 90 | 2021-04-28 17:08:30 to 2021-04-28 20:39:36 | |
| 21 | 166 to 168 | 2021-06-10 10:08:36 to 2021-06-10 13:59:58 | |
| 22 | 120 | 2021-06-18 13:09:54 to 2021-06-18 14:06:08 | |
| 23 | 230 to 231 | 2021-07-02 18:05:56 to 2021-07-02 20:06:31 | |
| 24 | 230 to 231 | 2021-07-12 16:04:28 to 2021-07-12 18:05:03 | |
| 25 | 153 | 2021-07-19 14:00:34 to 2021-07-19 15:16:50 | |

| | | | |
|---|---|---|---|
| 28 | 33 to 34 | 2021-08-13 15:29:57 to 2021-08-13 17:37:04 | |
| | 170 | 2021-08-18 23:51:46 to 2021-08-19 00:48:00 | |
| 29 | 78 | 2021-08-25 07:32:27 to 2021-08-25 08:48:32 | |
| | 106 | 2021-08-26 09:30:54 to 2021-08-26 11:10:31 | POS4 restart |
| | 251 | 2021-09-01 01:43:41 to 2021-09-01 02:39:55 | |
| 30 | 196 to 207 | 2021-09-08 20:09:12 to 2021-09-09 07:29:39 | |
| | 222 | 2021-09-09 20:28:35 to 2021-09-09 22:00:52 | |
| 31 | 82 to 86 | 2021-09-14 07:01:41 to 2021-09-14 12:05:01 | |
| | 88 to 95 | 2021-09-14 12:42:06 to 2021-09-14 21:10:01 | Switch from POS4-A to POS4-B |
| | 98 to 114 | 2021-09-14 21:47:06 to 2021-09-15 15:07:45 | |
| 32 | 62 to 72 | 2021-09-23 10:22:49 to 2021-09-23 21:36:32 | |
| | 120 | 2021-09-25 16:55:09 to 2021-09-25 17:51:23 | |
| | 224 | 2021-09-29 17:33:33 to 2021-09-29 20:00:36 | |
| 34 | 170 | 2021-10-17 11:42:56 to 2021-10-17 12:39:09 | |
| 35 | 120 | 2021-10-25 10:50:43 to 2021-10-25 11:46:57 | |
| 36 | 170 | 2021-11-06 07:39:57 to 2021-11-06 08:36:12 | |
| 38 | 120 | 2021-11-24 04:46:17 to 2021-11-24 05:42:31 | |
| 41 | 2 | 2021-12-19 08:03:51 to 2021-12-19 09:59:27 | |
| | 64 | 2021-12-21 18:04:25 to 2021-12-21 20:00:28 | |
| 42 | 162 | 2022-01-04 11:30:49 to 2022-01-04 13:40:22 | |
| 46 | 21 to 23 | 2022-02-07 15:49:15 to 2022-02-07 18:37:54 | |
| | 97 to 99 | 2022-02-10 15:01:33 to 2022-02-10 17:50:13 | |
| 50 | 251 | 2022-03-28 07:12:43 to 2022-03-28 08:08:56 | |
| 59 | 170 | 2022-06-22 09:06:02 to 2022-06-22 10:02:15 | |
| 61 | 36 | 2022-07-06 22:51:34 to 2022-07-07 01:01:04 | Ground segment anomaly (UNS 8401) |
| | 92 | 2022-07-09 03:53:10 to 2022-07-09 05:48:47 | Ground segment anomaly (UNS 8420) |
| | 246 | 2022-07-15 04:12:47 to 2022-07-15 05:44:02 | Ground segment anomaly (UNS 8449) |
| 62 | 20 | 2022-07-16 06:11:54 to 2022-07-16 08:07:30 | Ground segment anomaly (UNS 8451) |
| | 114 | 2022-07-19 22:13:23 to 2022-07-20 00:18:31 | Ground segment anomaly (UNS 8463) |
| | 120 | 2022-07-20 04:10:54 to 2022-07-20 05:07:08 | |
| | 160 | 2022-07-21 17:02:52 to 2022-07-21 19:03:37 | Ground segment anomaly (UNS 8487) |
| | 202 | 2022-07-23 08:49:45 to 2022-07-23 10:46:04 | Ground segment anomaly (UNS 8492) |
| | 254 | 2022-07-25 09:34:45 to 2022-07-25 11:31:20 | Ground segment anomaly (UNS 8495) |
| 63 | 120 | 2022-07-30 02:09:26 to 2022-07-30 03:05:39 | Ground segment anomaly (UNS 8602) |
| 64 | 124 | 2022-08-09 03:38:55 to 2022-08-09 05:34:53 | Ground segment anomaly (UNS 8546) |
| 69 | 144 | 2022-09-28 12:26:27 to 2022-09-28 14:08:05 | Ground segment anomaly (UNS 8718) |
| 72 | 45 | 2022-10-24 09:40:03 to 2022-10-24 10:36:16 | Ground segment anomaly (UNS 8803) |
| | 47 to 49 | 2022-10-24 11:32:29 to 2022-10-24 14:21:07 | |
| 74 | 19 to 22 | 2022-11-12 05:15:33 to 2022-11-12 09:00:24 | |
| | 35 | 2022-11-12 20:14:59 to 2022-11-12 21:11:12 | |
| | 68 | 2022-11-14 03:10:04 to 2022-11-14 04:06:17 | |
| | 147 to 148 | 2022-11-17 05:00:48 to 2022-11-17 07:46:36 | Ground segment anomaly (UNS 9059) |
| | 154 | 2022-11-17 10:52:57 to 2022-11-17 12:49:05 | |
| | 156 | 2022-11-17 13:34:47 to 2022-11-17 15:09:59 | |
| | 202 | 2022-11-19 08:42:05 to 2022-11-19 10:28:24 | |
| 77 | 148 | 2022-12-16 23:28:30.44 to 2022-12-17 01:42:11 | Ground segment anomaly (UNS 9117) |

*Table 4 – List of missing passes in HR*

### 3.1.2. Over ocean

Figure 9 shows the percentage of available measurements for Sentinel-6 MF LR and HR modes for ocean only. In average LR mode provides 99.4% of measurements over 75 cycles.

As expected, HR mode provides in average less measurements (97.9%) on the same time-period. From cycle 32 onwards, in LRMC mode only, the average percentage of available HR data is of 99.1%, which is still lower than LR, once again due to the Fairbanks Ground Station key hole effect.

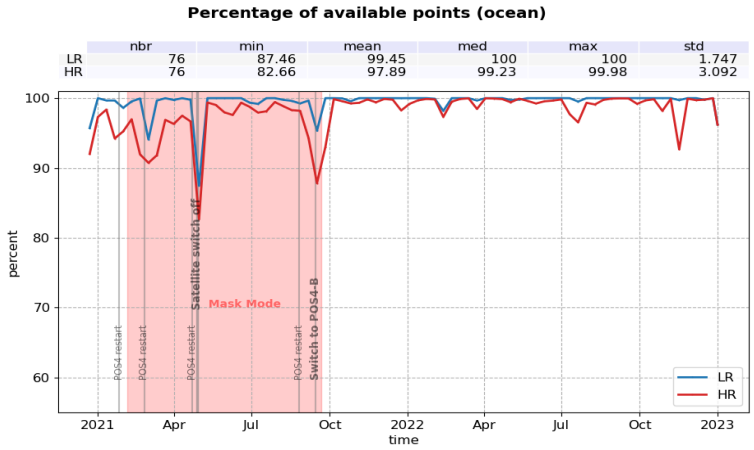


*Figure 9 – Percentage of available data over ocean for both LR (blue) and HR (red) per cycle.*

## 3.2. Edited measurements

### 3.2.1. Overview

The outlier detection or editing step of the Cal/Val process is applied to remove any measurement that is considered erroneous. Thus, it helps refining the various metrics which are provided in the specific sections dedicated to the performance over the ocean. The definition of an erroneous measurement, and of the accepted error level on the final sea level anomaly is of course a trade-off between accuracy and data coverage. The monitoring of the percentage of valid and edited measurements also provides relevant information about the mission performance.

A series of editing criteria are used to detect outliers over ocean. This process is divided into 3 main parts:

- removal of all measurements affected by sea-ice.
- removal of all measurements which exceed defined thresholds on different parameters.
- further checks on along-track SLA consistency.

For each step of the process, the number of outliers is routinely monitored at Cal/Val level. The number of removed data is used to detect processing anomalies which could be due to instrumental, geophysical or algorithmic changes. The process performed here is dedicated to ocean applications. Data over land are removed using a land/water mask prior to the analysis described in this section.

The percentage of edited data per cycle for HR and LR datasets over ocean is monitored on figure 10. In average, slightly less data is edited in HR mode (8.3%) compared to LR (8.7%). The main spikes observed are :

- Cycle 5, track 121 to 126 (01/01/21 00:31:12 to 06:08:28): Missing dry tropospheric correction files (see "Dry tropospheric correction" paragraph in section 3.2.3.2.).
- Cycle 8, track 12 to 60 (26/01/21 21:19 to 28-01-2021 10:14): Range anomaly (-9 m) following a POS-4 restart, for HR only (see "Sea level anomaly" paragraph in section 3.2.3.2.).
- Cycle 13, track 20 to 45 (17/03/21 09:36 to 18/03/21 09:38): AMR-C 24h warm target calibration (see "section 3.2.2.).

Before 21-09-2022 (cycle 32) and the switch to full LRMC-OL mode (section 2.3.), a higher percentage of data is edited in HR compared to LR, with additional spikes. This is due to less overall measurements being available in HR with the use of masks (see figure 9).

A annual signal is visible : the total percentage of edited data is lower during March/April/May (4-6%), then increasing during May to July and remains around 10-12%, and start to slowly decrease in mid-September. This expected behaviour is related to sea ice coverage (see dedicated part 3.2.2.), and was already observed on previous altimetry missions such as Jason-3.

The maps of figure 11 represent the percentage of edited data for LR and HR, over the year 2022. Equatorial wet zones or zones with sea ice appear on the maps as regions with less valid data, as it is also the case for other altimeters: measurements are corrupted by rain or sea ice. They were therefore removed by editing. HR and LR maps are in line, except in wet zones where less HR data are edited. It shows the better capability of HR processing to retrieve clean geophysical parameters over wet zones.

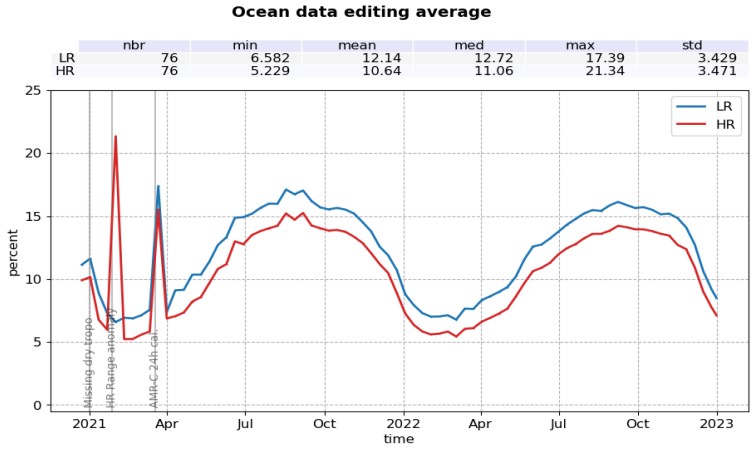


*Figure 10 – Percentage of edited data over ocean for both LR (blue) and HR (red) per cycle.*

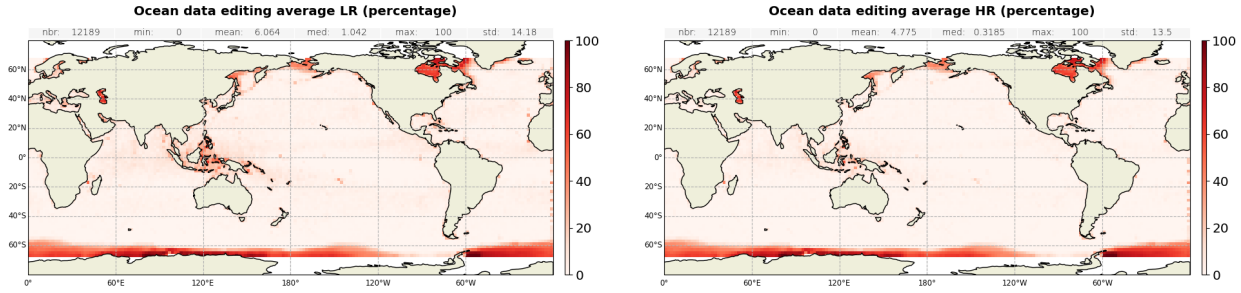


*Figure 11 – Maps of average percentage of edited ocean data for both LR (left) and HR (right), computed on cycles 42 to 79.*

### 3.2.2. Flagging quality : ice

The first step of the editing process includes the removal of points where ice is detected. The ice flag (based on rad_sea_ice_flag in L2 products) is used to remove measurements affected by sea ice within the altimeter footprint.

The percentage of measurements edited on the ice flag criterium over ocean is monitored on the figure 12.

On cycle 13, from pass 20 to 45 (17/03/21 09:36 to 18/03/21 09:38), an AMR-C 24h warm target calibration caused the unavailability of the radiometer derived ice flag, resulting in a spike in edited data. Over the shown period, no anomalous trend is detected but the nominal annual cycle is visible. Indeed, the maximum number of points over ice is reached during the southern winter (i.e. July - September). As Sentinel-6 MF satellite has an inclination of $66°$, it does not detect thawing of sea ice (due to global warming), which takes place especially in northern hemisphere over $66°$.

Note that the percentage of edited data on ice criterion is lower for Sentinel-6 MF (5.5 % in average) than on other mission such as Jason-3 (9.3 % in average), which uses altimeter sea ice flag. Indeed the radiometer sea ice flag performance does not allow to detect all measurements affected by sea ice. However these missed measurements are typically edited on other criteria down the process and the final impact is negligeable.

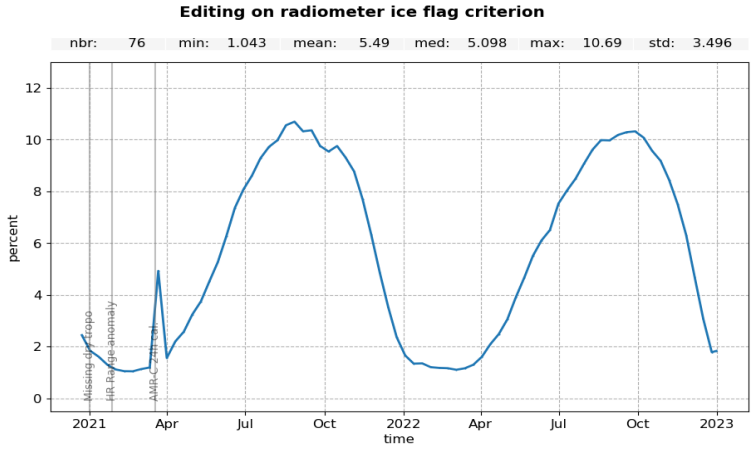


*Figure 12 – Percentage of data edited on ice criterion for both LR (blue) and HR (red) per cycle.*

### 3.2.3. Thresholds

#### 3.2.3.1. Overview

Once the measurements corrupted by sea ice surfaces are identified, the quality of the parameters retrieved by the altimeter, as well as that of the geophysical corrections are checked with respect to defined thresholds. These thresholds are detailed in table 5, with the corresponding percentage of detected outliers in LR and HR over Sentinel-6 MF lifetime. These percentages are closely monitored cycle by cycle, day by day and pass by pass by CLS Cal/Val routines. A distinction is made between indicators at default value, and indicators out of bounds.

This allows detection of anomalies in the number of removed data, which could have instrumental, geophysical or algorithmic origins. In particular, such monitoring has allowed to detect an anomaly on the dry tropospheric correction wich should not be missing or above thresholds (see dedicated paragraph below).

Note that no measurement is edited by the following corrections (these parameters are only verified in order to detect data at default values, which might happen during a processing anomaly):

- dynamical atmospheric correction (DAC),
- internal tide,
- earth tide,
- pole tide.

| Parameters | Min threshold | Max threshold | Unit | % rejected | |
|---|---|---|---|---|---|
| | | | | LR | HR |
| Sea surface height anomaly | -2 | 2 | m | 3.75 | 3.56 |
| Sea surface height | -130 | 100 | m | 2.52 | 0.02 |
| Nb measurements of range | 10 | N/A | | 0.14 | 0.1 |
| Std. deviation of range | 0 | See (*) | m | 2.75 | 0.62 |
| Backscatter coefficient | LR: 7<br>HR: 10 | LR: 30<br>HR: 35 | dB | 2.21 | 0.05 |
| Nb measurements of sigma0 | 10 | N/A | | 0.13 | 0.01 |
| Std. deviation of sigma0 | 0 | 1 | dB | 3.88 | 0.67 |
| Significant wave height | 0 | 11 | m | 2.66 | 0.10 |
| Altimeter wind speed | 0 | 30 | m.s-1 | 2.92 | 1.94 |
| Sea State Bias | -0.5 | 0 | m | 2.23 | 0.04 |
| Ionospheric correction filtered | -0.4 | 0.04 | m | 3.09 | 3.08 |
| Square off nadir angle | -0.2 | 0.64 | deg2 | 0.64 | N/A |
| Equilibrium tide | -0.5 | 0.5 | m | 0.01 | 0.01 |
| Combined atmospheric correction | -2 | 2 | m | 0.00 | 0.00 |
| Dry tropospheric correction | -2.5 | -1.9 | m | 0.07 | 0.07 |
| Internal tide | -5 | 5 | m | 0.00 | 0.00 |
| Ocean tide | -5 | 5 | m | 0.04 | 0.04 |
| Pole tide | -15 | 15 | m | 0.00 | 0.00 |
| Earth tide | -1 | 1 | m | 0.00 | 0.00 |
| AMR wet tropospheric correction | -0.5 | -0.001 | m | 0.20 | 0.20 |
| Global statistics of edited measurements by thresholds | | | | 6.64 | 5.16 |

*Table 5 – Table of parameters used for editing and the corresponding percentages of edited measurements for each parameter for Sentinel-6 MF LR and HR.*

(*) The maximum threshold for range standard deviation is set as function of significant wave height as follow:
- In LR:
  - for SWH $\leq$ 2m : 0.192
  - for SWH > 2m : 0.018 * SWH + 0.156
- In HR:
  - for SWH $\leq$ 2m : 0.087
  - for SWH > 2m : 0.033 * SWH + 0.121

The monitoring of edited data based on these thresholds criteria is shown on figure 13. Looking at data at default value (i.e. unavailable, right panel) and if we do not consider the events already listed above, a annual signal is visible. Part of this signal can be linked to sea ice. Indeed, as stated above, the radiometer sea ice flag performance does not allow to detect all measurements affected by sea ice. For the remaining measurements, MLE4 and Samosa retrackings failed to retrieve geophysical parameters, hence the default values detected here.
Looking at out-of-bounds data (left panel), less data are edited in HR (1.3 %) than in LR (2.5 %). Both monitoring are stable in time, with a small annual signal of about 1%-amplitude.

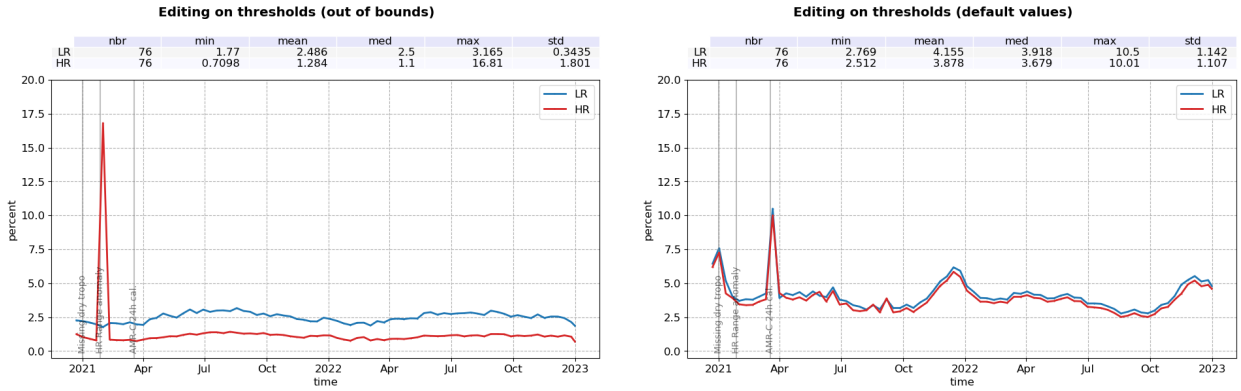


*Figure 13 – Percentage of data edited on threshold criteria for both LR (blue) and HR (red) per cycle, for out of bounds (left) and default value (right) indicators.*

The overall percentage of edited data with this threshold step is of 6.64 % for LR and 5.16 % for HR (table 5). These values are higher than on Jason-3 (3.45 %) due to sea ice flag performance. Indeed, the measurements affected by the sea ice but not flagged in Sentinel-6 MF radiometer sea ice flagged are rejected thanks to this threshold editing step.

### 3.2.3.2. Individual thresholds

**20 Hz range measurements number and standard deviation**

1 Hz range measurements computed with less than ten 20 Hz measurements are edited. Indeed they are considered as not consistent to compute 1Hz resolution range.

In LR, such situation usually occurs in regions with disturbed sea state or heavy rain, as shown on figure 15. Indeed, waveforms are distorted by rain cells, which makes them often meaningless for SSH calculation. As a consequence, edited measurements due to several altimetric criteria are often correlated with wet areas. HR processing is less impacted by this effect. Over the year 2022, the average percentage of removed measurements using this criterion is 0.14% for Sentinel-6 MF LR whereas it is only of 0.01% for HR (figure 14).

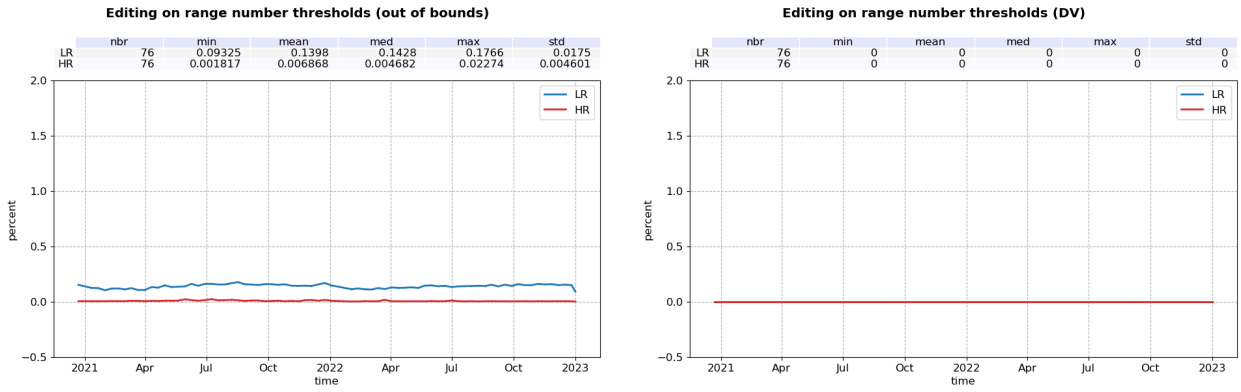


*Figure 14 – Percentage of data edited on range number threshold for both LR (blue) and HR (red) per cycle, for out of bounds (left) and default value (right).*

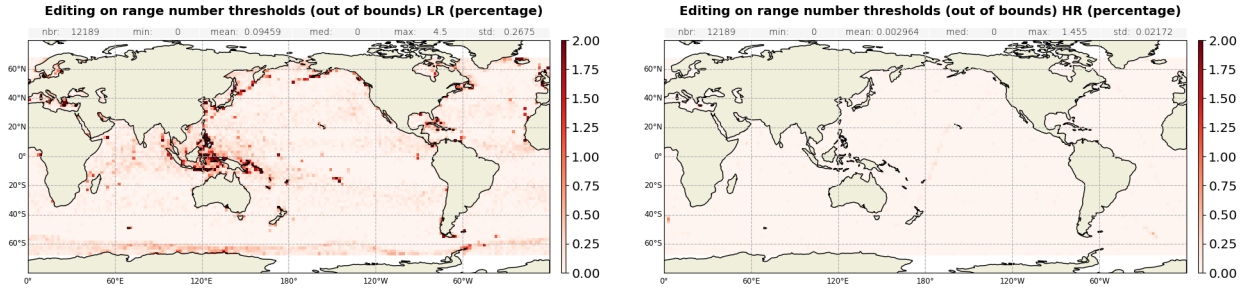


*Figure 15 – Maps of average percentage of data edited on range number threshold for both LR (left) and HR (right), for out of bounds, computed on cycles 42 to 79.*

Using the threshold editing on 20Hz measurements standard deviation (figure 16), 2.75% of data are removed in average in LR, higher than in HR (0.62%). This difference is explained by a higher percentage of values set to Default Value for LR than HR. It hightlights the HR processing capability to retrieve geophysical parameters on icy regions.
Additionally, an annual signal appears here for both modes. As for 20Hz range measurements number, edited measurements are correlated with wet areas (figure 17).

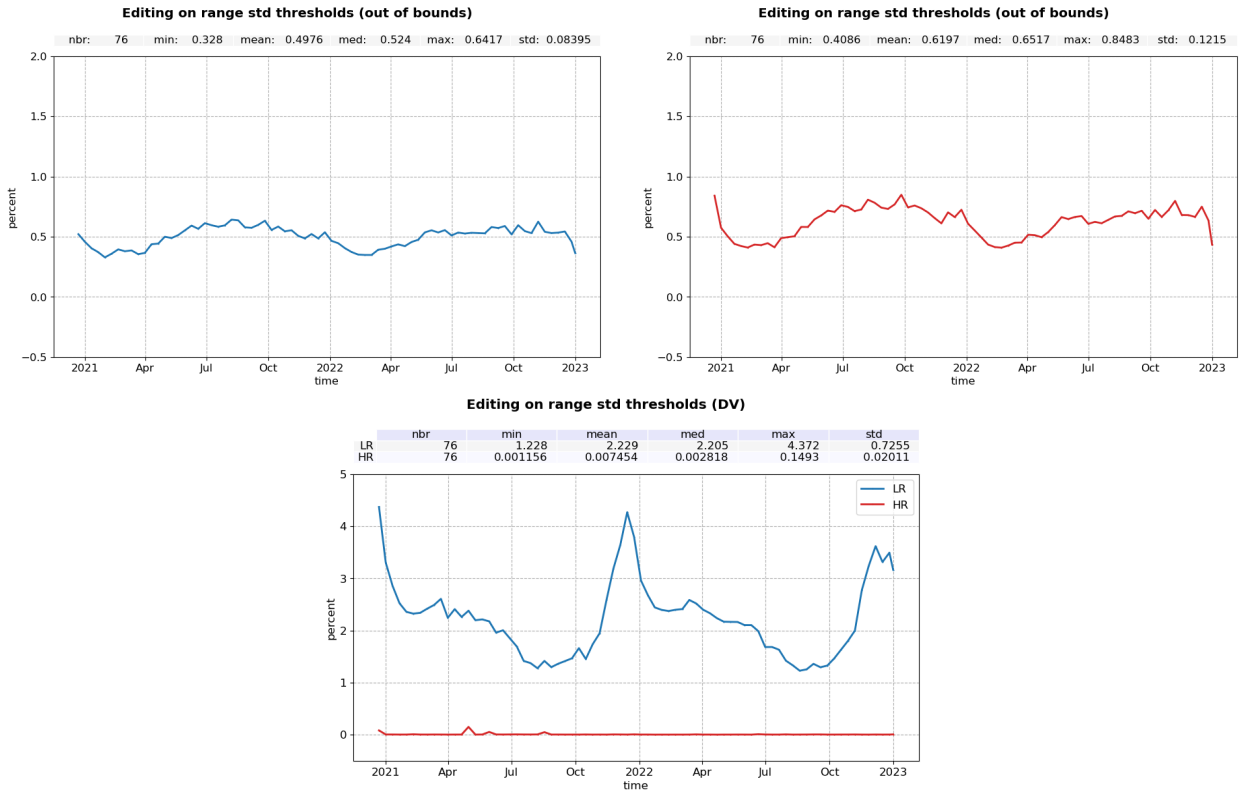


*Figure 16 – Percentage of data edited on range std threshold for both LR (blue) and HR (red) per cycle, for out of bounds (top) and default value (bottom).*

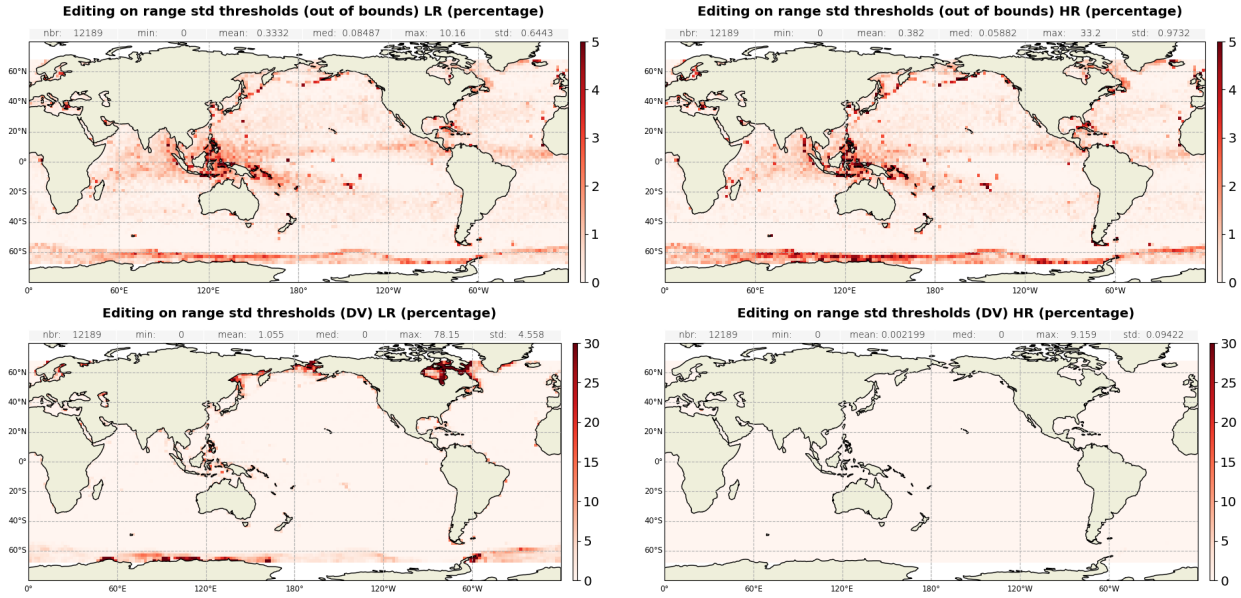


*Figure 17 – Maps of average percentage of data edited on range std threshold for both LR (left) and HR (right), for out of bounds (top) and default value (bottom), computed on cycles 42 to 79.*

### Backscatter coefficient

The percentage of edited measurements due to backscatter coefficient criterion is represented on top of figure 18. It is about 2.21% for LR and 0.05% for HR. For LR, most of these edited measurements are at DV and located in coastal areas, ice margins and wet zones (see figure 19).

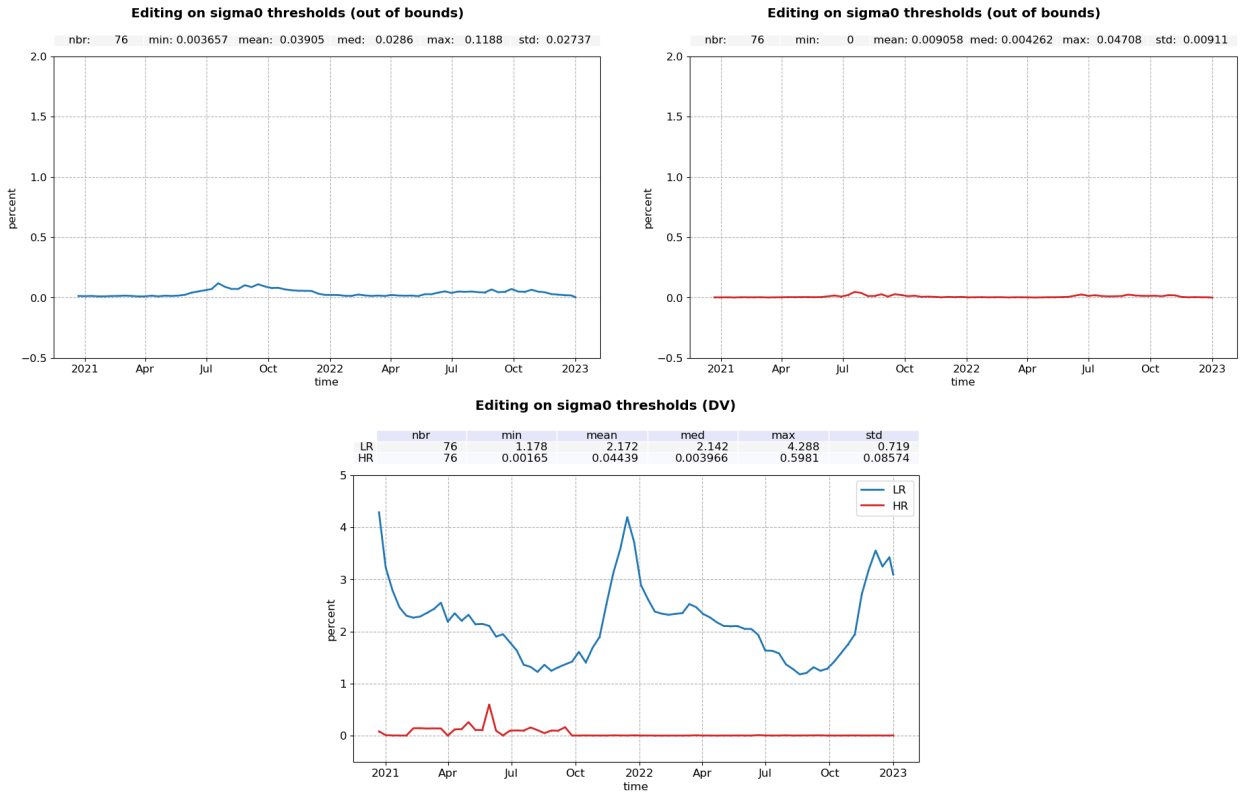


*Figure 18 – Percentage of data edited on sigma0 threshold for both LR (blue) and HR (red) per cycle, for out of bounds (top) and default value (bottom).*

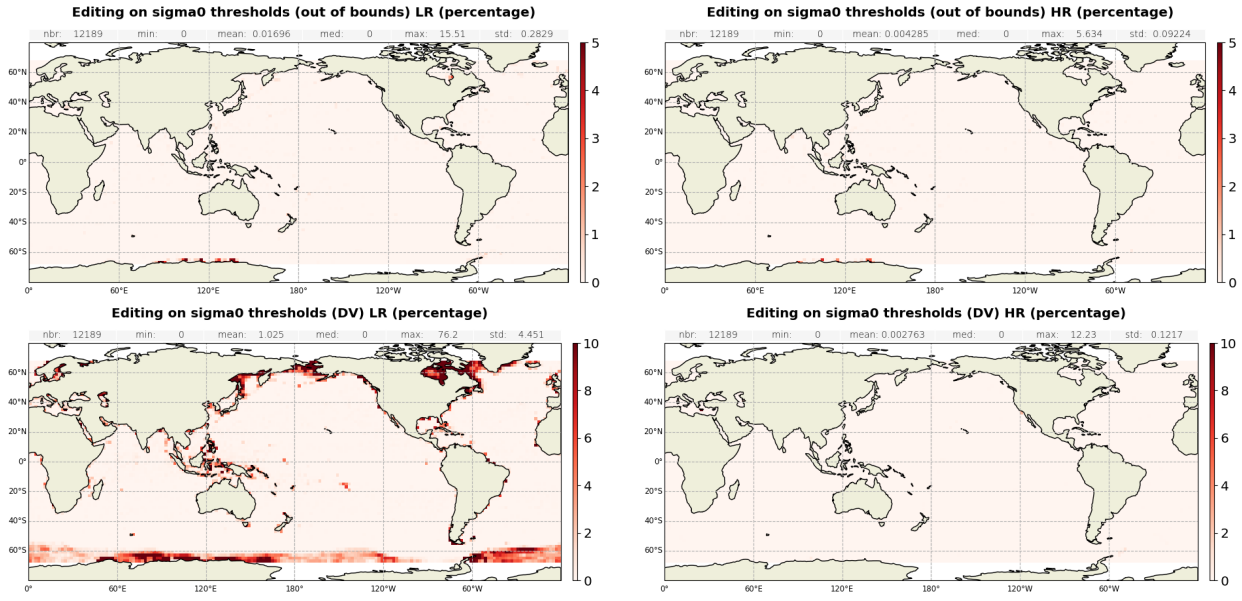


*Figure 19 – Maps of average percentage of data edited on sigma0 threshold for both LR (left) and HR (right), for out of bounds (top) and default value (bottom), computed on cycles 42 to 79.*

Similarly to range, sigma0 computed with less than 10 full resolutions (20Hz, 20 measurements/seconds)

are removed. As for the range, such situation usually occurs in regions with disturbed sea state or heavy rain (figure 21). While 0.13% of data are edited on this criterion in LR mode (figure 22), HR mode is almost unaffected with less than 0.01 % of data edited.

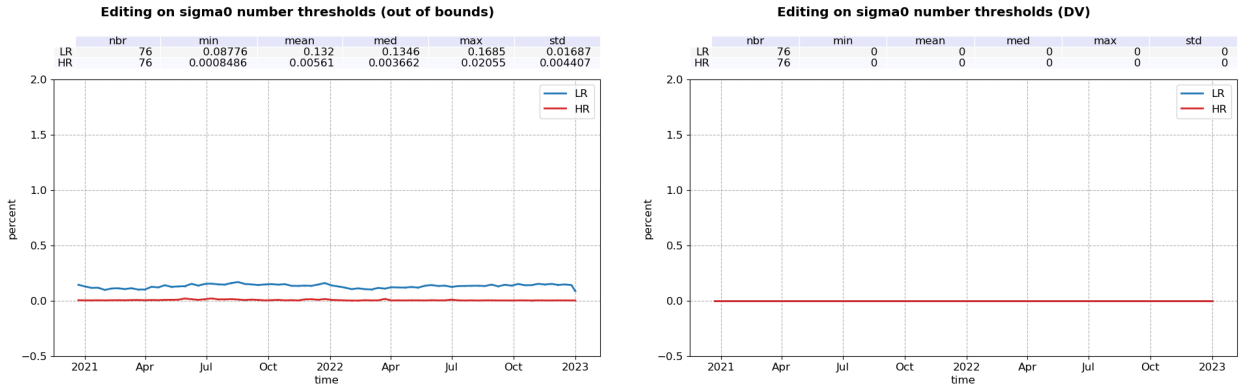


*Figure 20 – Percentage of data edited on sigma0 number threshold for both LR (blue) and HR (red) per cycle, for out of bounds (left) and default value (right).*

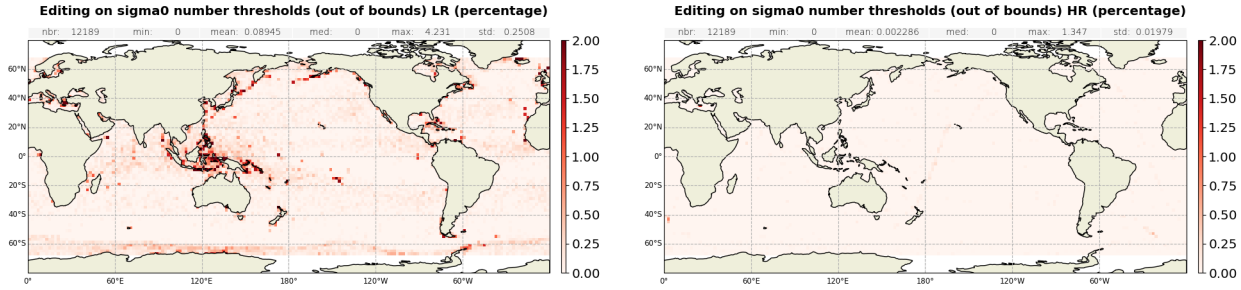


*Figure 21 – Maps of average percentage of data edited on sigma0 number threshold for both LR (left) and HR (right), for out of bounds, computed on cycles 42 to 79.*

Figure 22 presents the percentage of data edited base on sigma0 standard deviation criterion. It is about 3.88% for LR and 0.67% for HR. Most of the out of bound sigma0 STD are located in regions with disturbed sea state or heavy rain, primarly around Indonesia (figure 23).

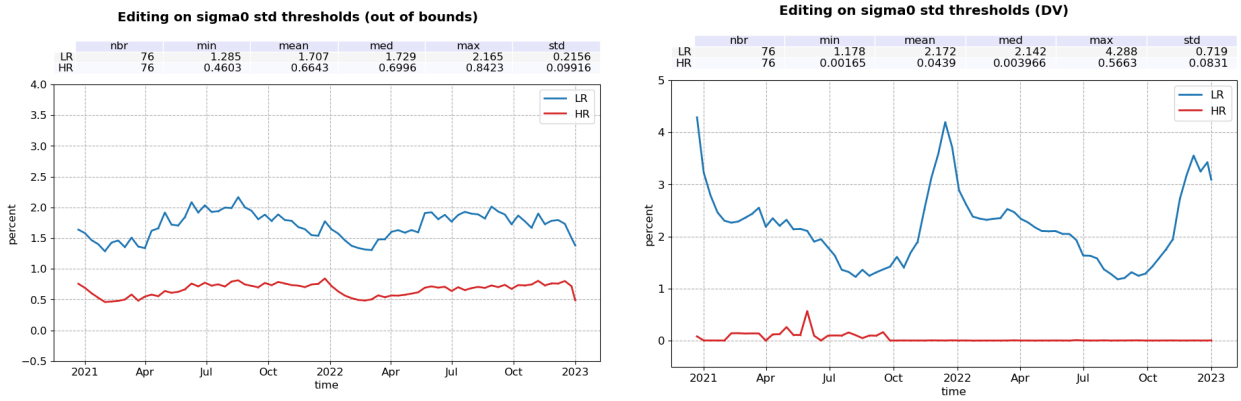


*Figure 22 – Percentage of data edited on sigma0 std threshold for both LR (blue) and HR (red) per cycle, for out of bounds (left) and default value (right).*

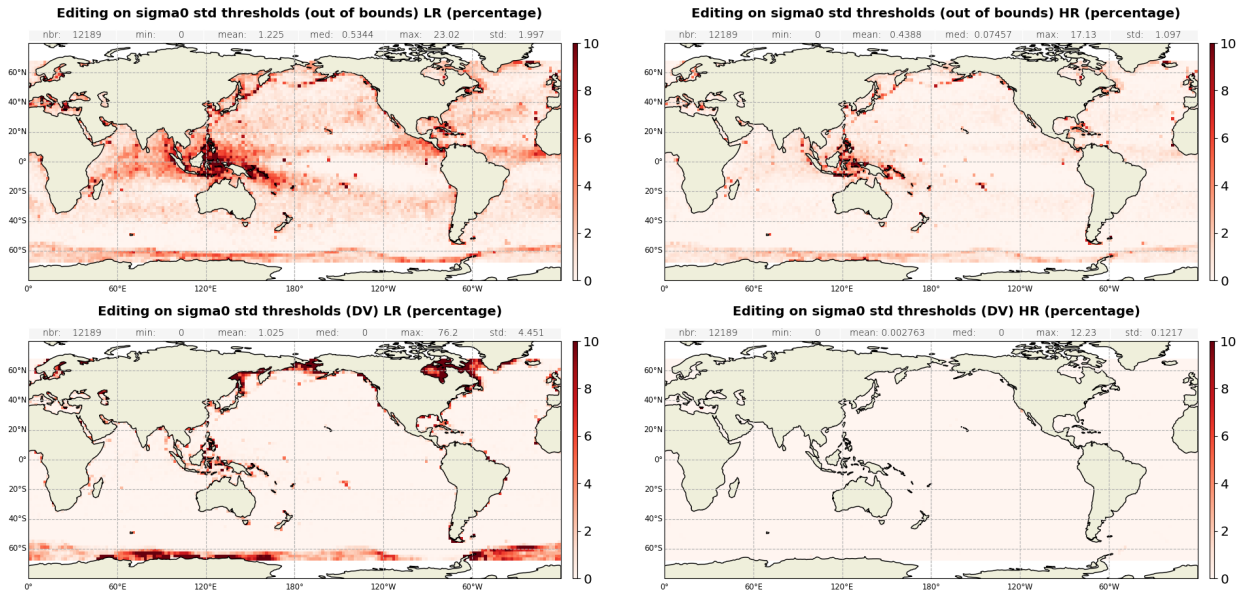


*Figure 23 – Maps of average percentage of data edited on sigma0 std threshold for both LR (left) and HR (right), for out of bounds (top) and default value (bottom), computed on cycles 42 to 79.*

## Significant wave height

The percentage of edited measurements due to significant wave heights criterion is represented on figure 24, and is about 2.66% for LR and 0.10% for HR. In LR mode, they are mostly due to default value data, and are located in circumpolar areas, while out of bounds values are located in coast regions, in the Mediterranean Sea and around Indonesia (figure 25).

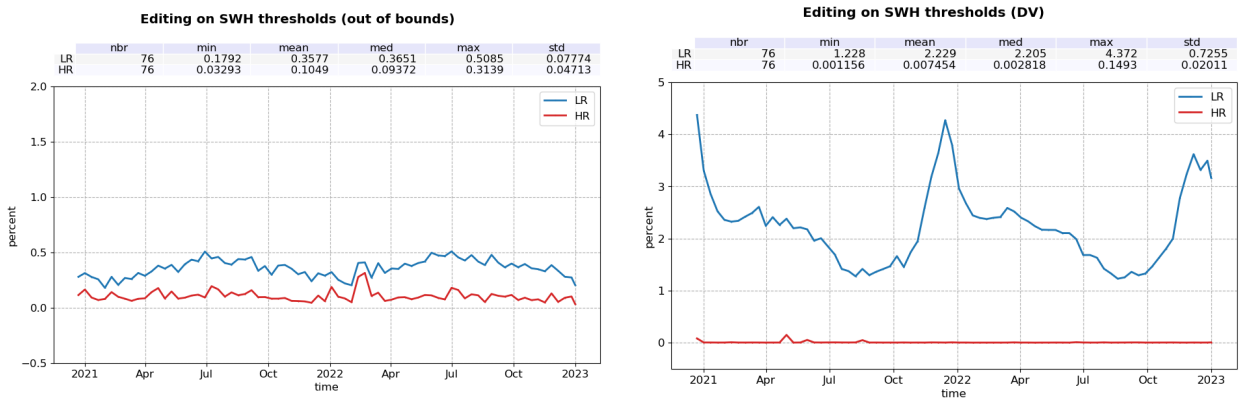


*Figure 24 – Percentage of data edited on SWH threshold for both LR (blue) and HR (red) per cycle, for out of bounds (left) and default value (right).*

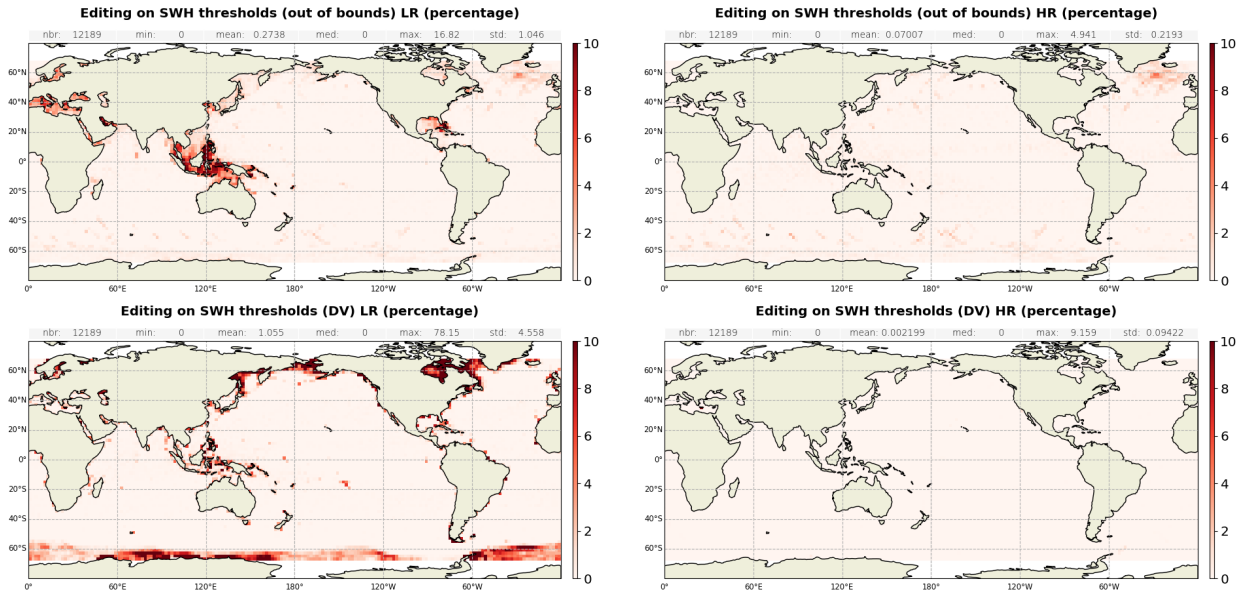


*Figure 25 – Maps of average percentage of data edited on SWH threshold for both LR (left) and HR (right), for out of bounds (top) and default value (bottom), computed on cycles 42 to 79.*

## Wind speed

The percentage of edited measurements due to altimeter wind speed criterion is represented on figure 26. It is about 2.92% for LR and 1.94% for HR. Measurements are exclusively edited because of default values.

Wind speed is also edited when it includes negative values. Nevertheless, sea state bias is available even for negative wind speed values. Therefore, the percentage of edited altimeter wind speed data is higher than the percentage of edited sea state bias data (Table 5). Maps on figure 27 showing percentage of measurements edited by altimeter wind speed criterion is correlated with maps 25 (SWH) and 19 (sigma0).

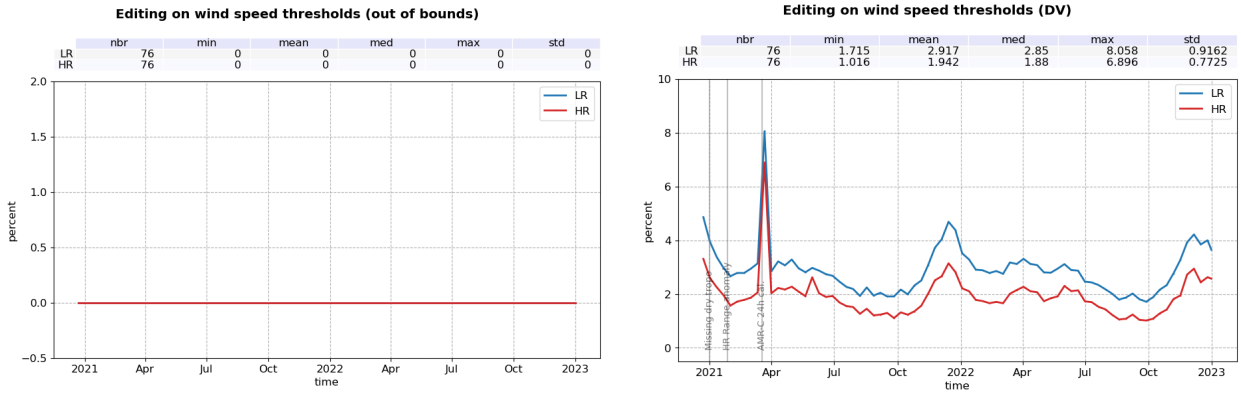


*Figure 26 – Percentage of data edited on wind speed threshold for both LR (blue) and HR (red) per cycle, for out of bounds (left) and default value (right).*

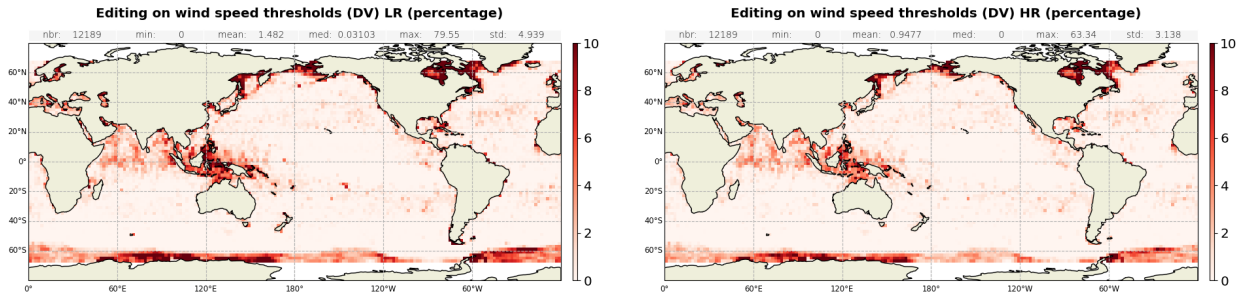


*Figure 27 – Maps of average percentage of data edited on wind speed threshold for both LR (left) and HR (right), for default value, computed on cycles 42 to 79.*

## Sea state bias

Regarding the sea state bias criterion, the percentage of LR edited measurements is about 2.23% and 0.04% for HR. These are exclusively due to default value data (figure 28). The difference can also be observed on wind-speed and significant wave height threshold criteria (which are both used for SSB computation).

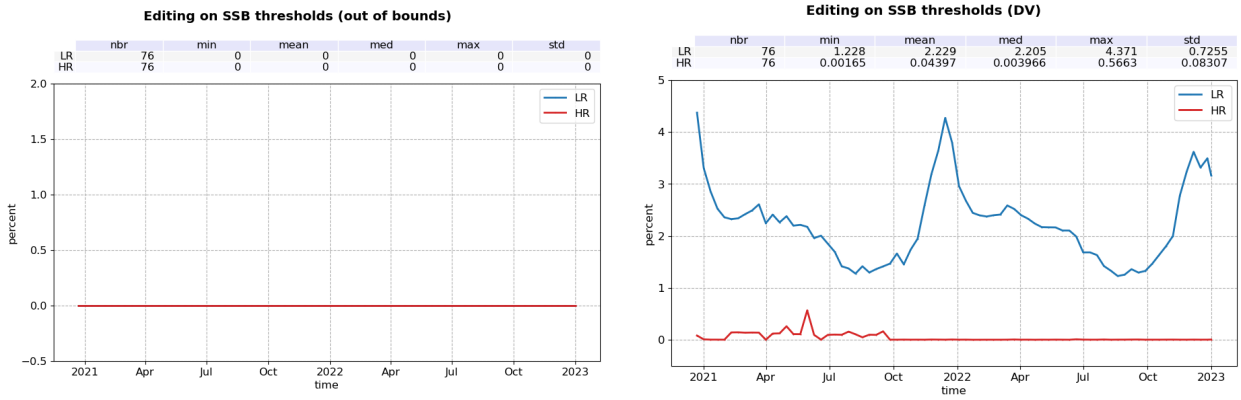


*Figure 28 – Percentage of data edited on SSB threshold for both LR (blue) and HR (red) per cycle, for out of bounds (left) and default value (right).*

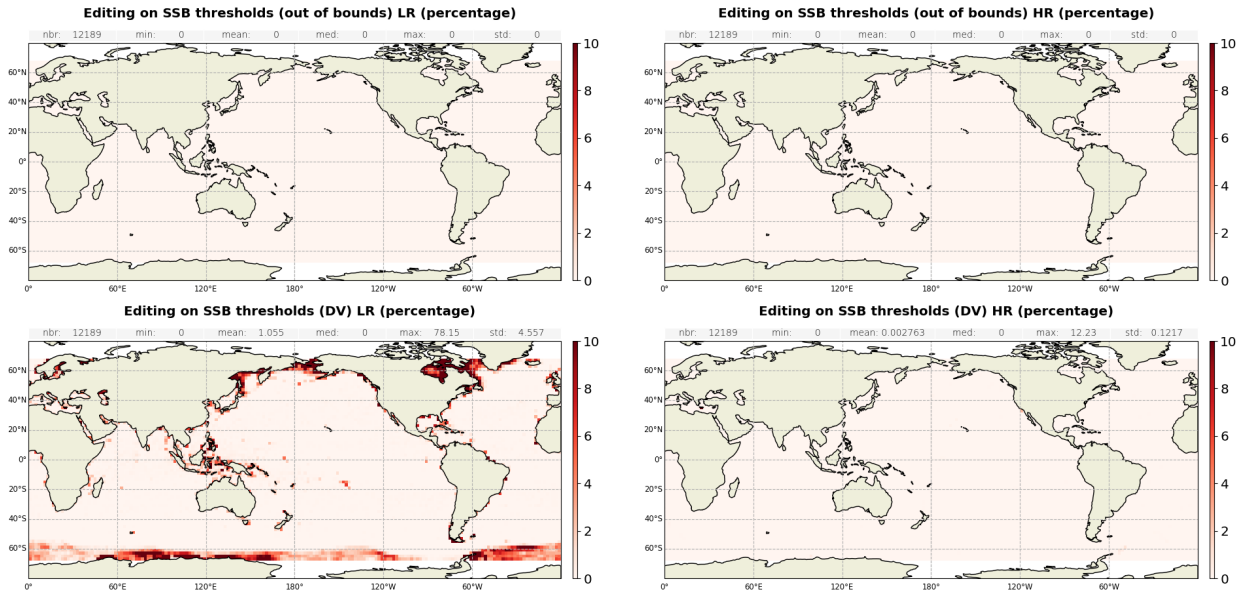


*Figure 29 – Maps of average percentage of data edited on SSB threshold for both LR (left) and HR (right), for out of bounds (top) and default value (bottom), computed on cycles 42 to 79.*

## Filtered ionospheric correction

The mean percentage of edited data by threshold criterion on filtered ionospheric correction is 3.09 % for both LR and HR. Indeed, the ionospheric correction is only computed in LR (C-band being only avalailable in LR) and LR ionospheric correction is used in HR. The small differences visible between LR and HR monitorings in figure 30 are due to the difference in data availability between the modes, especially during the Mode Mask phase. The maps on figure 31 show that measurements edited by filtered dual frequency ionosphere correction are mostly found near coasts and at ice frontiers.

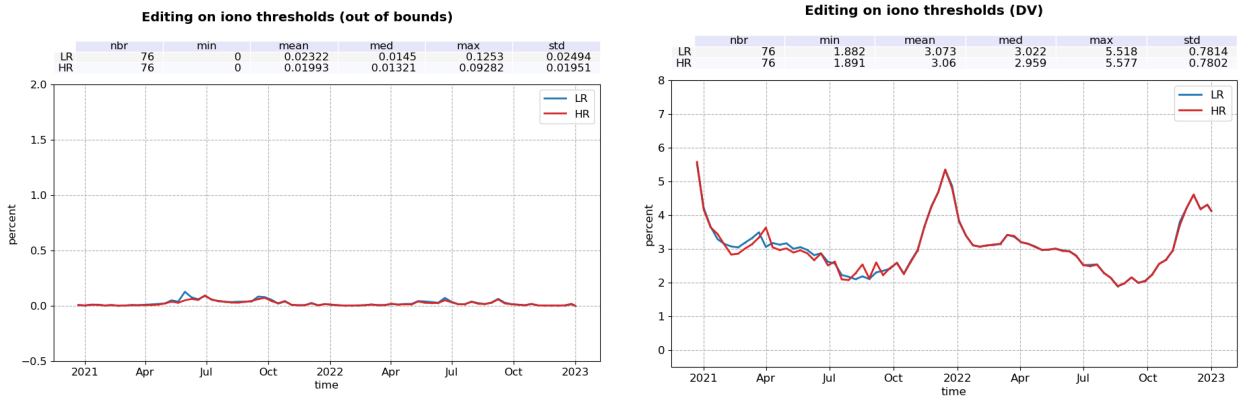


*Figure 30 – Percentage of data edited on filtered ionospheric correction threshold for both LR (blue) and HR (red) per cycle, for out of bounds (left) and default value (right).*

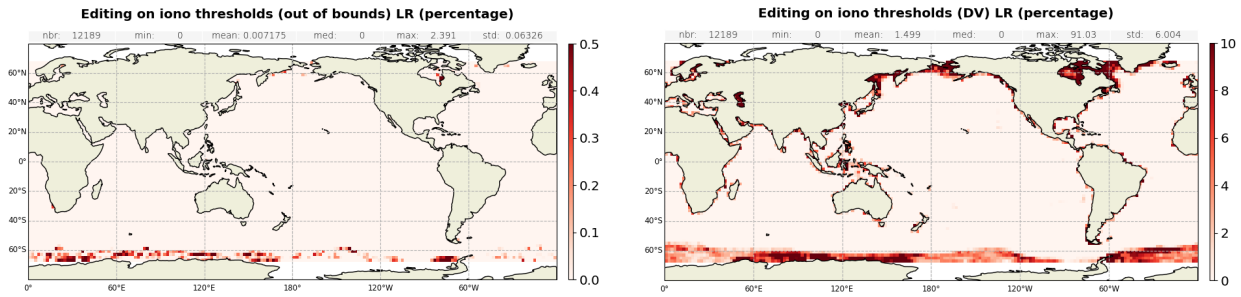


*Figure 31 – Maps of average percentage of data edited on LR filtered ionospheric correction threshold, for out of bounds (left) and default value (right), computed on cycles 42 to 79.*

## Square off nadir angle

The percentage of edited data on the square off nadir angle criterion (in LR data) is 0.64%, as shown in figure 32. Maps on figure 33 show that edited measurements are mostly found in coastal regions and regions with disturbed waveforms.

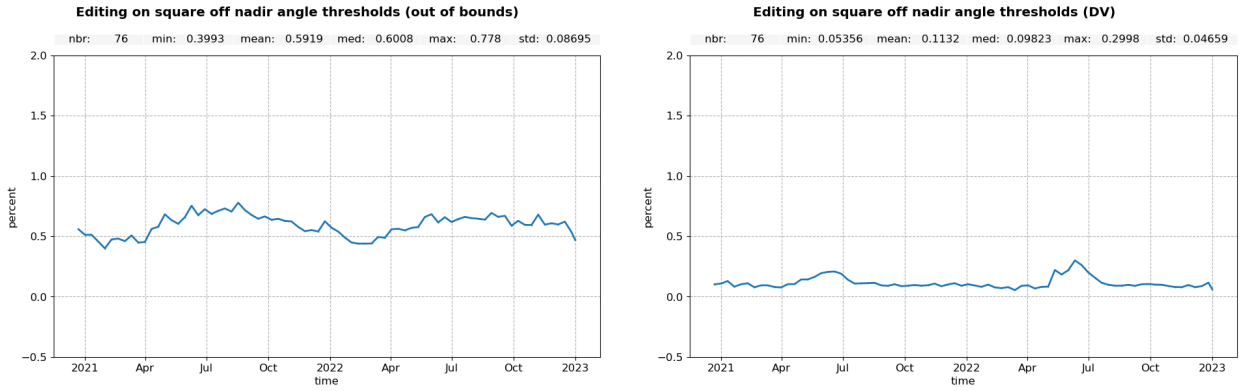


*Figure 32 – Percentage of data edited on square off nadir angle threshold for both LR (blue) per cycle, for out of bounds (left) and default value (right).*

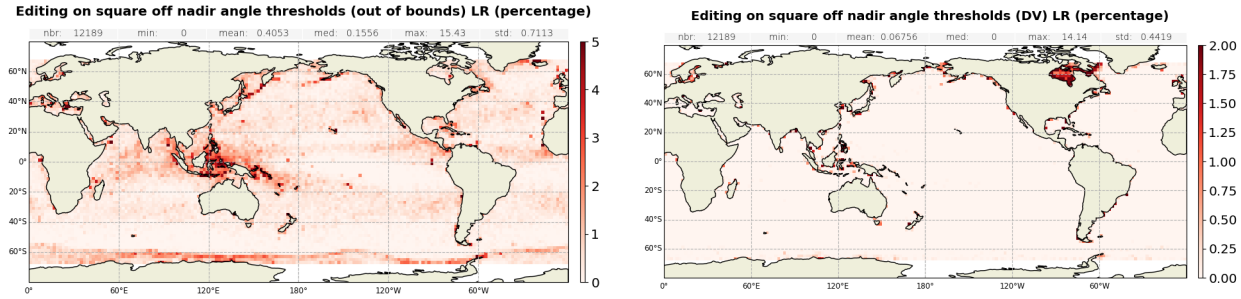


*Figure 33 – Maps of average percentage of data edited on square off nadir angle threshold for LR, for out of bounds (left) and default value (right), computed on cycles 42 to 79.*

### Dry tropospheric correction

On cycle 5, from passes 121 to 126 (01/01/21 00:31:12 to 06:08:28), the dry troposheric correction derived from ECMWF model is set to Default Value. It is due to a missing auxilary file for this period.
Over these 7 tracks, data are therefore entirely edited, as already seen in section 3.2.1..

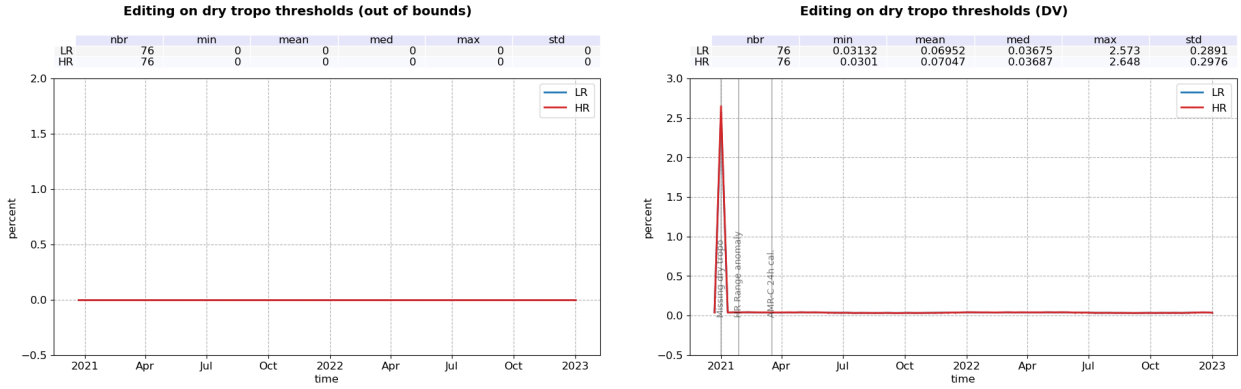


*Figure 34 – Percentage of data edited on dry tropospheric correcition threshold for both LR (blue) and HR (red) per cycle, for out of bounds (left) and default value (right).*

The editing criterion on the dry tropospheric correction has allowed to detect an anomaly in this model processing. As shown on figure 35, the dry tropospheric correction is not defined on the 0-longitude meridian. Investigation has shown that it is also the case for the model wet tropospheric correction and the inverse barometer (not shown). This anomaly might be related to an issue in the interpolation of pressure files. It affects LR and HR products, for all timeliness and since the beginning of the mission.
All data on this line are therefore always edited.

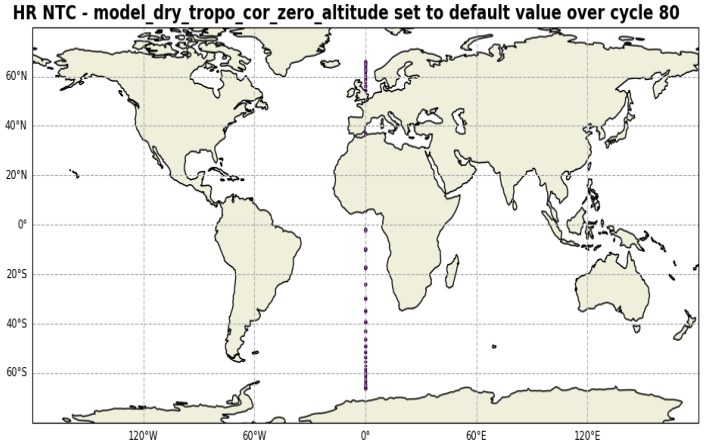


*Figure 35 – Map of model dry tropospheric correction set to default value. Computed for 1 cycle of HR NTC data.*

## Ocean tide equilibrium

A very small fraction of measurements, both in LR and HR, are edited based on the equilibrium ocean tide model being at default value. This impacts less than 0.01% of data in both modes (figure 36).

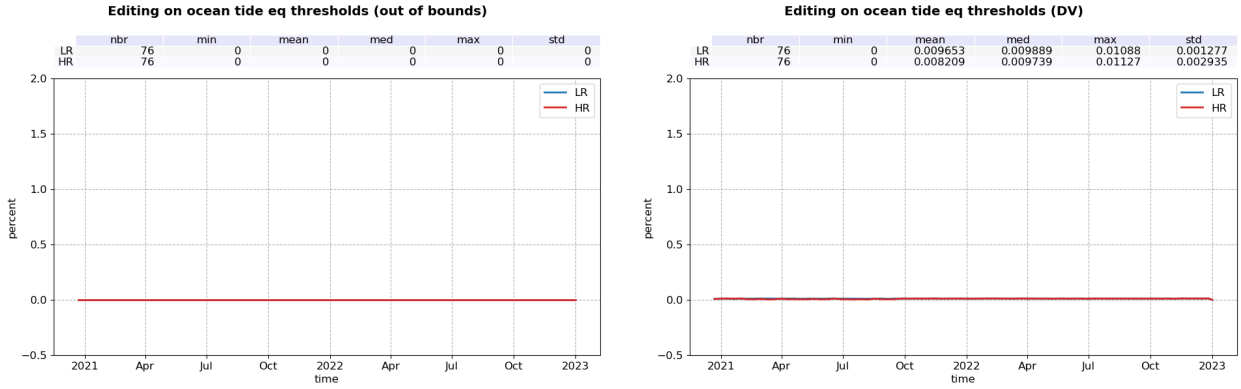


*Figure 36 – Percentage of data edited on equilibrium tide threshold for both LR (blue) and HR (red) per cycle, for out of bounds (left) and default value (right).*

## Ocean tide

The percentage of edited measurements due to ocean tide is about 0.035% for both modes (figure 37). The ocean tide correction is a model output, there should therefore be no edited measurement. Indeed there are no measurements edited in open ocean areas (figure 38). These measurements are exclusively at default values.

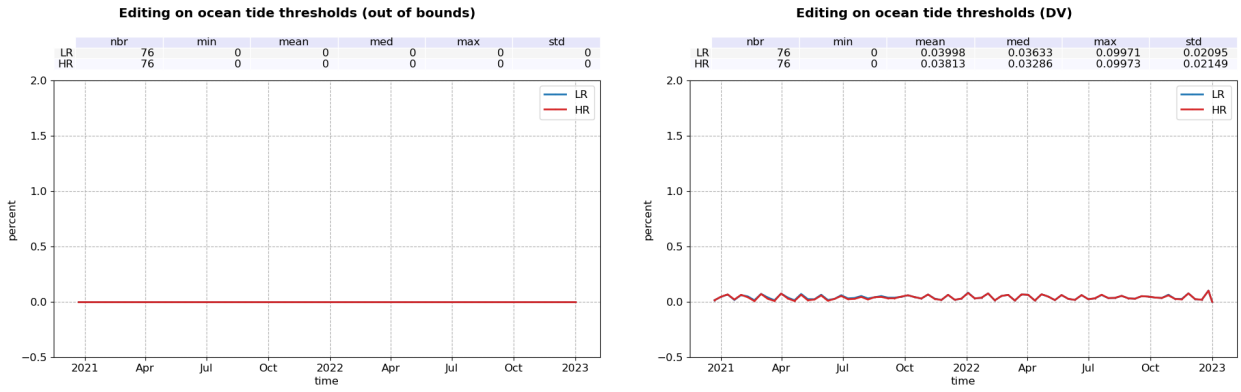


*Figure 37 – Percentage of data edited on ocean tide threshold for both LR (blue) and HR (red) per cycle, for out of bounds (left) and default value (right).*

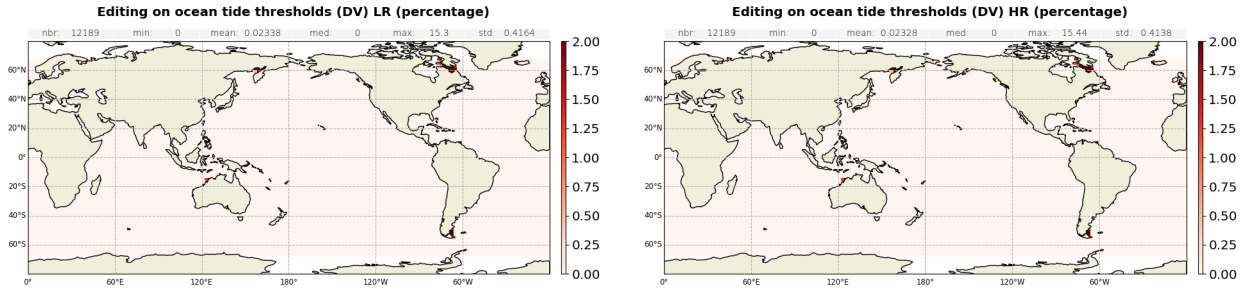


*Figure 38 – Maps of average percentage of data edited on ocean tide threshold for both LR (left) and HR (right), for default value, computed on cycles 42 to 79.*

### Wet tropospheric correction

The percentage of edited measurements due to radiometer wet troposphere correction criterion is represented in figure 39. It is about 0.20% in both modes. As expected, edited data are located in regions of high oceanic variability (see figure 40).

On cycle 13, from pass 20 to 45 (17/03/21 09:36 to 18/03/21 09:38), an AMR-C 24h warm target calibration caused an unavailability of the radiometer derived wet tropospheric correction, resulting in a peak in edited data, also visible in the sea ice flag (section 3.2.2.).

On cycle 74, pass 205 (2022-11-19 11:31:28 to 12:27:42) was originally missing in the LR dataset. The product file was made available a few weeks later, but with missing radiometer wet tropospheric correction, creating a small peak in edited data and signing in the map of figure 40, bottom left panel.

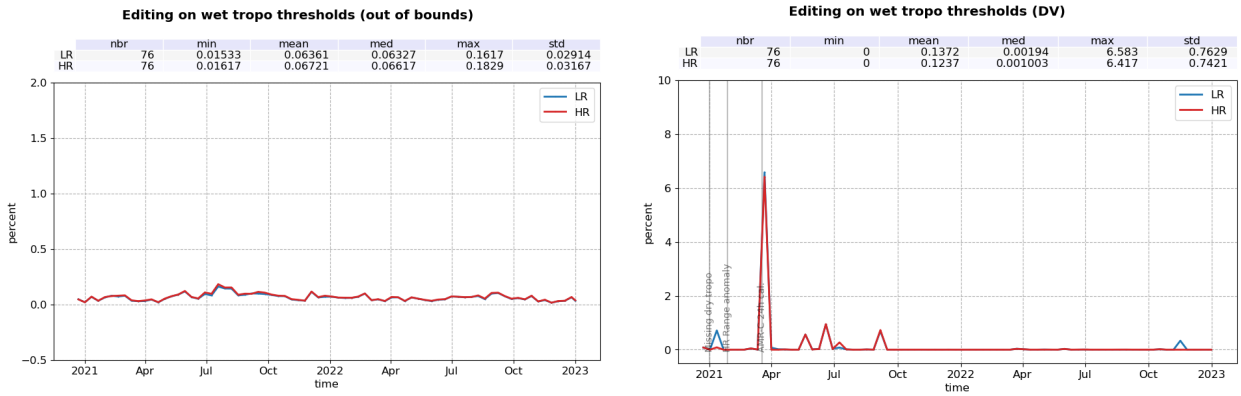


*Figure 39 – Percentage of data edited on wet tropospheric correction threshold for both LR (blue) and HR (red) per cycle, for out of bounds (left) and default value (right).*

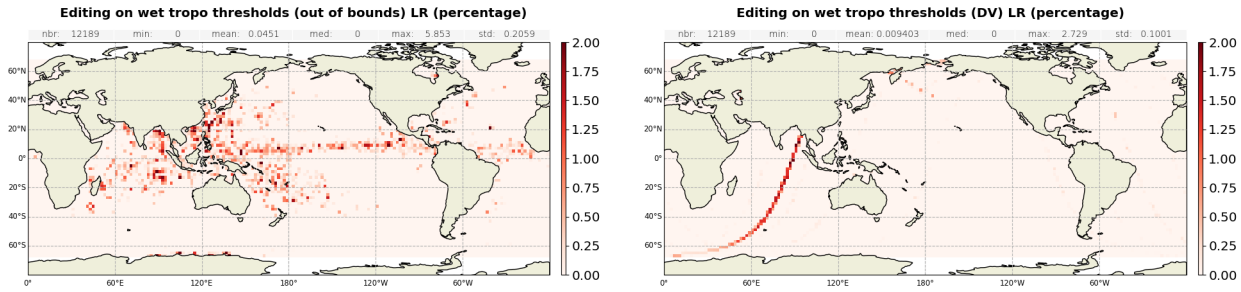


*Figure 40 – Maps of average percentage of data edited on radiometer wet tropospheric correction threshold, for out of bounds (left) and default value (right), computed on cycles 42 to 79.*

## Sea surface height

Uncorrected sea surface height represents the difference between the orbit and the altimeter range in Ku band. Figure 41 summarizes the editing resulting from the sea surface height threshold criterion. It removes in average 2.5% of data for LR and 0.02% of data for HR. In LR, the editing is exclusively due to range measurements at default values near coast, in wet zones, as well as regions with low significant wave heights or over sea ice (figure 42 left panel).

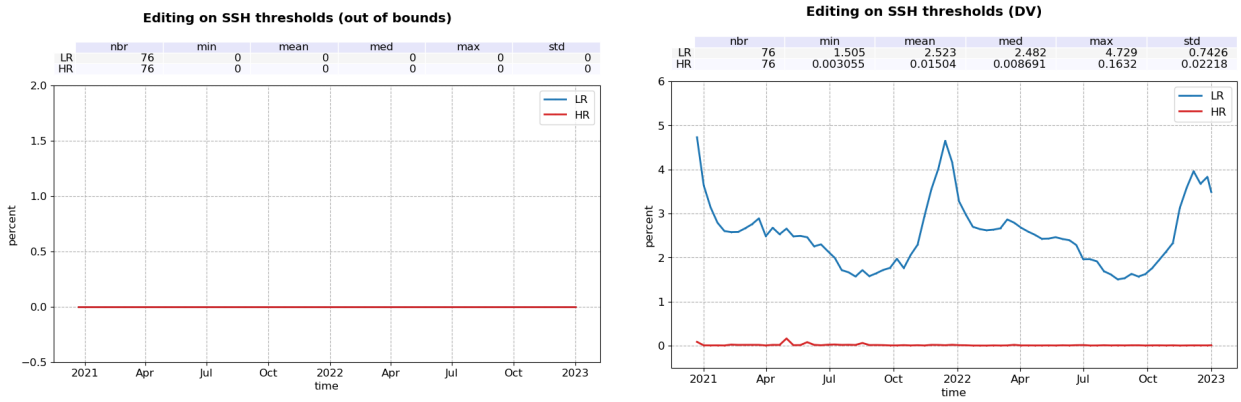


*Figure 41 – Percentage of data edited on SSH threshold for both LR (blue) and HR (red) per cycle, for out of bounds (left) and default value (right).*

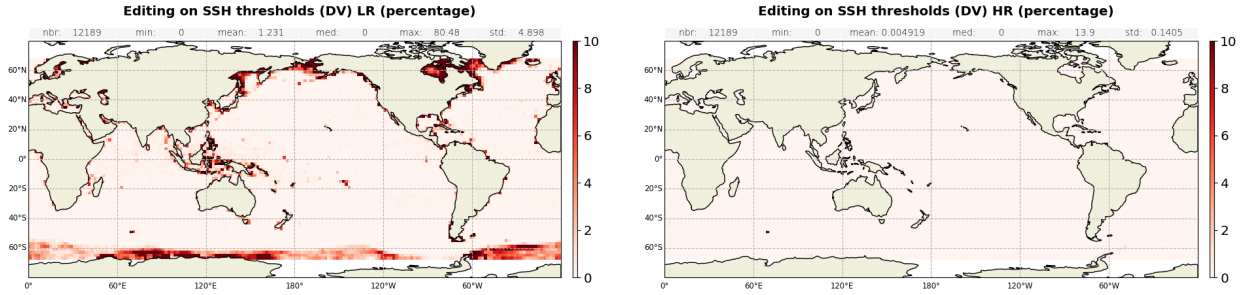


*Figure 42 – Maps of average percentage of data edited on SSH threshold for both LR (left) and HR (right), for default value, computed on cycles 42 to 79.*

### Sea level anomaly

The percentages of edited data by threshold criterion are 3.75% and 3.56% for Sentinel-6 MF for LR and HR SSHA respectively (figure 43).

The peaks already mentionned on the dry and wet tropospheric corrections are visible here. In addition, HR monitoring present a peak end of January 2021: on cycle 8, track 12 to 60 (26-01-2021 21:19 to 28-01-2021 10:14), an anomaly in HR range (-9 m) occured following a POS4 restart. The event was not above Sea Surface Height thresholds. SSHA thresholds are stricter and allows to edited HR data during this event.

When considering the median, less sensitive to these punctual events, the percentage of edited measurements drops to 3.7 and 3.3% for LR and HR respectively.

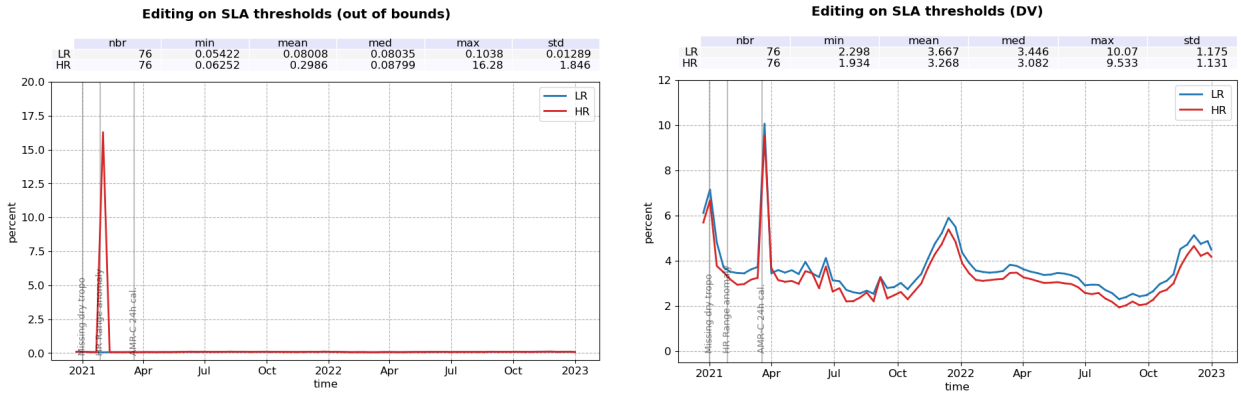


*Figure 43 – Percentage of data edited on SLA threshold for both LR (blue) and HR (red) per cycle, for out of bounds (left) and default value (right).*

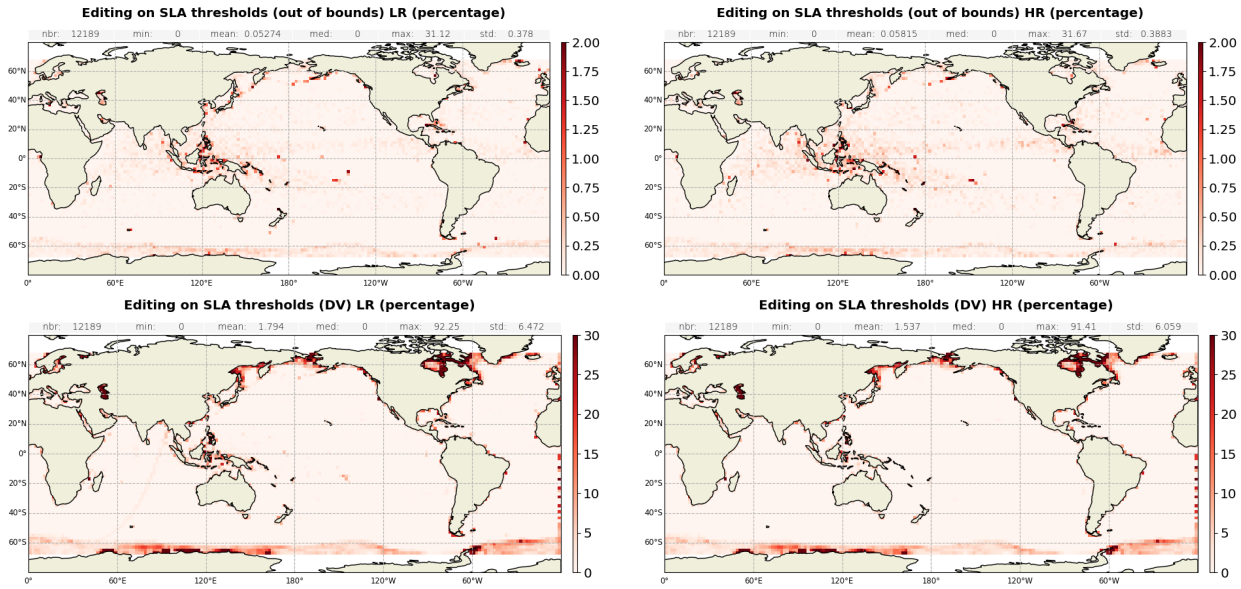


*Figure 44 – Maps of average percentage of data edited on SLA threshold for both LR (left) and HR (right), for out of bounds (top) and default value (bottom), computed on cycles 42 to 79.*

### 3.2.4. Along-track SSHA consistency

Once the thresholds editing is applied, the consistency of the along-track sea surface height anomaly is checked. The statistics of the SSHA by pass are computed (mean and standard deviation), with a selection over open ocean and in areas with low oceanic variability. A set of thresholds are set as editing criteria. The details are listed in table 6.

| Parameters | Set 1 | Set 2 |
|---|---|---|
| **Selection** | | |
| Bathymetry | <-1000m | <-1000m |
| Coastal distance | >100km | >100km |
| Oceanic variability | <0.3m | <0.1m |
| Min number of measurements | 3 | 200 |
| **Thresholds** | | |
| Mean (absolute value) | 0.3m | 0.15m |
| STD | 0.4m | 0.2m |

*Table 6 – Table of parameters used for the editing on the SSHA pass statistics. These parameters are identical in HR and LR.*

The percentage of edited points based on SSHA pass statistic is presented in figure 45. There is only one occurence on cycle 20 for LR : two consecutive passes (182 and 183) are edited, from 01-06-2021 03:18:11 to 05:10:35. In HR, the SSHA is set to default value for the two passes 182 and 183 and therefore do not appear in this diagnostic. No matching events have been found at these dates.

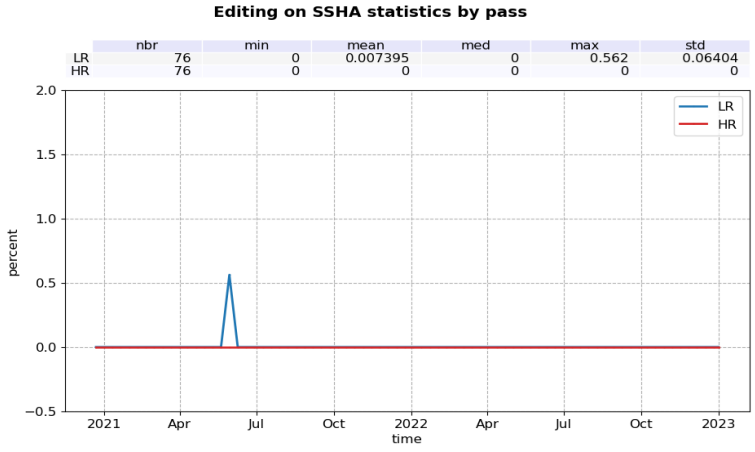


*Figure 45 – Percentage of edited data for both LR (blue) and HR (red) on pass SSHA statistics per cycle.*

# 4 Monitoring of altimeter and radiometer parameters

Means and standard deviations of Sentinel-6 MF main parameters have both been monitored since the beginning of the mission. Moreover, a comparison with Jason-3 parameters has been performed: it allows to monitor the bias between the parameters of the 2 missions.

- Till 2022-04-07, Sentinel-6 MF and Jason-3 are on the same ground track with only 30 seconds between the two satellites (tandem phase), the mean of the Sentinel-6 MF - Jason-3 differences can be computed using a point by point repeat track analysis (refered as 'residuals' in plots).
- From 2022-04-07 (Sentinel-6 MF cycle 52), a maneuver sequence was conducted to move Jason-3 to the new formation flight mission orbit. Jason-3 has a repeat ground-track which is interleaved with Sentinel-6 MF. It is the same ground-track as already used by Topex/Poseidon, Jason-1 and Jason-2. Because of a time shift of 5 days, geographical variations are then too strong to directly compare Sentinel-6 MF and Jason-3 parameters on a point by point basis. Therefore day per day global monitorings are performed and compared between the missions.

The goal of this chapter is to summarize these monitorings.
A detailed analysis of the tandem phase is available in the F06 Cal/Val reprocessing report [3]. Only the main results are included in this chapter.

## 4.1. 20 Hz range measurements

The monitoring of the number and standard deviation of 20 Hz elementary range measurements used to derive 1 Hz data is presented here. These two parameters are computed during the altimeter ground processing. Before performing a regression to derive the 1 Hz range from 20 Hz data, a MQE (mean quadratic error) criterion is used to select valid 20 Hz measurements. This first step of selection consists in verifying that the 20 Hz waveforms can be approximated by a Brown echo model (Brown, 1977 [7]) (Thibaut et al. 2002 [8]).
Then, through an iterative regression process, elementary ranges too far from the regression line are discarded until convergence is reached. Thus, monitoring the number of 20 Hz range measurements and the standard deviation computed among them is likely to reveal changes at instrumental level.

### 4.1.1. 20 Hz range measurements number

Figure 46 presents the average number of 20 Hz elementary range measurements used to derive 1 Hz ranges in Ku and C-band. In Ku-band, more elementary measurements are used in average in LR mode (19.6) than in HR (18.5), with LR C-band in between (19.1).
These values are stable over time and are in line with Jason-3 for LR data.

A slight latitude dependancy can be seen in Ku-band for LR and HR data (figure 47), with lower values at high latitude. This is linked to a specific feature of Sentinel-6 MF, which has a latitude dependant PRF value. The behavior is different on Jason-3, more dependent of sea state conditions. For the C band, values are lower near the coast and at high latitudes. This is expected as C band has a larger footprint than Ku band, and is more sensitive to coastline and ice presence.

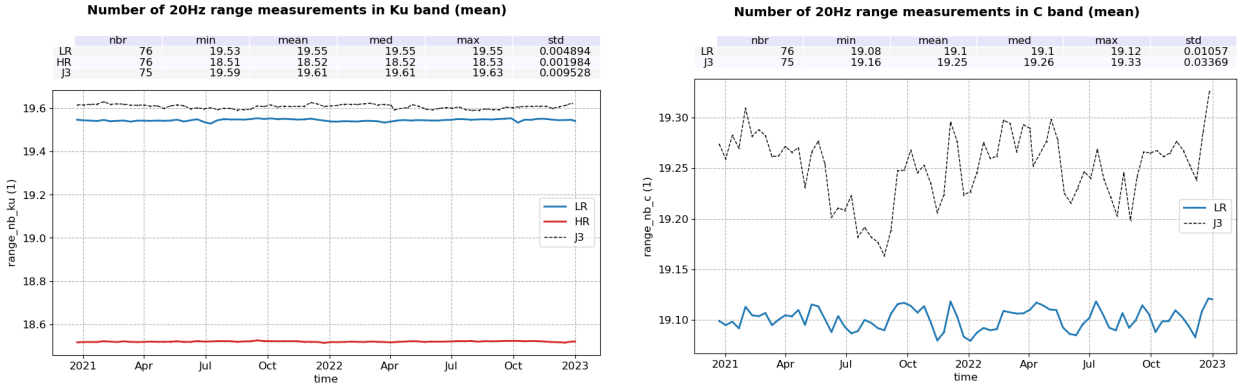


*Figure 46 – Mean number of 20Hz range measurements for LR (blue) and HR (red) per cycle, in Ku-band (left) and C-band (right).*

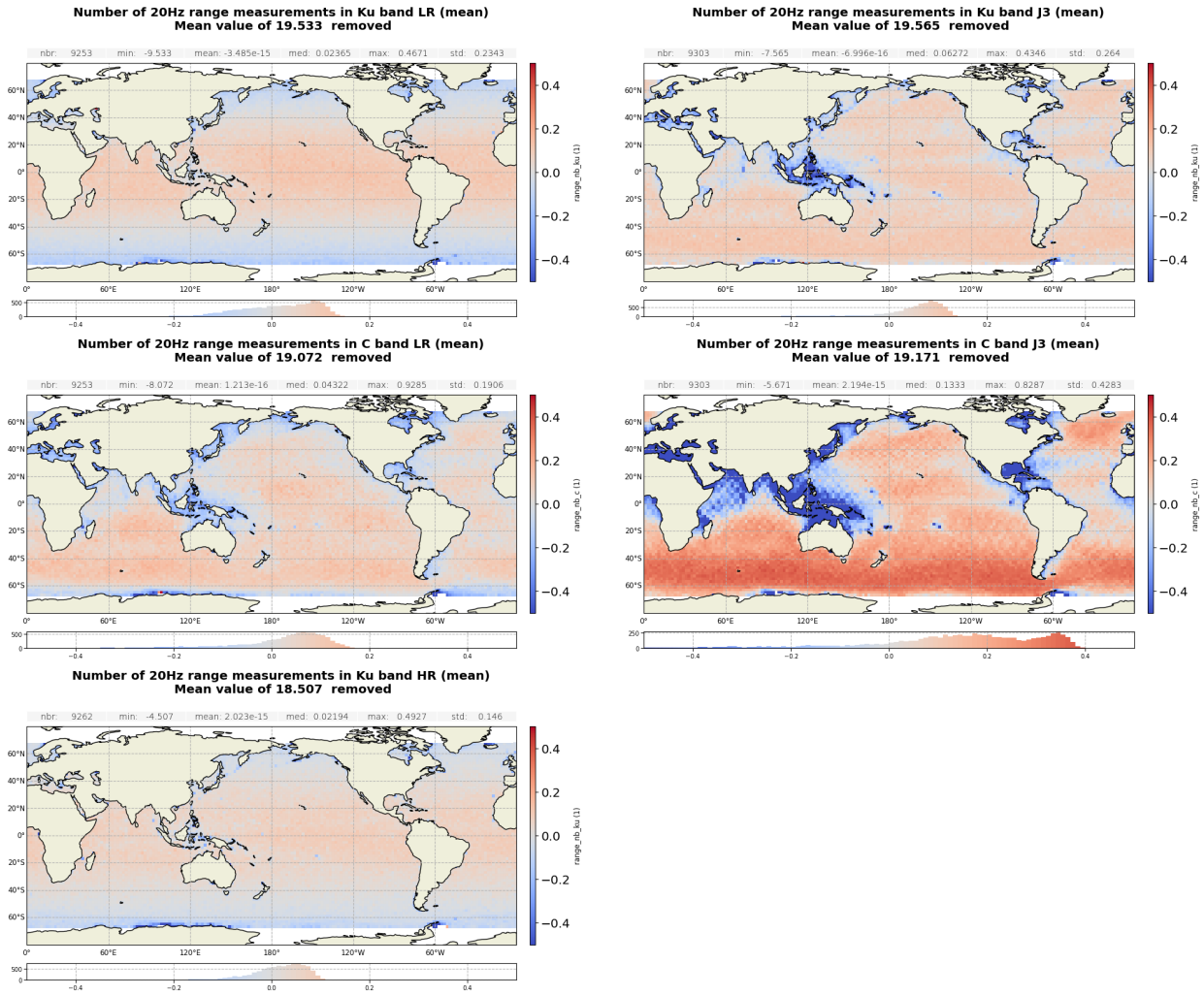


*Figure 47 – Centred maps of mean number of 20Hz range measurements for Sentinel-6 MF (left) and Jason-3 (right). Top: maps in LR Ku-band, middle: maps for LR C-band, bottom : map for Sentinel-6 MF HR Ku-band. Computed on Sentinel-6 MF cycles 42 to 79.*

### 4.1.2. 20 Hz range measurements standard deviation

Figure 48 presents the standard deviation of the 20 Hz elementary range measurements used to derive 1Hz ranges in Ku and C-band (left and right panels respectively) per cycle. In Ku-band, Sentinel-6 MF LR range standard deviation is lower than Jason-3 by 1 cm in average. It shows the improvement brought by Sentinel-6 MF in terms of noise.
Sentinel-6 MF HR range noise is even lower than LR, by 2.7 cm, thanks to the HR processing.

Due to the reduced number of pulses, C-band range standard deviation is the highest (0.26 m).

Standard deviation of measurements is correlated to significant wave height (figure 49), as shown in sections 8.1.2. and 8.1.3..

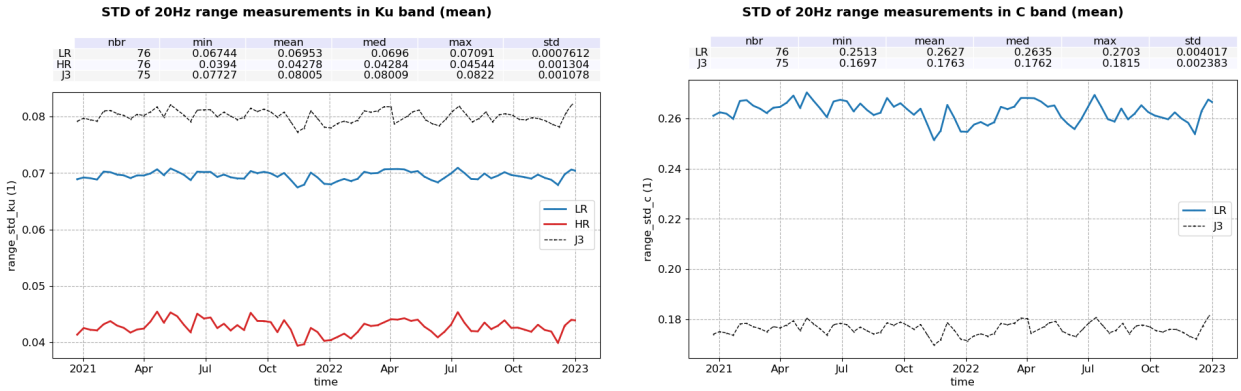


*Figure 48 – Mean STD of 20Hz range measurements for LR (blue) and HR (red) per cycle, in Ku-band (left) and C-band (right).*

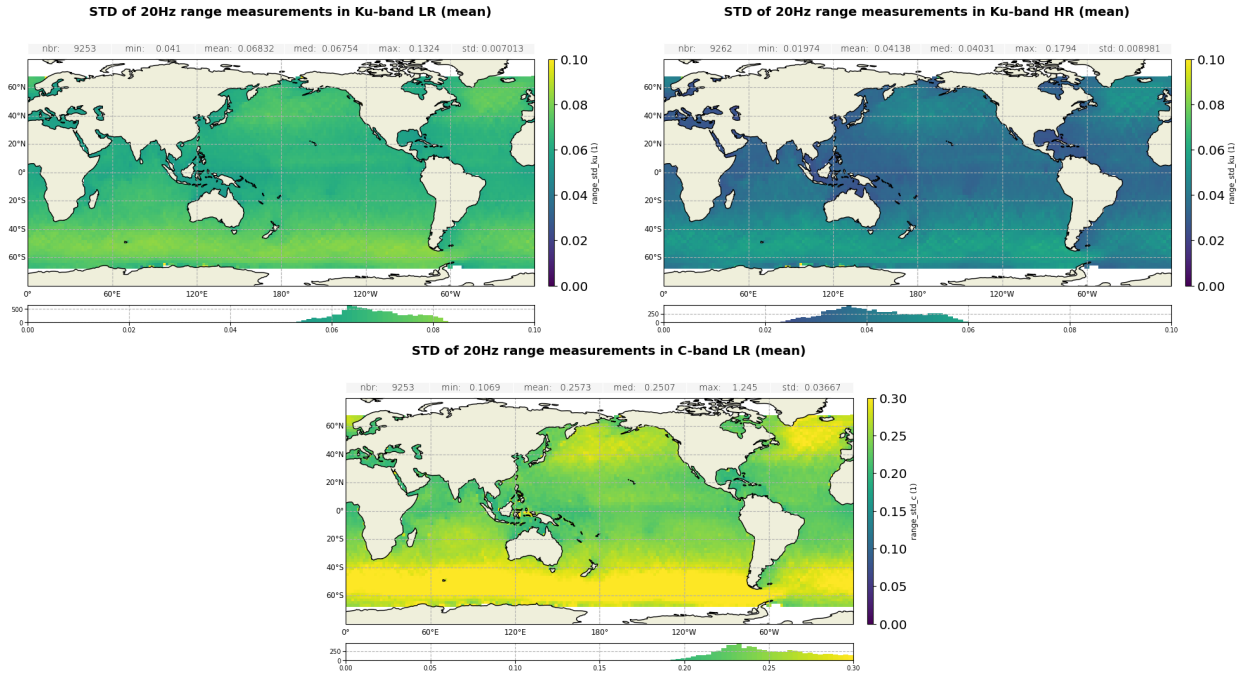


*Figure 49 – Maps of mean STD of 20Hz range measurements for Ku-band LR (top left) and HR (top right) and C-band (bottom). Computed on cycles 42 to 79.*

## 4.2. Off nadir angle from waveform

In this section is analysed the square of the off-nadir angle derived from the MLE4 waveform retracking from LR dataset.

The off-nadir angle is derived from the slope of the trailing edge of the waveform during the altimeter processing: it can either be caused by real platform mispointing or by backscattering properties of the surface. The square of the off-nadir angle, averaged on a cyclic and daily basis (taking into account valid measurements only), has been plotted for Sentinel-6 MF and Jason-3 on figure 50. A jump is visible in both mean and standard deviation on 18/01/2021, which is related to a star-tracker update that resulted in improved pointing performance of the satellite. Spikes are visible in an otherwise stable timeseries, that correspond to manoeuvers during the commissionning phase.

The corresponding map for 2022, presented on figure 51, shows higher square off nadir angle in coastal areas and around Indonesia. Figure 52 shows the dependancy between the waveform mispointing and the SWH. Mispointing is higher at low SWH (up to 0.02 square degrees at 0m). Between 2 and 8m SWH, the slope is about 0.0003 $deg^2$/m.
The standard deviation of the square off nadir angle is also much higher at low SWH.
Curves for year 2022 only (solid lines) are aligned with curves for the entire timeseries (dotted lines).

The mispointing distribution is presented in Figure 53 for Sentinel-6 MF and Jason-3. Sentinal-6A distribution is centred around 0.012 square degrees, while Jason-3's is centered on 0. Curves for year 2022 only (solid lines) are perfectly aligned with curves for the entire timeseries (dotted lines).
Note that with the processing baseline F08, deployed in March 2023, the antenna aperture angle has been updated from 1.33° to 1.34°. It leads to a better approximation of the mispointing, which mean value is reduced to 0.008 $deg^2$.

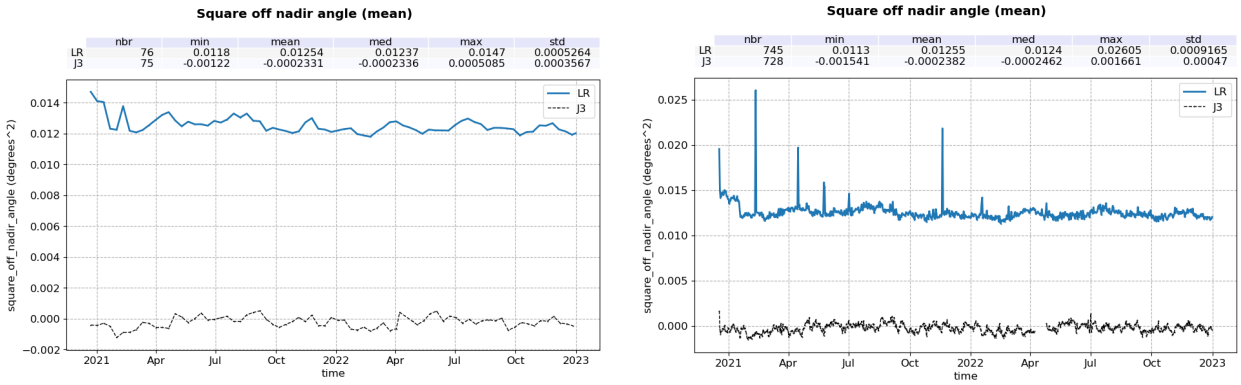


*Figure 50 – Mean square off nadir angle per cycle (left) and day (right).*

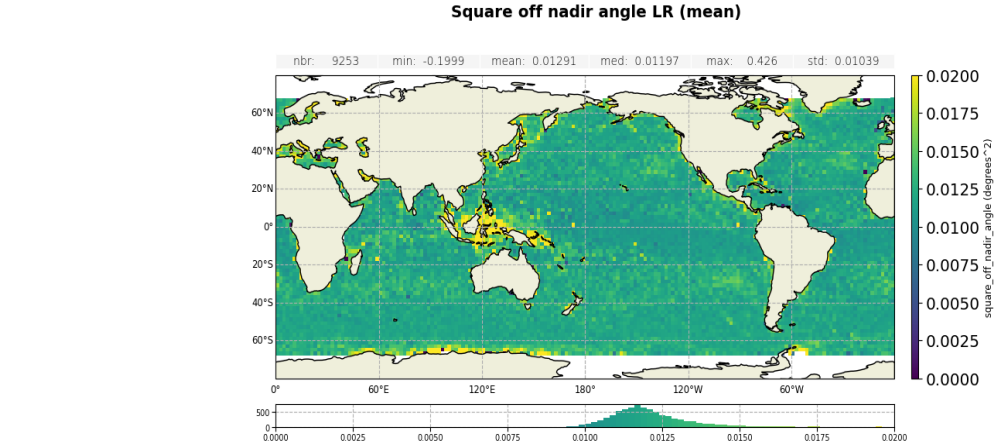


*Figure 51 – Map of mean square off nadir angle. Computed on cycles 42 to 79.*

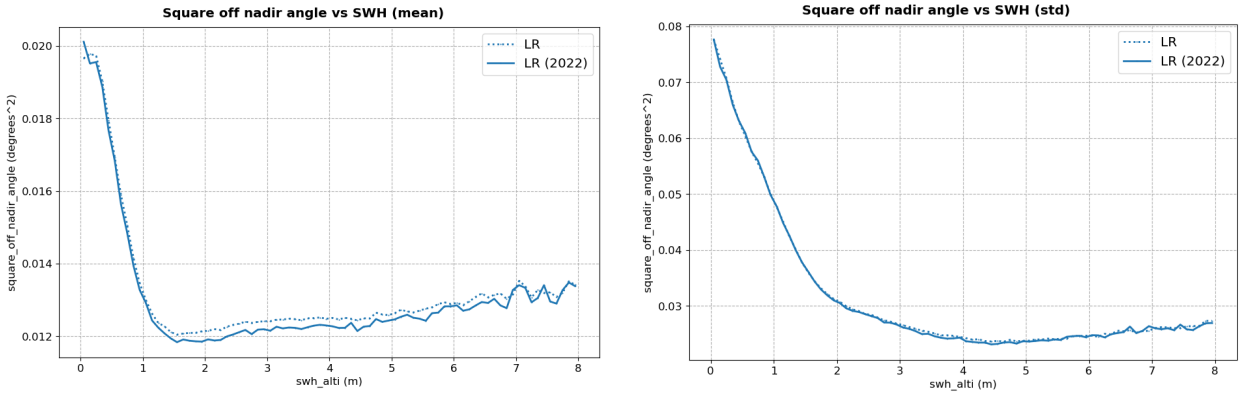


*Figure 52 – Square off nadir angle wrt SWH. Computed on the entire timeseries (dotted line) and on 2022 only (solid line).*

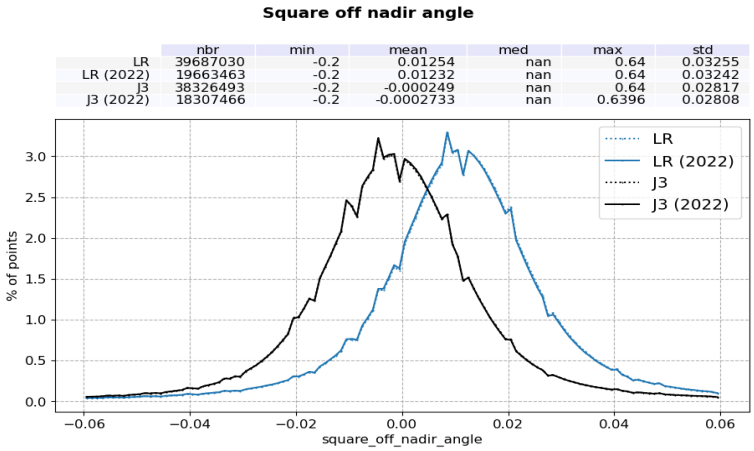


*Figure 53 – Histogram of square off nadir angle for Sentinel-6 MF (blue) and Jason-3 (black). Computed on the entire timeseries (dotted line) and on 2022 only (solid line).*

## 4.3. Range

The mean difference between Sentinel-6 MF HR and LR range is centred around 1.9 cm (figure 54). Looking at the temporal evolution of this difference (figure 55), a slight negative drift is visible. This drift between LR and HR range is most likely caused by the degradation of the PTR shape in the azimuth di-

rection, impacting HR data. The drift resulting from this degradation has been estimated at 3.1 mm/year on POS4-B (Dinardo, 2022 [9]). Please note that this analysis was performed on the 9 months of side B, from September 2021 to June 2022, and values may be different for the second half of 2022 because of an expected on-going stabilization.
The implementation of the range walk correction in the HR processing will correct from the range walk effects and reduce the drift. It is planned for the future processing baseline F09.

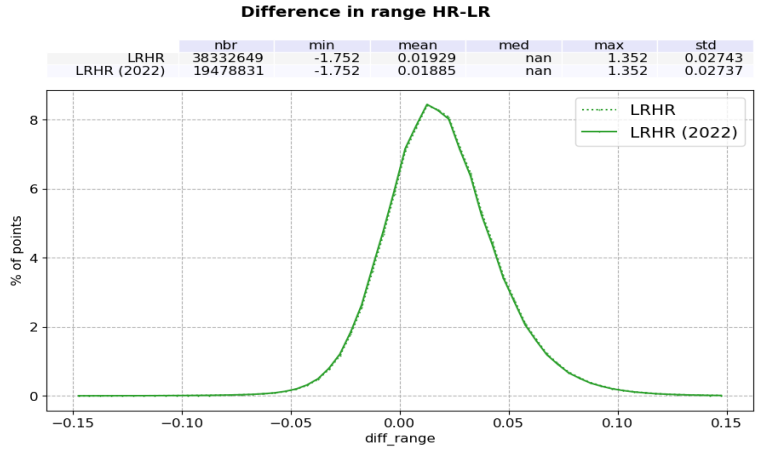


*Figure 54 – Histogram of HR-LR difference in range. Computed on the entire timeseries (dotted line) and on 2022 only (solid line).*

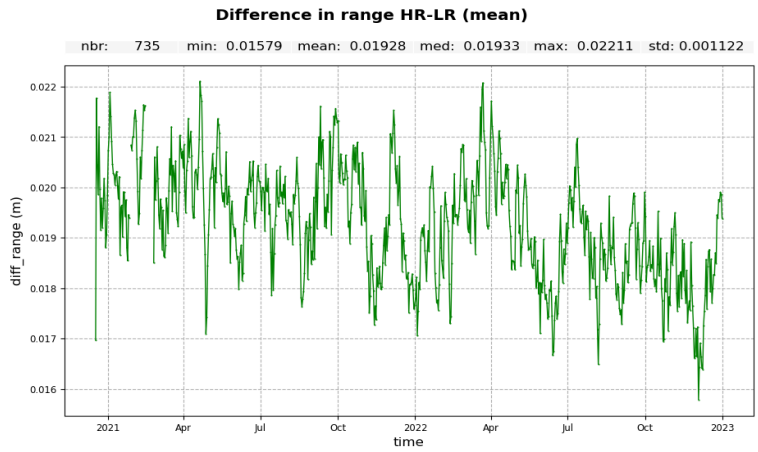


*Figure 55 – HR-LR difference in range per day.*

Maps of the range difference between HR and LR (figure 56 top panel) shows a strong correlation to SWH. The range bias increases by 3.8 cm between 2 and 7-m wave. Such comparison highlights the impact of the different value of wave skewness coefficient used in the LR MLE4 retracking (skewness -0.1) and in the HR SAMOSA retracking side (skewness 0.0)

Along track wind has a known impact on HR data and more particularly on HR range [5]. To highlight this impact, two gridded maps of HR versus LR range difference are drawn, one for ascending tracks and the other one for descending tracks. Next, the difference between these two maps is computed (ascending minus descending). Such process allows to remove all systematic error on the bias (such as waves) and to only highlight HR variations with respect to LR that depend on track orientation. Figure 56 bottom panel clearly shows the wind patterns, ranging between -1 and 1 cm.

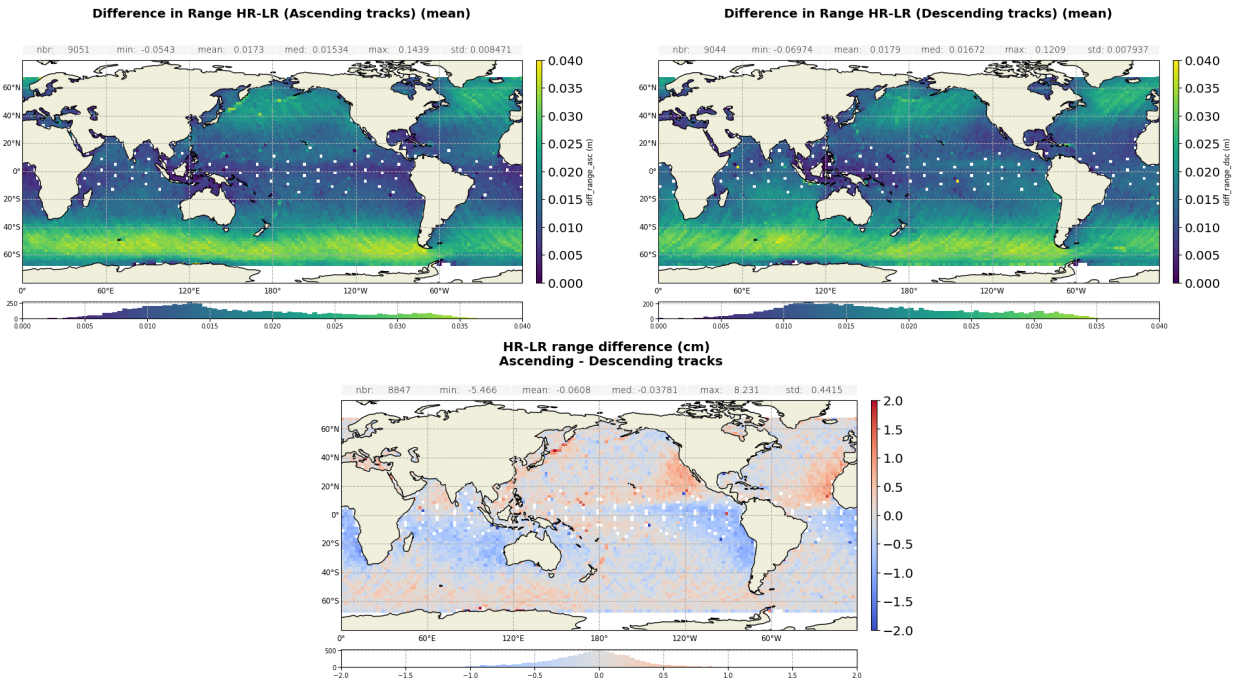


*Figure 56 – Maps of HR-LR difference in range, for ascending tracks (top left) and descending tracks (top right). Bottom: difference of the two maps above*

Over the tandem phase, direct comparisons of Sentinel-6 MF and Jason-3 retrievals have been performed. Looking at Ku-band range difference between the two missions, an average bias of 0.76 cm is found, with a clear correlation to SWH (figure 57 left panel). Studies have shown that part of this correlation will be corrected thanks to the future numerical retracking in LR (Processing Baseline F08). It will most likely remain the pulse to pulse correlation effect, also correlated to waves and not taken into account in the processing yet.
In addition, an equatorial band of 5 mm amplitude is also visible on the map. Investigations have shown that this behavior is most likely coming from Jason-3. The root cause is still to be identified.

In C-band, the range differences are of the same order (0.97 cm) but with a larger noise in C-band due to the reduced number of pulses. The map of this difference (figure 57 right panel) shows at first order a correlation to the total electron content of the atmosphere, which origin still need to be understood. These differences might also be correlated to the sea state bias.

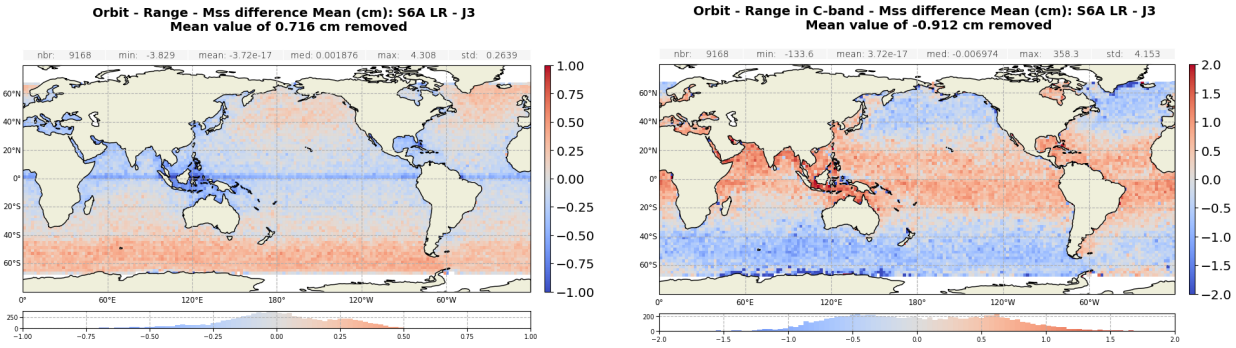


*Figure 57 – Orbit - Range - MSS difference: Sentinel-6 MF LR minus Jason-3 computed over the complete tandem period. Gridded map for Ku-band (left panel) and C-band (right panel).*

In HR, over the tandem period, the skewness difference between Sentinel-6 MF HR and Jason-3 processings induces a strong correlation to sea state conditions, as shown on figure 58.

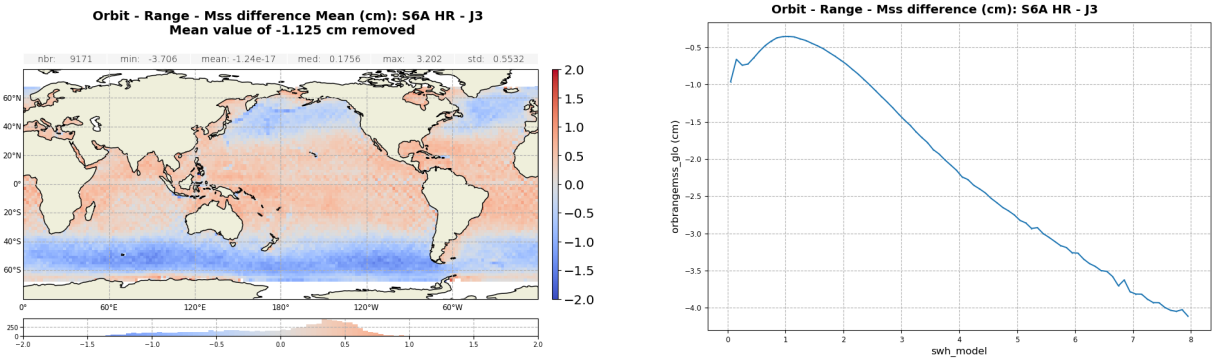


*Figure 58 – Orbit - Ku-band Range - MSS difference: Sentinel-6 MF HR minus Jason-3 computed over the complete tandem period. Gridded map (left panel) and difference function of ERA5 SWH (right panel).*

## 4.4. Significant wave height

The geographical distribution of SWH over 2022 is presented on figure 59 for Ku-band LR and HR and for

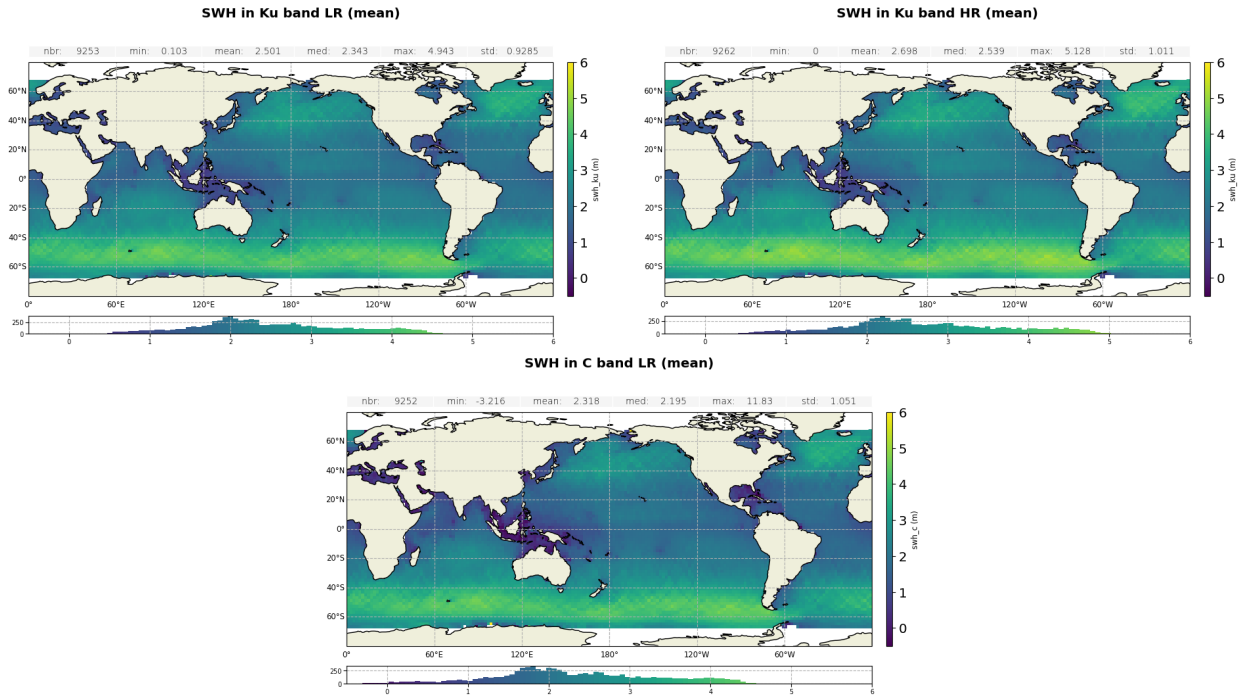


*Figure 59 – Maps of mean SWH for Ku band LR (top left), HR (top right) and C band (bottom). Computed on cycles 42 to 79.*

C-band LR. All SWH average over 2022 share similar geographical patterns.

Ku-band SWH are centred around 2.69 m for Sentinel-6 MF LR and 2.89 m for Sentinel-6 MF HR. In C-band, the average SWH is of 2.52m for Sentinel-6 MF and 2.70m for Jason-3. This values are stable along time, as shown on figure 60.

Sentinel-6 MF LR SWH is in line with Jason-3, also centred around 2.69 m. The spike visible in the monitoring in April 2022 is due to missing measurements in Jason-3 during its move to the interleaved orbit (see section 2.1.). Sentinel-6 MF and Jason-3 SWH histograms are aligned, except at very low wave heights, where Sentinel-6 MF performs better, due to its improved handling of low wave heights in the Level 2 processing.

Precise bias between Sentinel-6 MF LR and Jason-3 SWH have been estimated during the tandem phase. The Ku-band SWH bias between Sentinel-6 MF LR and Jason-3 is centred around -1.29 cm (figure 61 left panel). The map of SWH difference (figure 61 right panel) mainly shows a good consistency between the two missions, except in small waves areas where the bias is higher. The root cause of this higher bias is the improved handling of low wave heights in Sentinel-6 MF Level 2 processing: Sentinel-6 MF processing allows negative SWH values while it is not the case for Jason-3. It can lead to differences up to -9 cm for very low SWH (below 0.5 m). For SWH $>$ 1 m, Sentinel-6 MF LR and Jason-3 SWH are in line, with differences within 2 cm in absolute value.

Sentinel-6 MF HR SWH is not in line with Sentinel-6 MF LR and Jason-3 due to the impact of ocean vertical velocity on HR data [11]. Note that this impact has been reduced thanks to PB F06 (see section 2.4. for more details about the PB update). The average HR-LR SWH difference (bottom panel) is centred around 23.2cm (figure 62 left panel). This bias is stable over time but strongly depends on SWH values (figure 62 right panel). It ranges from 9 to 42 cm between 1 and 7m SWH.

As expected, comparison between Sentinel-6 MF HR and Jason-3 SWH over the tandem phase higlights

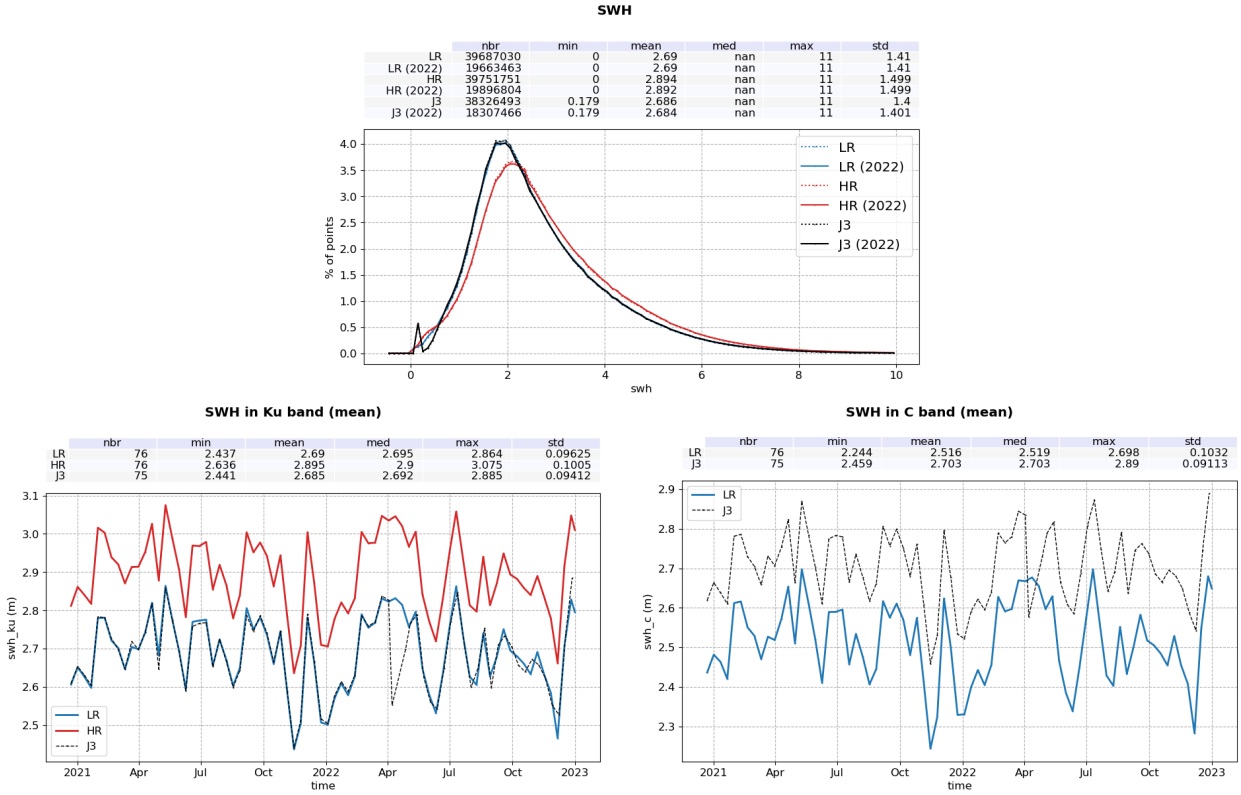


*Figure 60 – Top : Histogram of Ku-band SWH for Sentinel-6 MF LR (blue), Sentinel-6 MF HR (red) and Jason-3 (black), Computed on the entire timeseries (dotted line) and on 2022 only (solid line). Bottom: Cyclic monitoring of SWH mean in Ku-band (left) and C-band (right).*

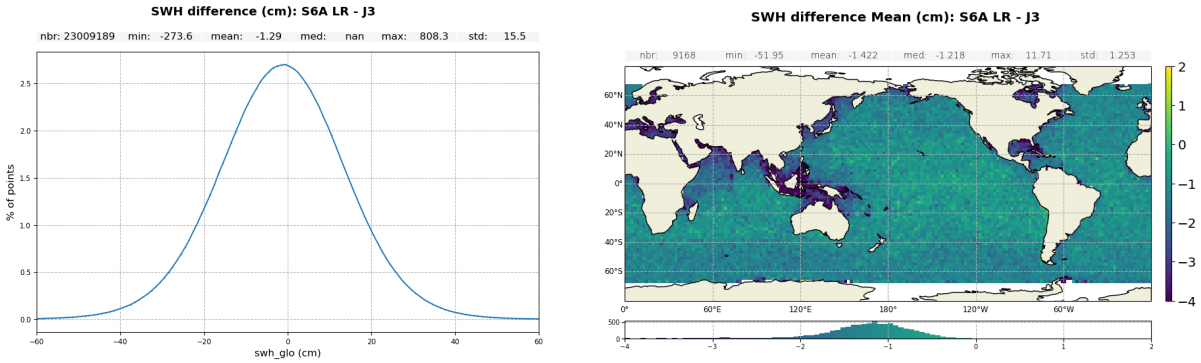


*Figure 61 – Ku-band SWH difference: Sentinel-6 MF LR minus Jason-3 computed over the complete tandem period. Left: Histogram, Right: Map.*

again the effect of ocean vertical velocity. The bias is centred around 22.1 cm, with correlation to SWH. The bias is of 18 cm at 2m-wave and reaches 40 cm at 6m-wave (figure 63 right panel)

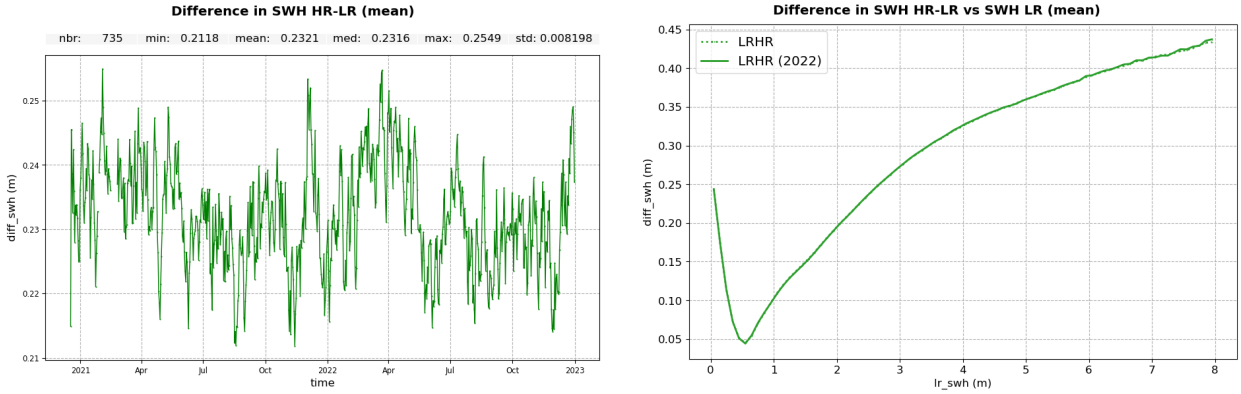


*Figure 62 – HR-LR difference for Ku-band SWH. Left: mean per day. Right: difference with respect to LR SWH, computed on the entire timeseries (dotted line) and on 2022 only (solid line).*

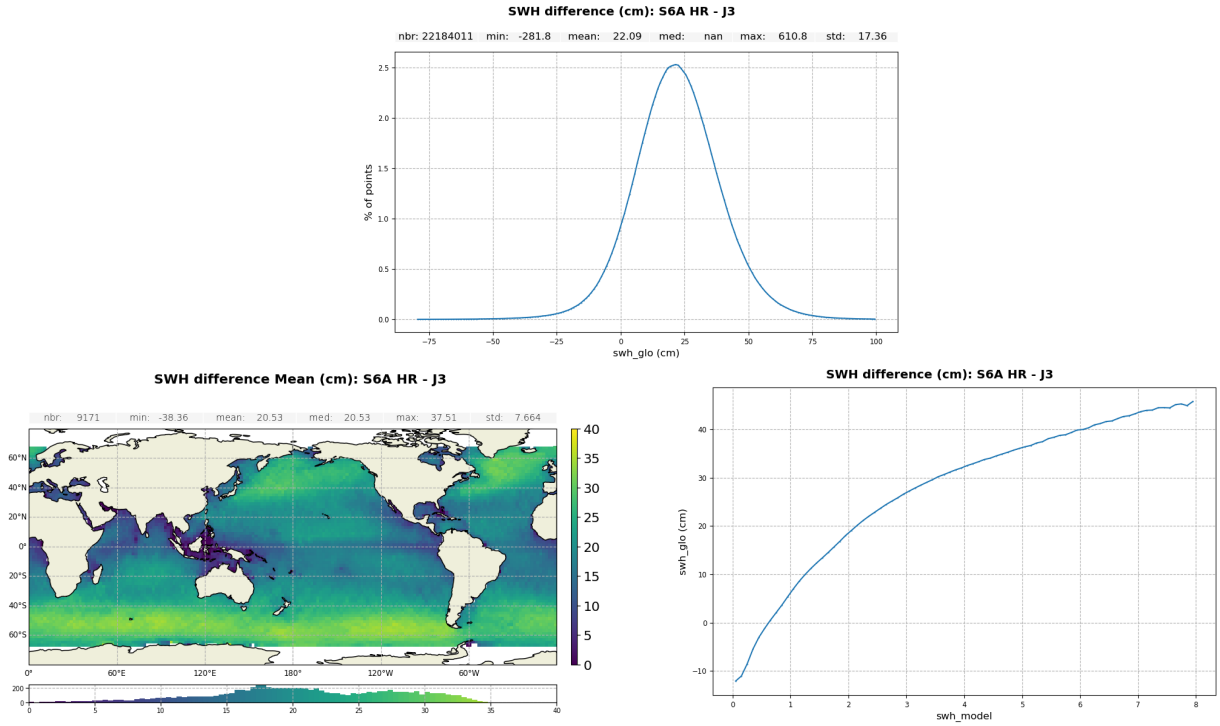


*Figure 63 – Ku-band SWH difference: Sentinel-6 MF HR minus Jason-3 computed over the complete tandem period. Histogram (top), gridded map (bottom left) and difference function of ERA5 SWH (bottom right).*

## 4.5. Backscatter coefficient

The monitoring of the backscatter coefficient (sigma0) per cycle is presented on figure 64 along with the corresponding distribution (for Sentinel-6 MF Ku-band side B only and Jason-3 on the same time period). Ku-band Sentinel-6 MF LR sigma0 is centred around 12.4dB, Sentinel-6 MF HR around 18.1dB and Jason-3 around 13.6dB.
No jump or drift is visible in the data.

In C-band, Sentinel-6 MF sigma0 is centred around 12.4dB and Jason-3's around 13.7dB, due to processing differences. No jump or drift is visible in the data.

The geographical distributions of the Ku band HR, Ku band LR and C band sigma0 are presented on figure 65. No significant difference in geographical patterns is visible.

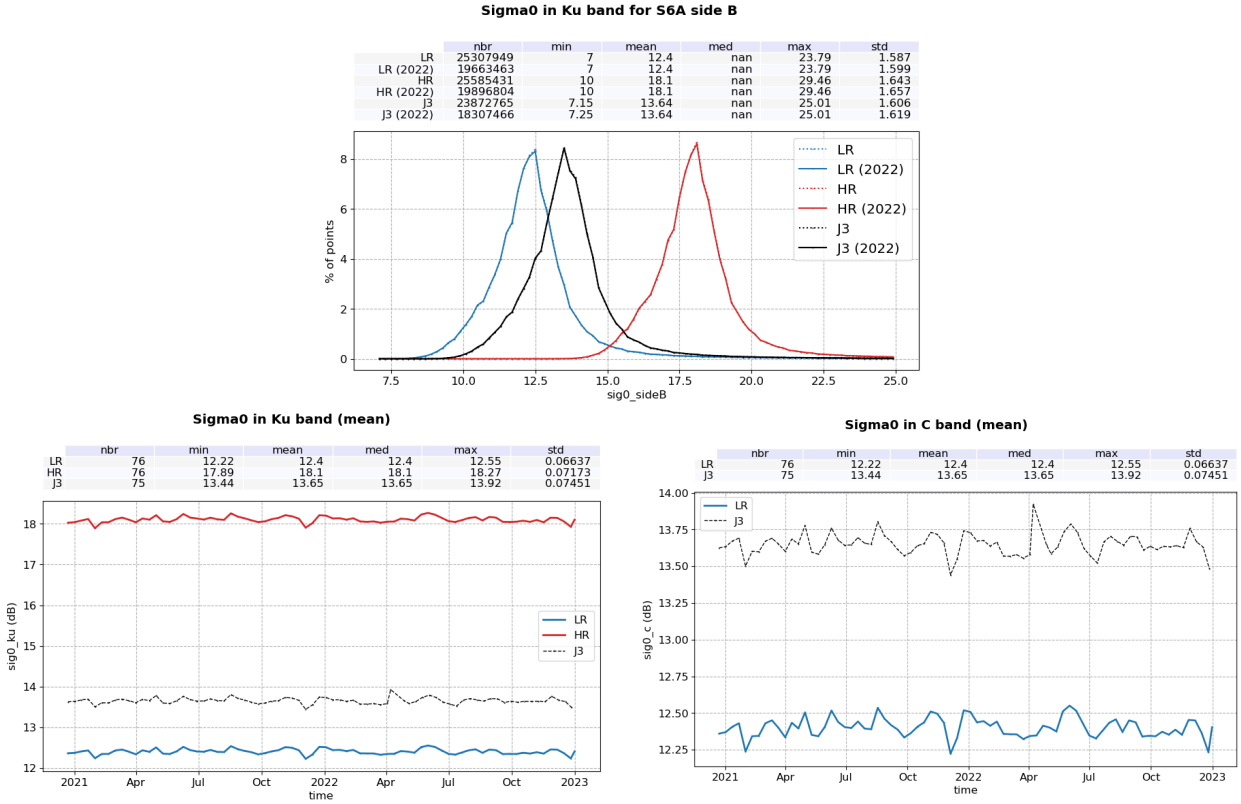


*Figure 64 – Top : Histogram of Ku-band Sigma0 for Sentinel-6 MF LR (blue), Sentinel-6 MF HR (red) and Jason-3 (black), computed on POS4-B entire time period (dotted line) and on 2022 only (solid line). Bottom: Cyclic monitoring of Sigma0 mean in Ku-band (left) and C-band (right).*

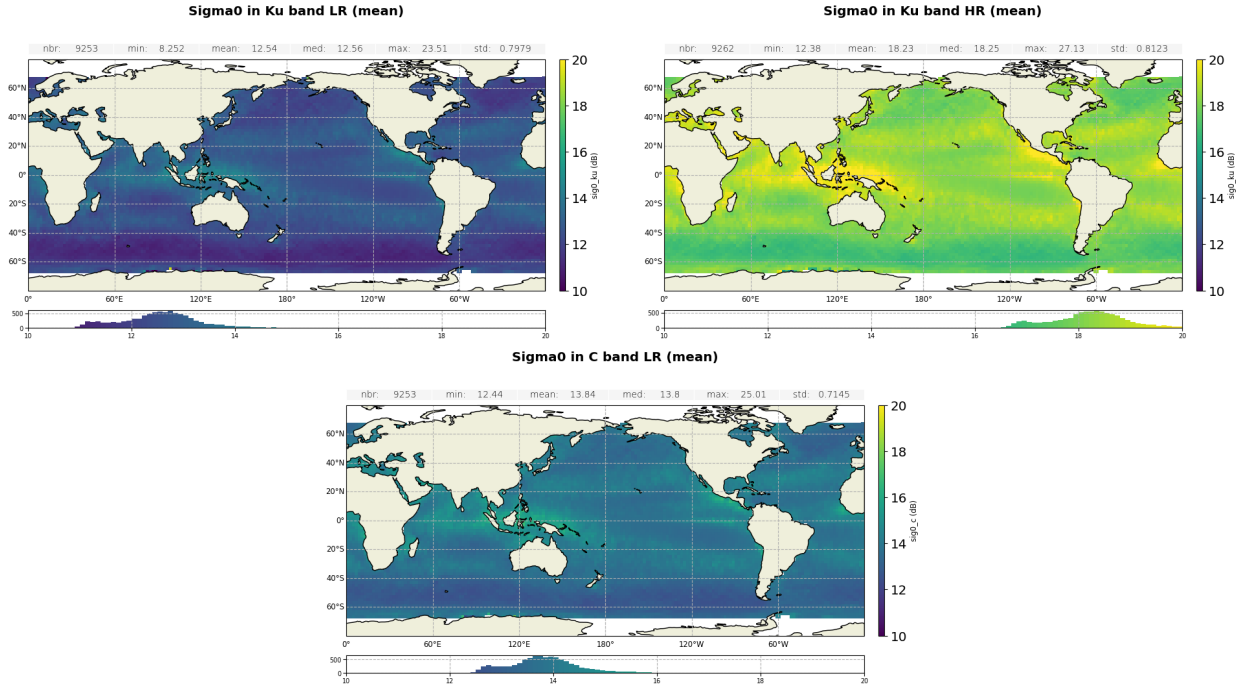


*Figure 65 – Maps of mean sigma0 for Ku band LR (top left), HR (top right) and C band (bottom). Computed on cycles 42 to 79.*

Figure 66, left panel, presents the HR-LR sigma0 difference, which is centred around 5.64dB. At the very beginning of the time serie, before a jump during cycle 7, the HR-LR difference is about 0.02dB lower. This change can be traced back to a star-track patch on 18/01/2021 that improved the nadir satellite pointing. This impacted HR and LR sigma0 differently as in HR, SAMOSA retracking does not estimate the mispointing from the waveform, as opposed to LR with MLE4 retracking (figure 67).

As shown on figure 66 (right panel), the HR-LR sigma0 difference is slightly correlated with LR SWH, from about 5.6dB at 1m SWH to 5.69dB at 8m SWH.
The curve for year 2022 only (solid lines) is aligned with the curve for the entire timeseries (dotted lines).

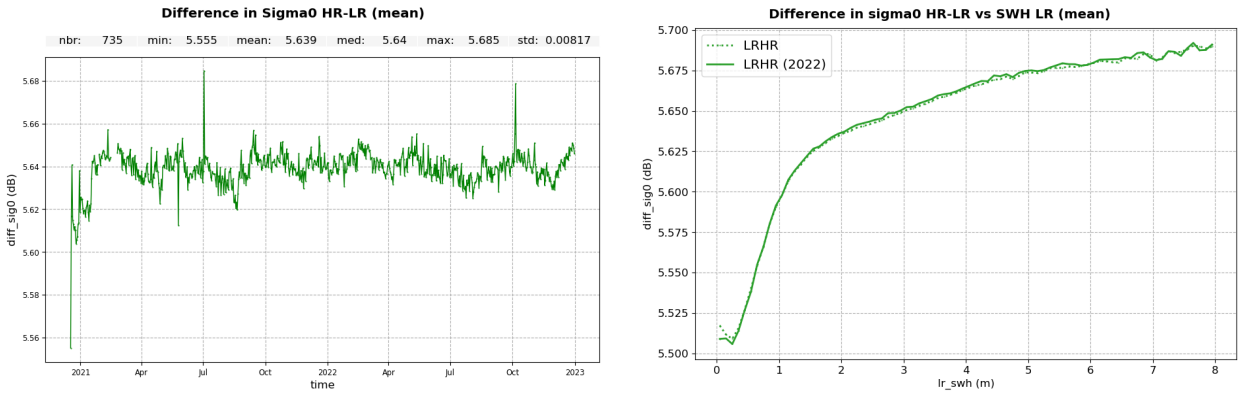


*Figure 66 – HR-LR sigma0 difference: Daily mean (left) and with respect to LR SWH (right). Computed on the entire timeseries (dotted line) and on 2022 only (solid line).*

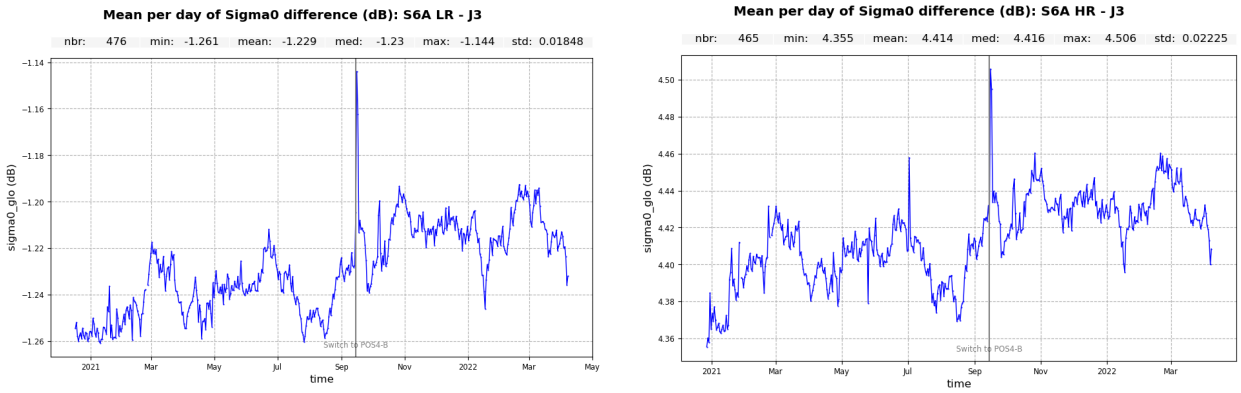


*Figure 67 – Daily mean of Ku-band backscatter coefficient difference: Sentinel-6 MF minus Jason-3, for Sentinel-6 MF LR (left) and Sentinel-6 MF HR (right).*

Figure 68 shows the distribution of the difference in Ku sigma0 between Sentinel-6 MF and Jason-3 over the tandem phase, splitted between POS4 sides. Values are not identical: -1.24 dB for side A and -1.21 dB for side B in LR ; and 4.4 dB for side A and 4.43 for side B in HR. These biases should be taken into account for the calibration bias applied on sigma0 for the wind speed computation (see section 4.6. for more details).

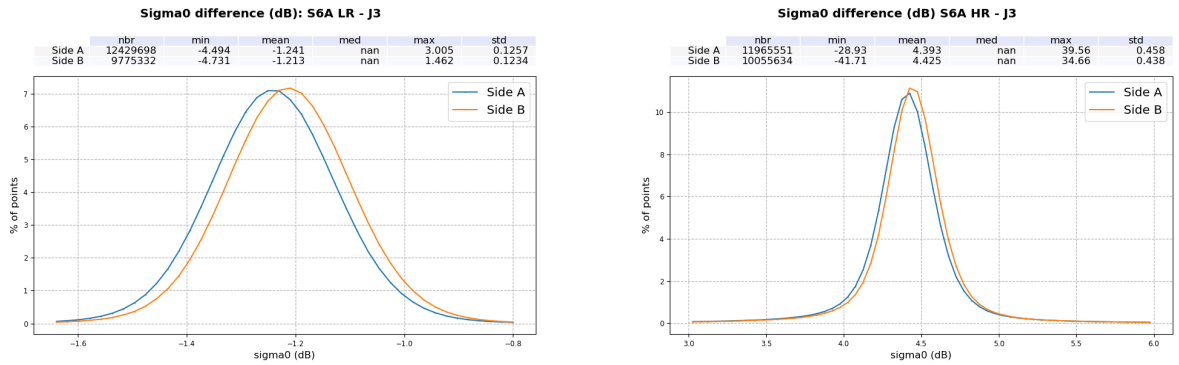


*Figure 68 – Histogram of Ku-band backscatter coefficient difference: Sentinel-6 MF minus Jason-3, over POS-4 side A and side B periods of the tandem phase for LR (left) and HR (right).*

## 4.6. Wind speed

For Sentinel-6 MF wind speed computation, the same algorithm as for Jason-3 GDR-F is applied (Collard). The geographical distribution of altimeter wind speed over 2022 is presented on figure 59 for Sentinel-6 MF LR and HR, and Jason-3. All wind speed average over 2022 share similar geographical patterns.

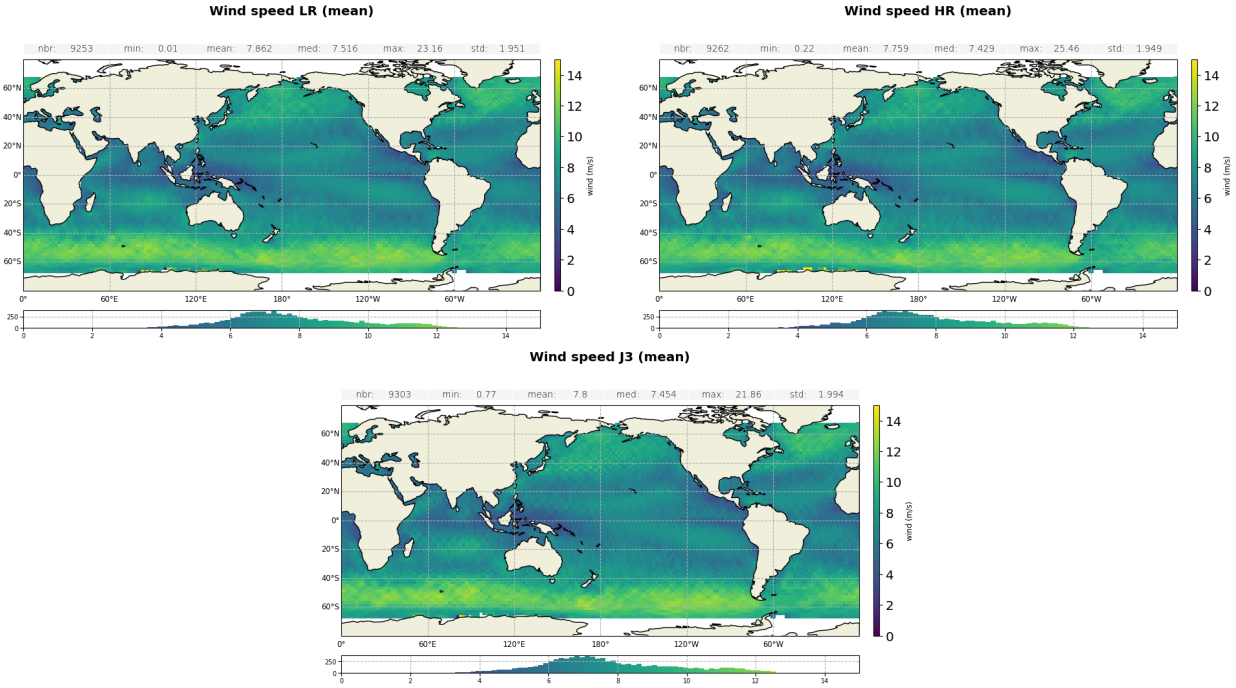


*Figure 69 – Maps of mean wind speed for LR (top left), HR (top right) and Jason-3 (bottom). Computed on cycles 42 to 79.*

The monitoring of the wind speed per cycle is presented on figure 70 and the corresponding distribution on figure 71. Wind speed is of the same order between LR and HR modes, as well as Jason-3, and centred around 8.2m/s, 8.0m/s and 8.1m/s respectively. Variations are similar between all three datasets with no drift or jump.
In the monitoring of the standard deviation, a yearly cycle is visible, due to seasonal evolution of the wind speed : higher standard deviation during northern hemisphere summer (about 3.8m/s) than during the northern hemisphere winter (about 3.6m/s).

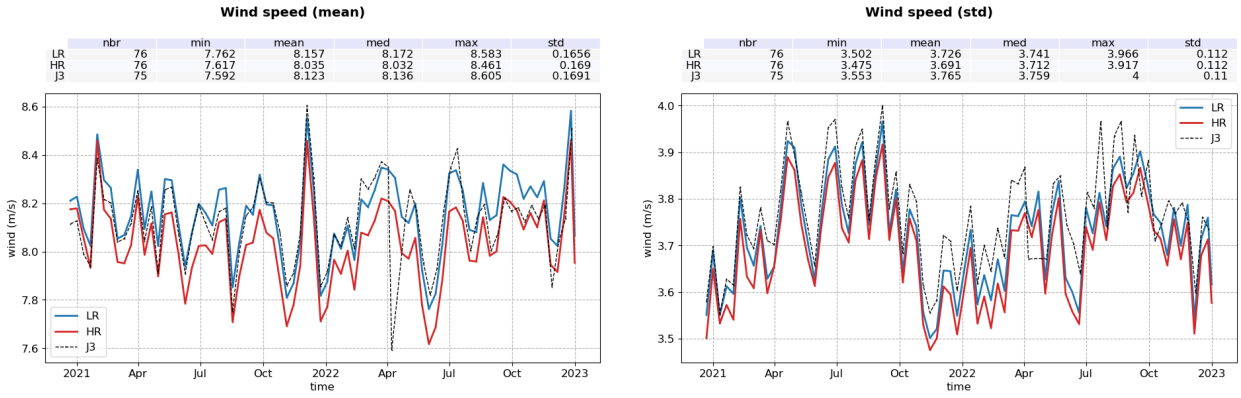


*Figure 70 – Mean (left) and standard deviation (right) wind speed per cycle for LR (blue), HR (red) and Jason-3 (black).*

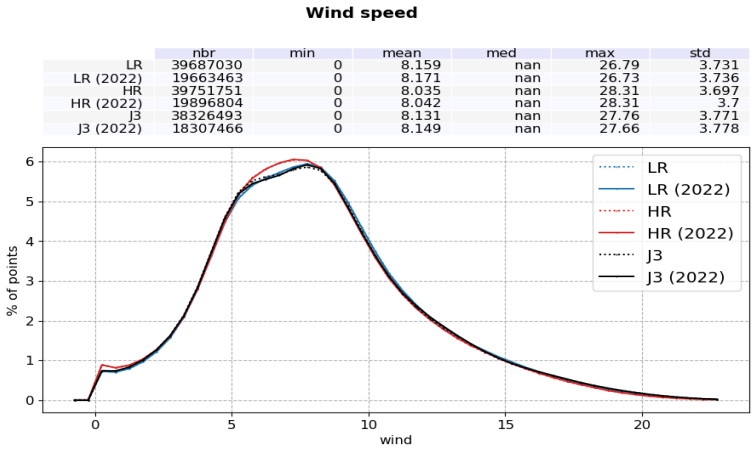


*Figure 71 – Histogram of wind speed for Sentinel-6 MF LR (blue), Sentinel-6 MF HR (red) and Jason-3 (black). Computed on the entire timeseries (dotted line) and on 2022 only (solid line).*

The monitoring of the HR-LR wind speed difference is presented on figure 72. A jump is visible in the beginning of the timeseries on 18/01/2021 that corresponds to a star-tracker update that improved the satellite pointing. This impacted HR and LR wind speed differently as in HR, SAMOSA retracking does not estimate the mispointing from the waveform, as opposed to LR with MLE4 retracking. The difference is centred around -0.04m/s and stable in time, with a seasonal variability (the variability is higher in summer and lower in winter)

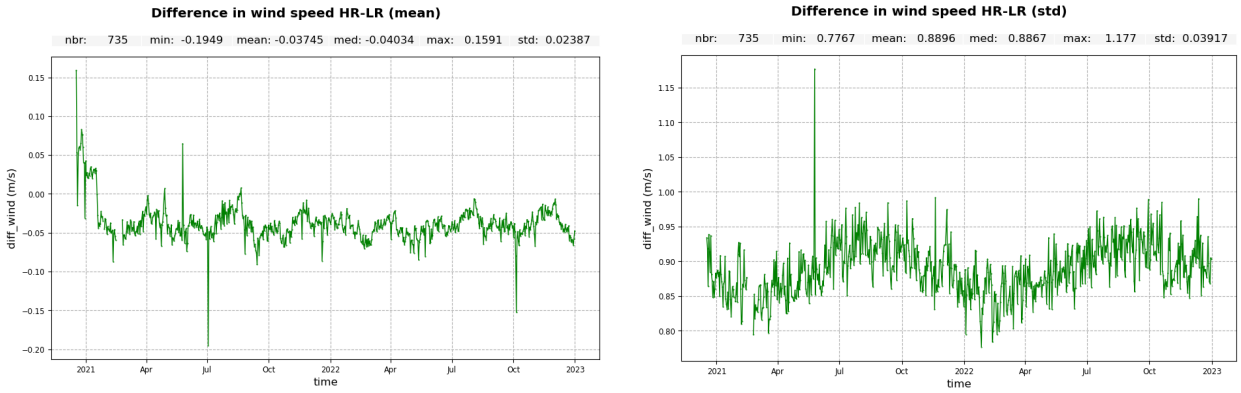


*Figure 72 – Mean (left) and standard deviation (right) HR-LR wind speed difference per day.*

Over the tandem period, the bias between Sentinel-6 MF wind speed and Jason-3 is not constant at the switch to POS4-B, for both LR and HR data (figure 73 left panel). Such differences are due to the variation of Ku-band sigma0 between POS4-A and POS4-B. Even though these variations are small, the impact on the wind speed are visible. Therefore, it should be taken into account in the wind speed computation. In the F06 reprocessing report [3], new values of sigma0 calibration bias for wind speed computation have been recommended for LR and HR, with different value for POS4-A and POS4-B. Note that in the PB F08, deployed in march 2023, these calibration biases have been applied, after some adjustement linked to update of the antenna aperture angle.

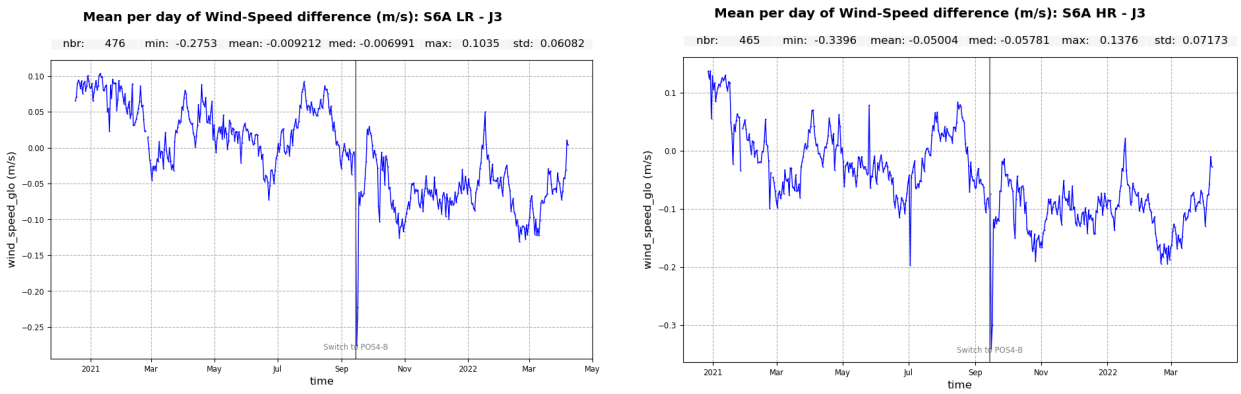


*Figure 73 – Time monitoring of Ku-band Wind-Speed difference: Sentinel-6 MF minus Jason-3. Mean per day for LR (left) and HR (right), computed over the complete tandem period.*

The monitoring of the difference between the altimeter-derived wind speed and the model is plotted on figure 74. The mean difference per cycle is relatively close between Sentinel-6 MF (19.9 cm/s and 15.2 cm/s for LR and HR respectively) and Jason-3 (20.0 cm/s), however there are significant behavior differences between the two missions.
Sentinel-6 MF and Jason-3 are loosely in line at the beginning of the timeseries, but seem to diverge after the switch to POS4-B in September 2021, although high cycle to cycle variability makes this estimation imprecise at best. This could be due to the fact that there is not yet specific calibration biases in sigma0 for POS4-A and POS4-B, as stated above.
The jump in the Sentinel-6 MF curves in August 2022 might be caused by the switch to PB F07 which impacted the sigma0 through the usage of ECHO CAL (see section 2.4.).
Additionally, short term oscillations in the Sentinel-6 MF monitoring are much more significant than in Jason-3, with an amplitude of about 10 cm/s and a period of about 2 months.
The monitoring of the standard deviation yields close values in average (1.45 m/s for Sentinel-6 MF LR, 1.39 m/s for Sentinel-6 MF HR and 1.41 m/s for Jason-3), but yearly oscillations in the Sentinel-6 MF data have a significantly higher amplitude (about 15 cm/s) than Jason-3 (about 10 cm/s).
These differences in behavior between Sentinel-6 MF and Jason-3 are under investigation.

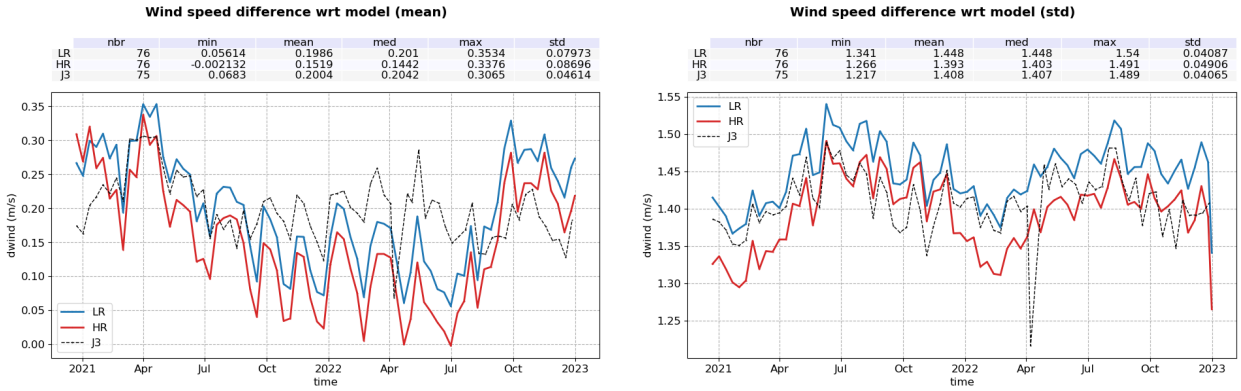


*Figure 74 – Mean (left) and standard deviation (right) wind speed difference wrt model per cycle for LR (blue), HR (red) and Jason-3 (black).*

## 4.7. Sea state bias

Sentinel-6 MF sea state biases (SSB) are computed using Jason-3 GDR-F SSB parameterizations.

Maps of Ku-band SSB averaged over the year 2022 show the same geographical patterns between Jason-3 and Sentinel-6 MF LR and HR (figure 75).

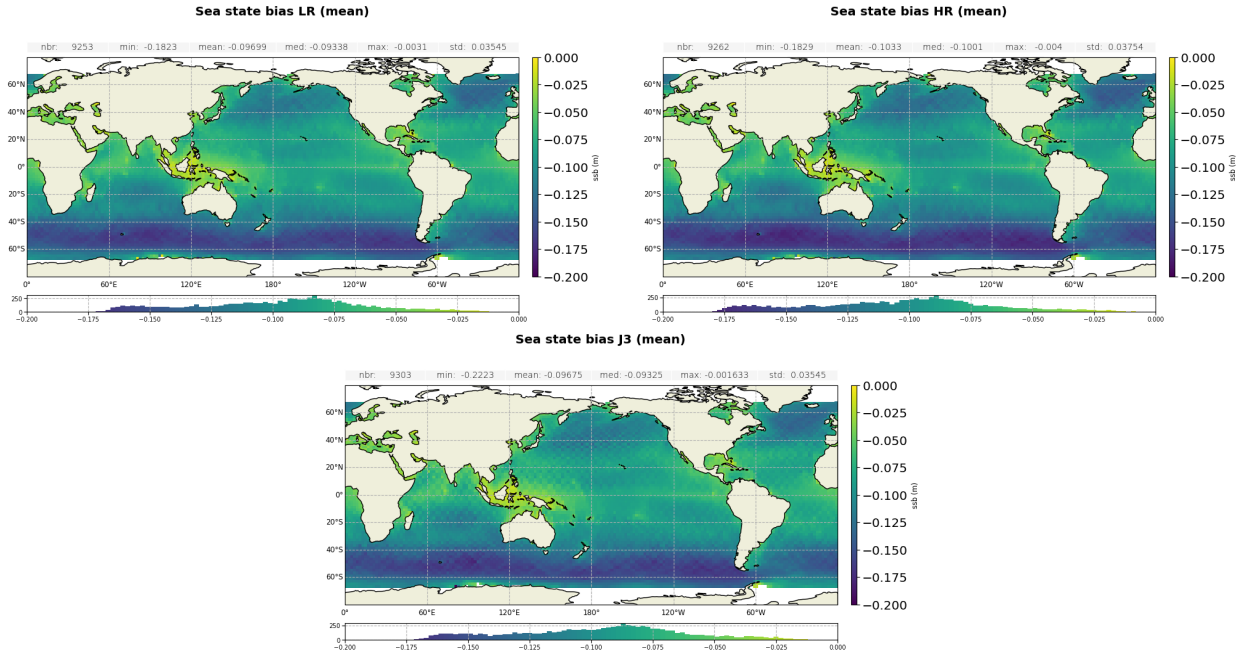


*Figure 75 – Maps of mean SSB for LR (top left), HR (top right) and Jason-3 (bottom). Computed on cycles 42 to 79.*

Ku-band SSB are centred around -10.4 cm for Sentinel-6 MF LR and -11.1 cm for Sentinel-6 MF HR. In C-band, the average SSB is of -9.5 cm for Sentinel-6 MF and Jason-3. This values are stable along time, as shown on figure 76.

Sentinel-6 MF LR SSB is very good agreement with Jason-3, also centred around -10.4 cm. Direct difference over the tandem phase however shows a jump in the SSB bias between the two missions, from 0.2 to 0.6 mm in average (figure 77). It is linked to sigma0 variation and should be removed with PB F08. The differences are mostly located in low SWH areas. It is in line with what is observed for SWH differences in figure 61, and is linked to the difference in low SWH management between Sentinel-6 MF and Jason-3 processing.

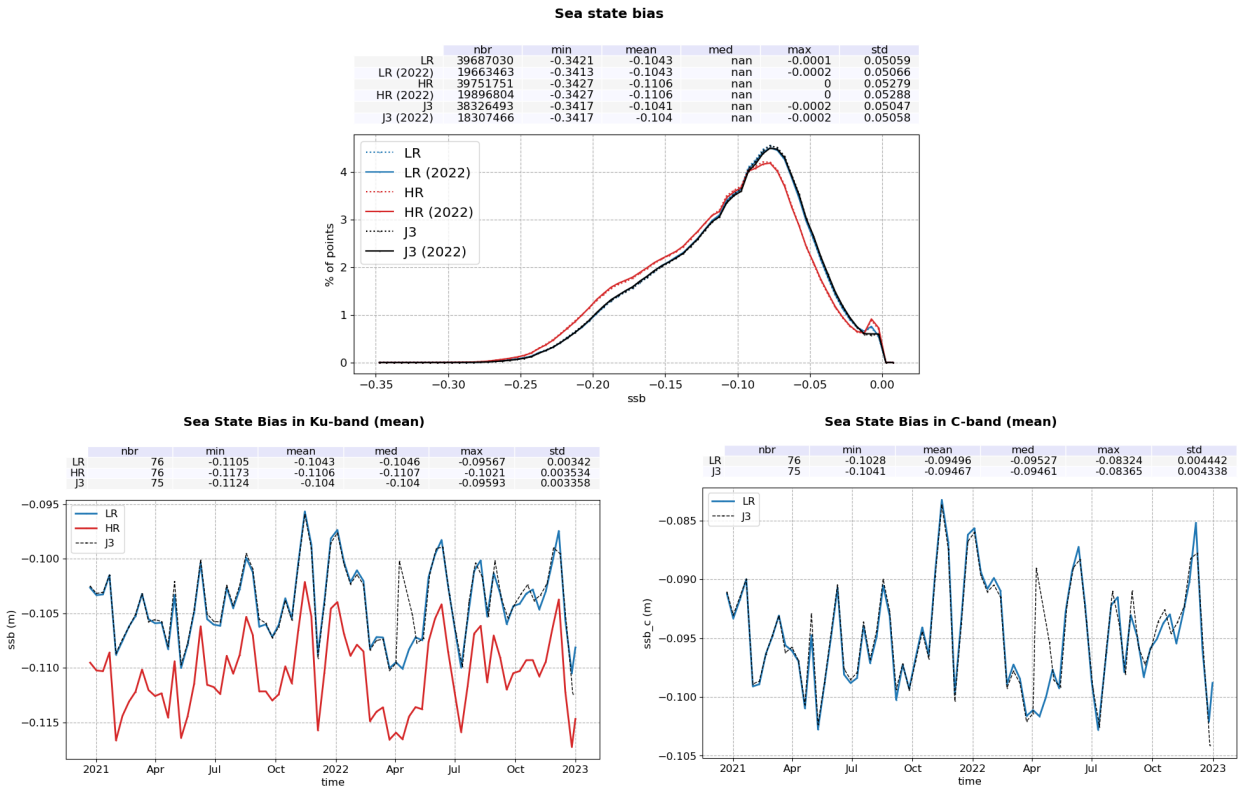


*Figure 76 – Top : Histogram of Ku-band SSB for Sentinel-6 MF LR (blue), Sentinel-6 MF HR (red) and Jason-3 (black), Computed on the entire timeseries (dotted line) and on 2022 only (solid line). Bottom: Cyclic monitoring of SSB mean in Ku-band (left) and C-band (right).*

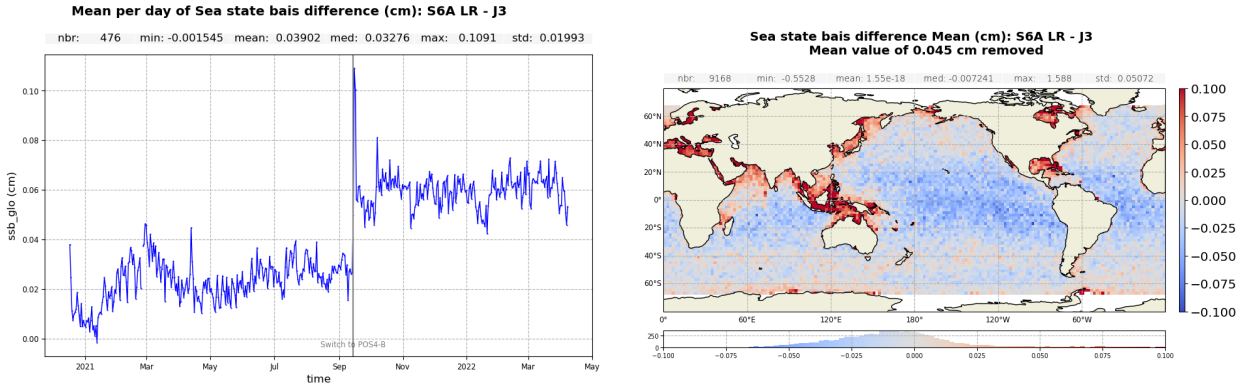


*Figure 77 – Ku-band SSB difference: Sentinel-6 MF LR minus Jason-3. Mean per day (left) and gridded map (right) computed over the complete tandem period.*

The monitoring of the HR-LR SSB difference is presented on figure 78. The difference is centred around 0.75cm in average and 0.58cm in standard deviation with yearly oscillations in both cases, as observed on the wind speed (figure 72, right panel). This seasonal variability is induced by the SWH.
Because of its small impact on HR wind speed, the switch to POS4-B does not seems to impact the HR SSB retrieval in comparison to Jason-3 (figure 79). A clear correlation to sea state condition is observed on the difference map. It is important to note here that the SSB algorithm used for HR SSB computation is the same as for LR data, i.e. Jason-3 GDR-F Ku-band algorithm. This algorithm is not adapted to HR data. It can be the cause of the patterns observed here.

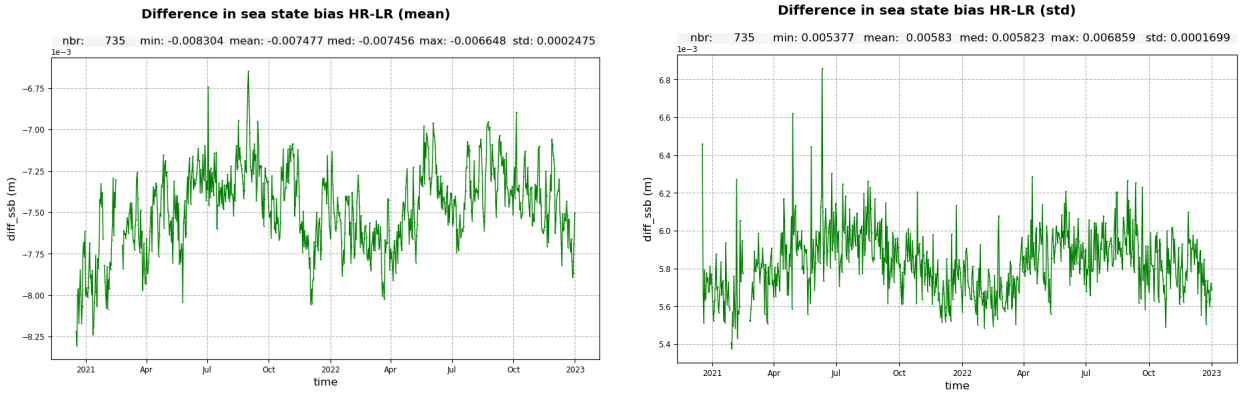


*Figure 78 – Mean (left) and standard deviation (right) HR-LR SSB difference per day.*

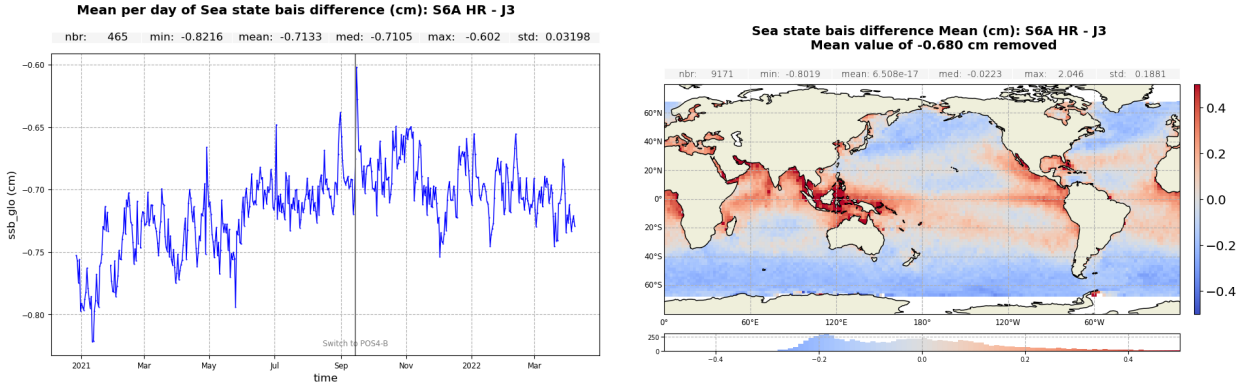


*Figure 79 – Ku-band SSB difference: Sentinel-6 MF HR minus Jason-3. Mean per day (left) and gridded map (right) computed over the complete tandem period.*

## 4.8. Ionospheric correction

Sentinel-6 MF altimeter ionosphere correction is derived from LR data, in Ku and C band. The ionosphere correction in HR products is copied from LR products and thus identical.

The filtering process of dual-frequencies ionospheric correction is described in [13]. If system performance for SLA estimations over open ocean are significantly improved thanks to filtering of the dual-frequencies ionospheric correction, the filtering process tends to set the correction to default value near coast and ice frontiers, and as a consequence a loss of SSHA valid points over these areas.

The monitoring of the filtered dual-band ionospheric correction is presented on figure 80, along with the corresponding distributions. There is a very good agreement between Sentinel-6 MF and Jason-3 ionospheric corrections, that follow the same variations with a downward trend due to the intensification of the current solar cycle. Averages over the whole period are -3.1 cm for Sentinel-6 MF and -2.6 cm for Jason-3, the 5 mm bias being stable over time.
The geographical distribution of Sentinel-6 MF filtered ionospheric correction is presented on figure 81.

The monitoring of the filtered - GIM model ionospheric corrections is presented on figure 82. As expected, both the Sentinel-6 MF and Jason-3 curves follow identical variations. Sentinel-6 MF altimeter ionosphere correction shows in average a better consistency to GIM model than Jason-3. The bias with respect to GIM is centred around 0.9 cm for Sentinel-6 MF data while 1.2 cm for Jason-3. However, looking at the corresponding maps of altimeter versus GIM difference (figure 83), the amplitude of the difference is stronger for Sentinel-6 MF than Jason-3. This behavior can be linked to the reduced smoothing in Sentinel-6 MF ionosphere correction filtering, thus giving more accurate reflection of the peaks and troughs in the

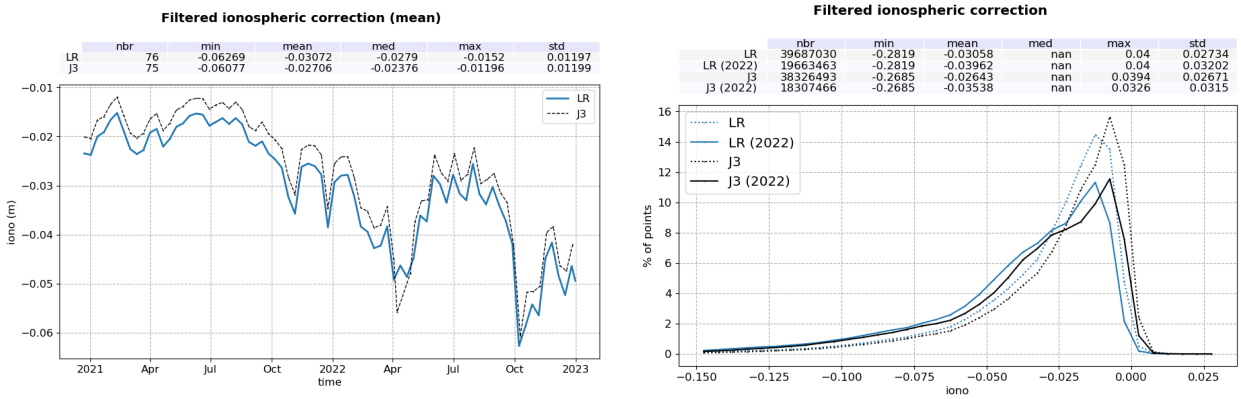


*Figure 80 – Monitoring of filtered ionospheric correction for Sentinel-6 MF LR (blue) and Jason-3 (black). Left: Mean per cycle. Right : Histogram computed on the entire timeseries (dotted line) and on 2022 only (solid line).*

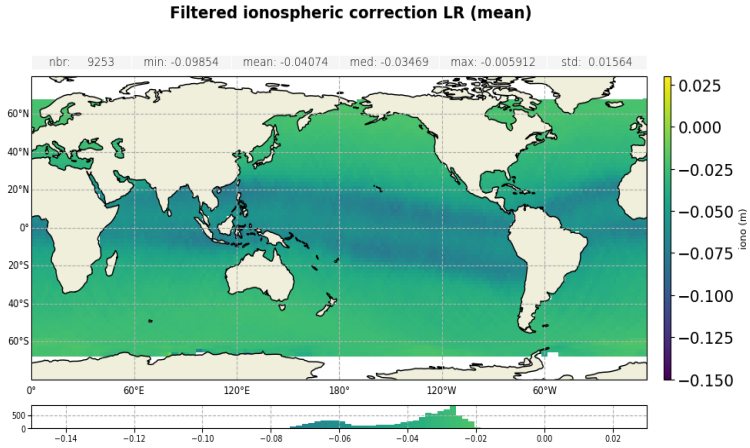


*Figure 81 – Maps of mean filtered ionospheric correction for Sentinel-6 MF. Computed on cycles 42 to 79.*

ionospheric content. This is also visible in the higher standard deviation for Sentinel-6 MF compared to Jason-3 (0.8 and 0.7 cm respectively, see figure 82, right panel).

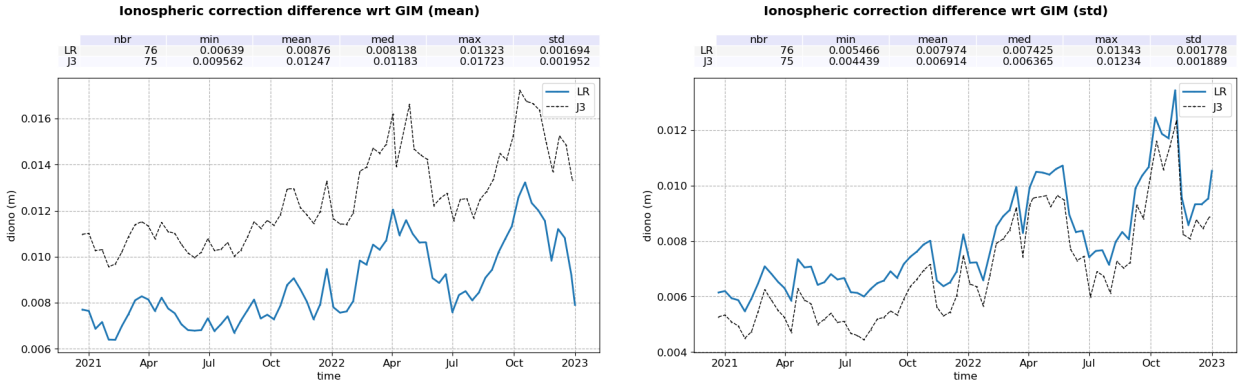


*Figure 82 – Mean (left) and standard deviation (right) filtered iono - GIM iono per cycle for Sentinel-6 MF LR (blue) and Jason-3 (black).*

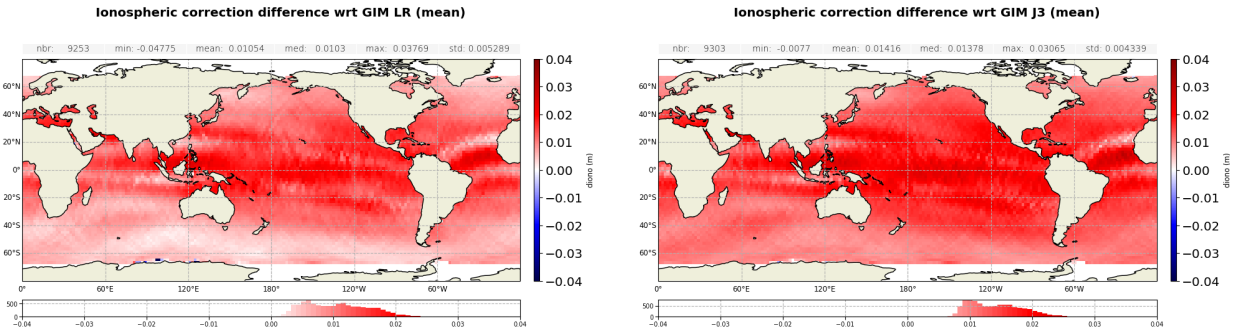


*Figure 83 – Maps of mean filtered ionospheric correction - GIM iono for Sentinel-6 MF LR (left) and Jason-3 (right). Computed on cycles 42 to 79.*

Over the complete tandem phase, the bias between the Sentinel-6 MF and Jason-3 solutions is centred around -0.4 cm. The time monitoring of this bias (figure 84) shows a clear jump of -0.7 mm at the POS4-B switch. This value is small but the jump is clearly visible on the plot due to the stability of the bias over each POS4 side period. This jump is due to Sentinel-6 MF Ku-band sigma0 change at the switch to POS4-B (see Figure 68). This change has not been taken into account in the altimeter wind speed computation, leading to jump in Ku-band and C-band SSBs and thus impacting the altimeter ionosphere correction.

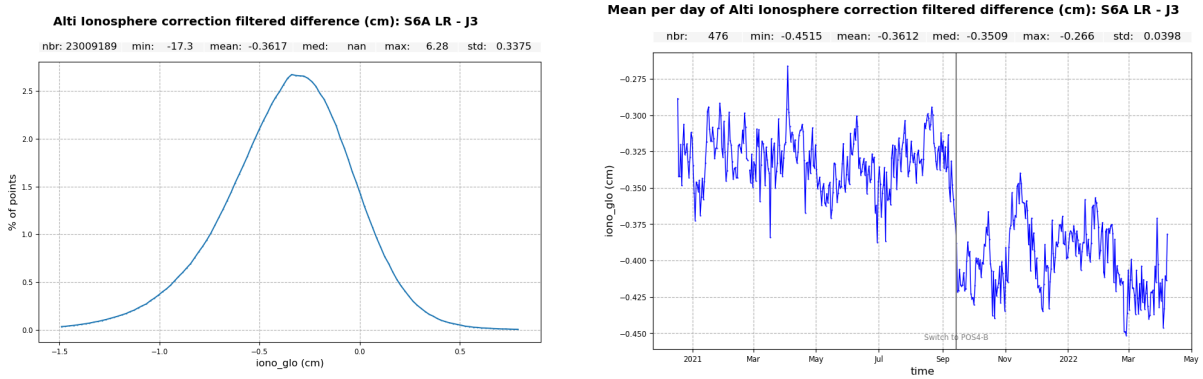


*Figure 84 – Altimeter Filtered Ionosphere correction difference: Sentinel-6 MF LR minus Jason-3. Histogram (left) and Mean per day (right) computed over the complete tandem period.*

The map of the filtered ionosphere correction differences is presented in figure 85, left panel. We observe a correlation with ERA-5 SWH (right panel): -0.5 cm between 2 and 7m wave.

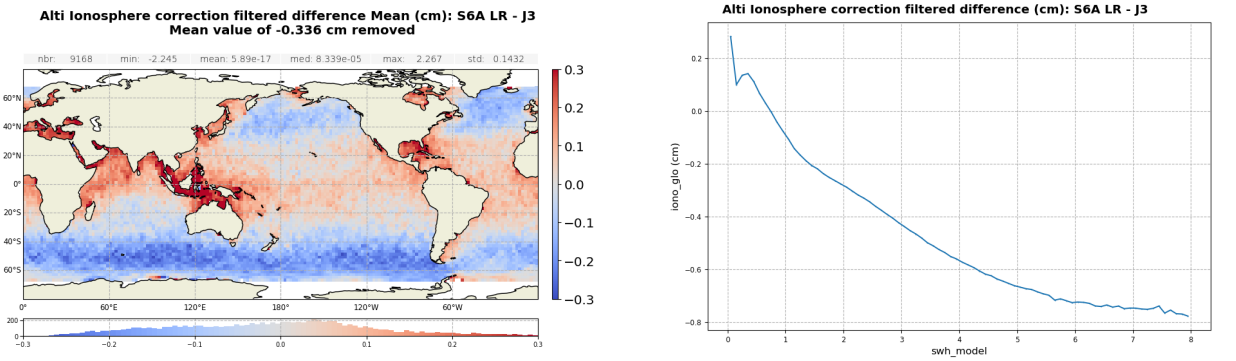


*Figure 85 – Altimeter Filtered Ionosphere correction difference: Sentinel-6 MF LR minus Jason-3 computed over the complete tandem period. Gridded map (left panel) and difference function of ERA5 SWH (right panel).*

## 4.9. AMR wet troposphere correction

### 4.9.1. Overview

In order to evaluate radiometer wet troposphere correction, liquid water content, water vapor content and atmospheric attenuation, Sentinel-6 uses a three-frequencies AMR radiometer (18.7, 23.8 and 34.0 GHz), similar to the one used on Jason-3.

Note that the 23.8 GHz channel is the primary water vapor sensing channel, meaning a higher water vapor concentration leads to larger 23.8 GHz brightness temperature values. As a consequence, top right and bottom right parts of figure 86 are anti-correlated. Moreover, the 34 GHz channel and the 18.7 GHz channel, which have less sensitivity to water vapor, facilitate the removal of the contributions from cloud liquid water and excess surface emissivity of the ocean surface due to wind, which also act to increase the 23.8 GHz brightness temperature.

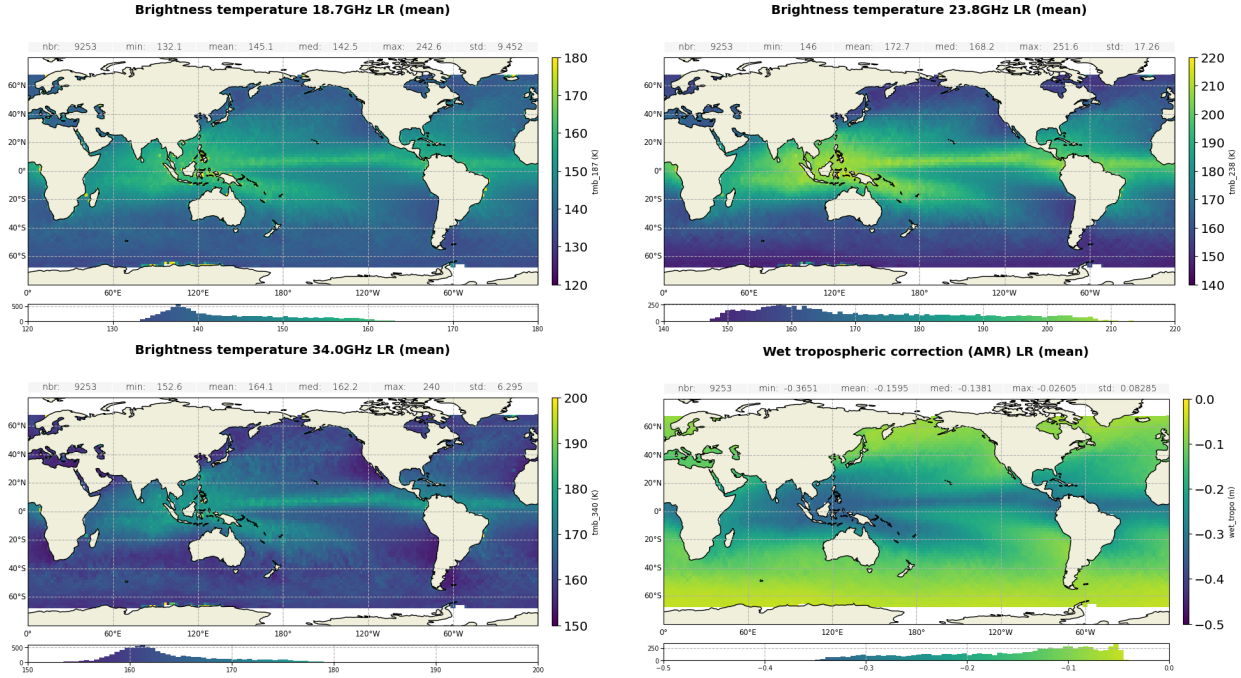


*Figure 86 – Maps of mean brightness temperature for chanels 18.7 GHz (top left), 23.8GHz (top right), 34.0GHz(bottom left) in K and mean wet tropospheric correction (bottom right) in m. Computed on cycles 42 to 79.*

The distributions of the wet tropospheric corrections for Sentinel-6 MF and Jason-3 are presented on figure 87. Both distributions are similar, with Sentinel-6 MF centred around -15.2 cm and Jason-3 around -15.1 cm.
Curves for year 2022 only (solid lines) are aligned with curves for the entire timeseries (dotted lines).

From processing baseline F07 (2022-08-15 in NTC), all variables within the Level 2 altimeter products derived from the radiometer (such as WTC) result from the combination of AMR-C and HRMR data. Such update allows to improve WTC retrieval near the coast, by extending the wet path delay measurements into coastal areas

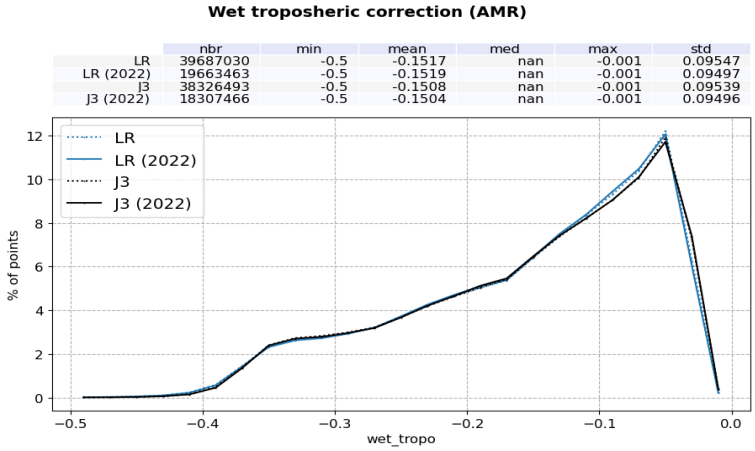


*Figure 87 – Histogram of wet tropospheric correction in m for Sentinel-6 MF (blue) and Jason-3 (black). Computed on the entire timeseries (dotted line) and on 2022 only (solid line).*

### 4.9.2. Comparison with model

The wet troposphere correction computed from ECMWF model data has been used to check the Sentinel-6 MF and Jason-3 radiometer corrections. The cross-comparison between all radiometers and models available is necessary to analyze the stability of each wet troposphere correction. An overview of the wet troposphere correction importance for mean sea level is given in Obligis et al. [14]. The difference between AMR and model data is computed on a daily basis and is plotted on figure 88 for Sentinel-6 MF and Jason-3 for comparisons. Looking more closely to Sentinel-6 MF data, the monitoring per day of the bias between radiometer and model highlights several phases and events (figure 88 left panel):

- on 27-28 April 2021, a jump of -4 mm is observed in the bias preceded by a progressive increase of the bias (from beginning of March 2021) by the same amplitude. The jump visible on 27-28 April 2021 is concomitent with a satellite restart and follows an AMR deep sky calibration occuring on the 25/04/2021. It is not observed in Jason-3 time series (figure 88 left panel). This jump is most likely linked either to the AMR calibration or to the satellite restart that occured on the 22/04/2021, during which significant thermal variations could have permanently impacted the radiometer antenna.
- on 13 October 2021, a jump of +2 mm is observed on both Sentinel-6 MF and Jason-3 monitoring. It is linked to an update in the ECMWF model (see [10] for more details).
- around mid-February 2022, another change is observed on Sentinel-6 MF monitoring. This change is more progressive and spanned over about 3 days. Over this period, Jason-3 and Sentinel-6 monitorings split from one-another and comparison cannot be done. The origin of this small change (-1 mm) on Sentinel-6 MF is under investigation.
- An anomalous -2mm/month drift in Sentinel-6 MF wet-troposphere correction is visible from 2022-10-01, which is absent from Jason-3. This drift has been identified as resulting from a calibration error in the microwave radiometer. On 2022-12-14, the error was fixed, causing a jump of about +5mm back to previous levels.

The events of April 2021 and October 2021 are also visible in the comparison to Jason-3 over the tandem phase, as shown on figure 89.

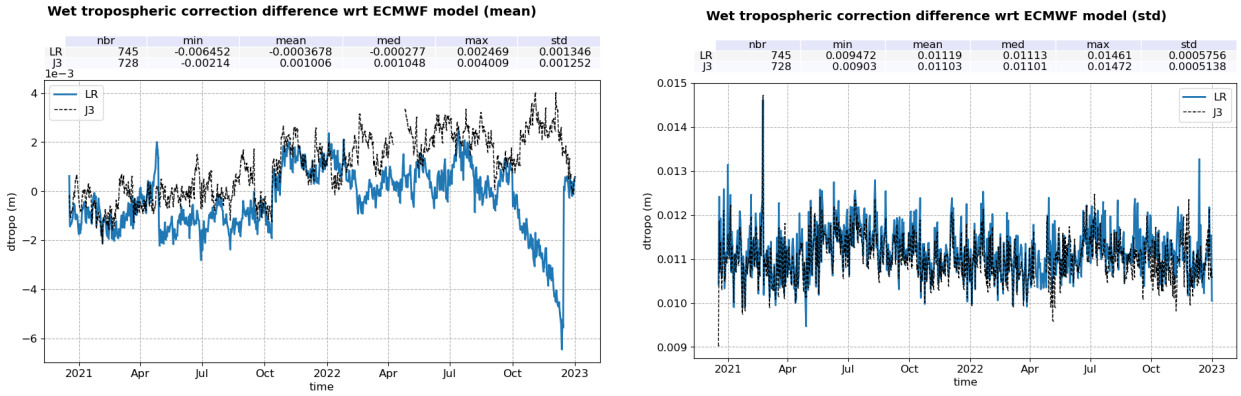


*Figure 88 – Mean (left) and standard deviation (right) AMR wet troposhperic correction - ECMWF model per day for Sentinel-6 MF LR (blue) and Jason-3 (black).*

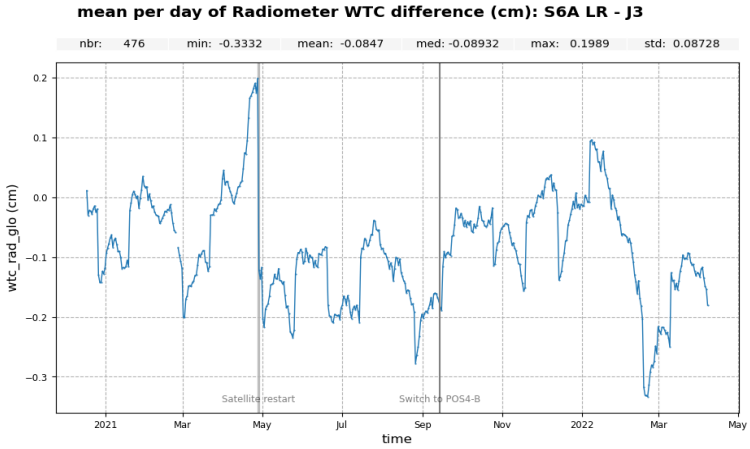


*Figure 89 – Radiometer wet troposphere correction difference: Sentinel-6 MF LR minus Jason-3. Mean per day computed over the complete tandem period.*

# 5 SSH crossover analysis

## 5.1. Overview

Sea Surface Height crossover differences are the SSH differences between ascending and descending passes where they cross each other. Sea Surface Heights are computed as follow :

$$SSH = Orbit - AltimeterRange - \sum(GeophysicalCorrections)$$

Crossover differences are systematically analyzed to estimate data quality and the Sea Surface Height (SSH) performance. SSH crossover differences are computed from the valid data set on a one cycle basis, with a maximum time lag of 10 days, in order to limit the effects of ocean variability which are a source of error in the performance estimation. The mean SSH crossover differences should ideally be close to zero and standard deviation should ideally be small.

Nevertheless SLA varies also within 10 days, especially in high variablity areas. Furthermore, due to lower data availability (due to seasonal sea ice coverage), models of several geophysical corrections are less precise in high latitude. Therefore an additional geographical selection - removing shallow waters, areas of high oceanic variability and high latitudes ($> |50|$ deg) - is applied for cyclic monitoring.

## 5.2. Mono-mission SSH crossovers

The cycle by cycle mean of SSH crossover differences is plotted in figure 90. All curves follow similar variations and average close to zero, Sentinel-6 MF HR having a slightly higher mean at 0.8 mm compared to Sentinel-6 MF LR and Jason-3 (-0.2 and -0.1 mm). These results are summarized in table 7. Similarly to Jason-3, a 120-day signal is observed for Sentinel-6 MF LR and HR monitoring. Prior Sentinel-6 MF launch, the origin of this signal was linked to Jason-3 platform. As the two satellites do not have the same platform, this hypothesis seems not to be the right one. Further investigations are required to fully understand this behavior.

The map of LR SSH differences at crossovers are smooth and does not hightlight any strong discrepancies between ascending and descending tracks in terms of SSH (figure 91 left panel). The map of HR SSH difference at crossover highlight patterns correlated to along-track wind (right panel). It is linked to the impact of along-track wind on HR data and more particularly on HR range (see section 4.3.).

Figure 92 presents the monitoring of the standard deviation of crossover SSH differences, for Sentinel-6 MF LR, HR, and Jason-3. All datasets show very good performance, very similar and stable in time. No anomaly is detected. Sentinel-6 MF LR and Jason-3 have similar standard deviation, 4.7 cm and 4.6 cm in average respectively, while Sentinel-6 MF HR STD is lower at 4.5 cm. These results are summarized in table 7.
This metric allows to estimate the system noise by dividing by $\sqrt{2}$ (which leads to 3.32 cm for Sentinel-6 MF LR, and 3.18 cm for Sentinel-6 MF HR).

The cyclic monitoring of the crossover differences of the SSH using model wet tropospheric correction is plotted on figure 93. The mean of the Sentinel-6 MF LR dataset is slightly higher in absolute value with model WTC (-0.4 mm vs -0.2 mm with radiometer-derived WTC), which is also true for Jason-3 (-0.2 mm

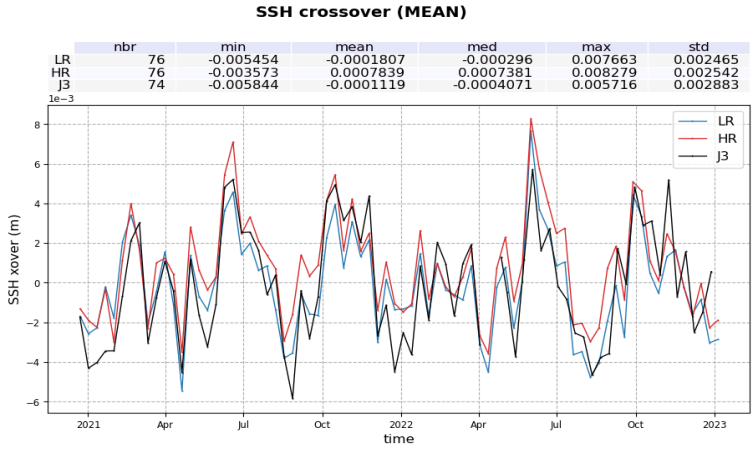


*Figure 90 – Mean SSH differences at crossovers by cycle for Sentinel-6 MF LR (blue), HR (red) and Jason-3 (black).*

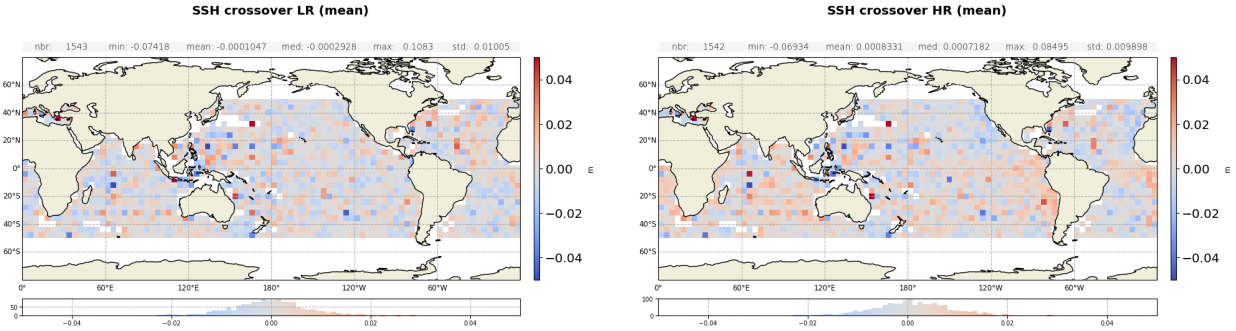


*Figure 91 – Maps of mean SSH differences at mono-mission crossovers in m for both LR (left) and HR (right), computed on cycles 42 to 79.*

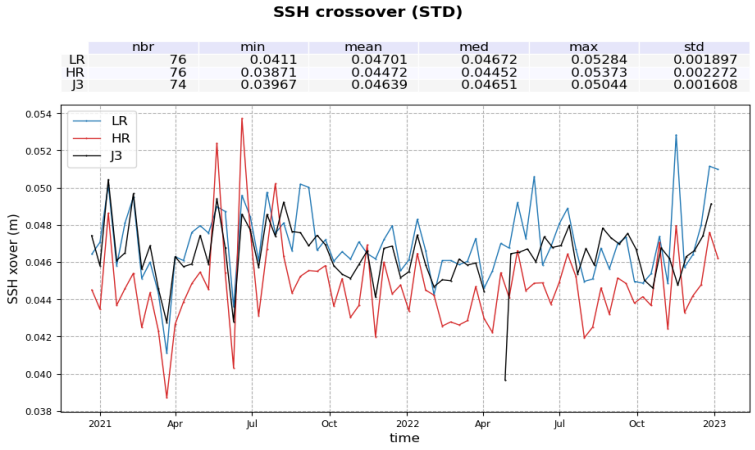


*Figure 92 – Standard deviation of SSH differences at crossovers by cycle for Sentinel-6 MF LR (blue), HR (red) and Jason-3 (black).*

vs -0.1 mm). However the mean of the HR dataset is slightly closer to zero (0.6 mm vs 0.8 mm).
The differences in standard deviation are more significant. For all datasets, the use of model wet tropospheric correction degrades the standard deviation of the SSH crossover differences by 2 mm. These results are summarized in table 7.

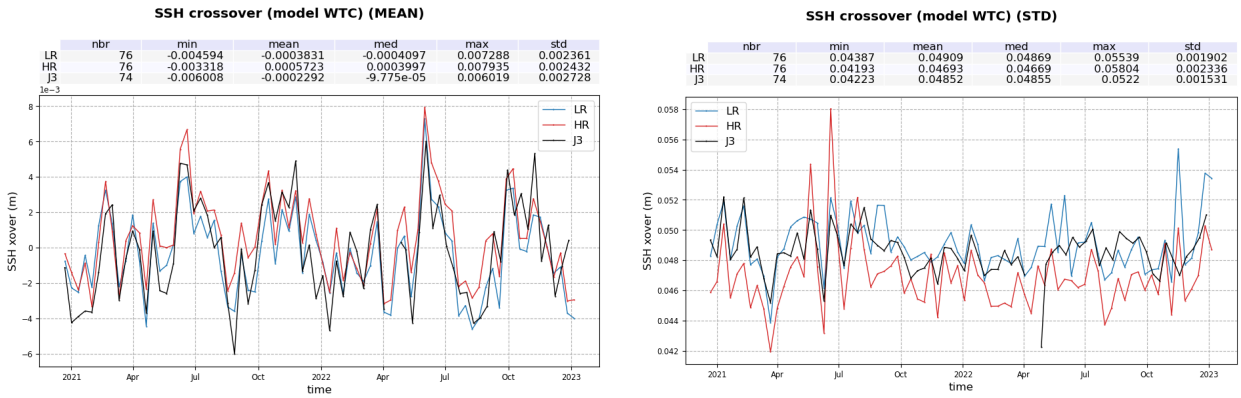


*Figure 93 – Mean (left) and standard deviation (right) SSH differences at crossovers by cycle for Sentinel-6 MF LR (blue), HR (red) and Jason-3 (black).*

| **Mission** | **Mean (mm)** | | **Standard deviation (cm)** | |
|---|---|---|---|---|
| | AMR WTC | Model WTC | AMR WTC | Model WTC |
| Sentinel-6 MF LR | -0.1 | -0.2 | 4.7 | 4.9 |
| Sentinel-6 MF HR | 0.8 | 0.6 | 4.5 | 4.7 |
| Jason-3 | -0.1 | -0.2 | 4.7 | 4.9 |

*Table 7 – Mean and standard deviation of monomission SSH crossover differences for Sentinel-6 MF LR and HR and Jason-3*

## 5.3. Multi-mission SSH crossovers

The monitoring of multi-mission SSH differences at crossovers is plotted on figure 94. Both LR/Jason-3 and HR/Jason-3 follow the same variations, with means of -1.3cm and 0.1cm respectively.
The spike in April 2022 is due to missing measurements in Jason-3 during the orbit change after the end of the tandem phase (cf section 2.1.).
A downward drift is visible. It might be caused by different PTR shape degradation between both satellites. Between October and December 2022, the Sentinel-6 MF/Jason-3 differences at crossover increase in absolute value. This is due to the WTC drift described in section 4.9.2. that impacted Sentinel-6 but not Jason-3.

The corresponding geographical distributions and their differences are presented in figure 95. While no significant regional pattern can be seen in the Sentinel-6 MF LR/Jason-3 SSH crossovers differences, Sentinel-6 MF HR/Jason-3 SSH crossovers differences are higher at high latitudes. This difference in geographical pattern in clearly visible in the bottom panel, with differences up to about 10cm at high latitudes, while is is about 0cm in the equatorial regions. This is expected as the skewness used in HR processing is different from LR and Jason-3 processings, leading to a strong correlation of the range to sea state conditions (see section 4.3.).

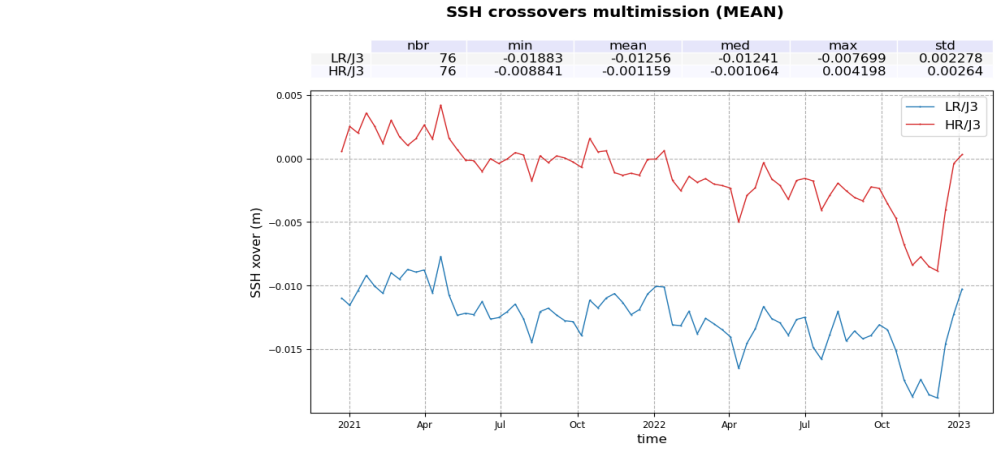


*Figure 94 – Mean multimission SSH differences at crossovers by cycle for Sentinel-6 MF LR/Jason-3 (blue) and HR/Jason-3 (red).*

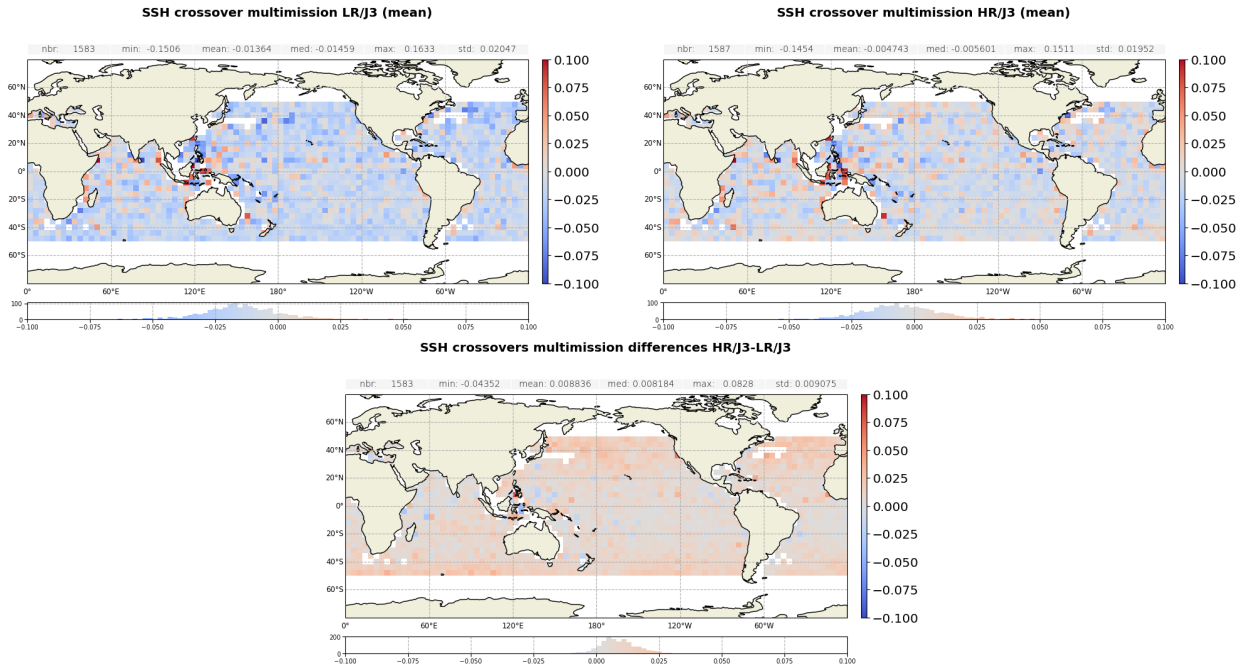


*Figure 95 – Maps of multimission mean SSH differences at crossovers for LR/Jason-3 (top left), HR/Jason-3 (top right) and their difference (bottom). Computed on cycles 42 to 79.*

Figure 96 presents the monitoring of the standard deviation of multimission crossover SSH differences, for LR/Jason-3 and HR/Jason-3. Both datasets show very good performance at 4.7 and 4.6 cm respectively. The spike in April 2022 is due to missing measurements in Jason-3 during the orbit change after the end of the tandem phase (cf section 2.1.). After the end of the tandem phase, the standard deviation increases slightly for both LR/Jason-3 and HR/Jason-3 crossover differences.

The cyclic monitoring of the multimission crossover differences of the SSH using model wet tropospheric correction is plotted on figure 97. The average SSH crossover difference per cycle follows the same variation as the crossover SSH with radiometer-derived WTC, with only minor value differences. The only notable exception is the expected absence of the dip at the end of 2022 caused by the radiometer drift.
As for monomission crossover differences, however, using a corrected troposphere model degrades the standard deviation of the multimission SSH crossover differences by about 2 mm in both LR/Jason-3 and HR/Jason-3 datasets.

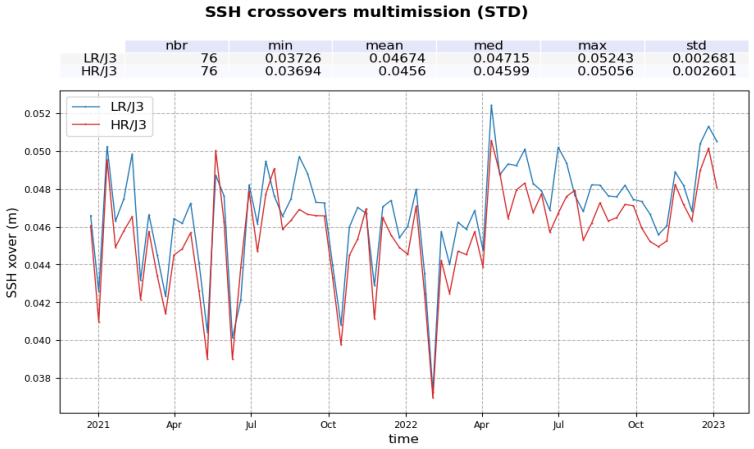


*Figure 96 – STD multimission SSH differences at crossovers by cycle for Sentinel-6 MF LR/Jason-3 (blue) and HR/Jason-3 (red).*

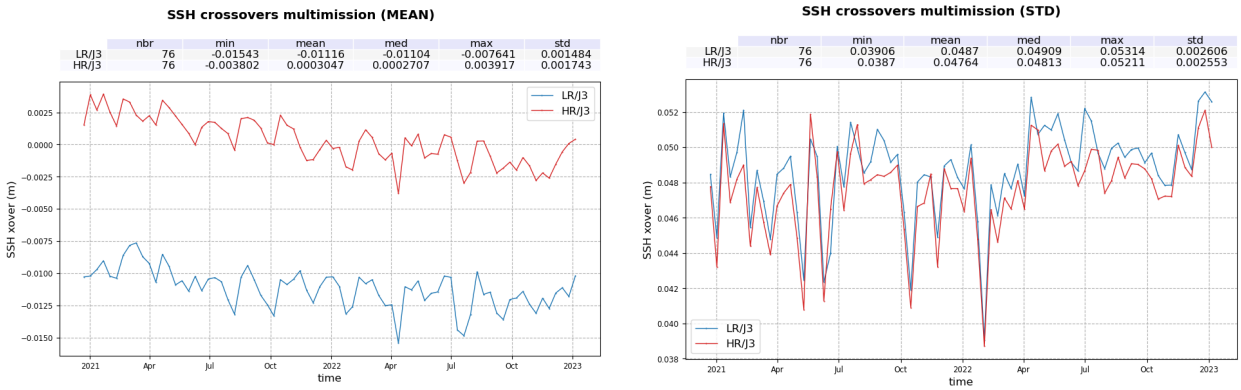


*Figure 97 – Mean (left) and standard deviation (right) of multimission SSH differences at crossovers by cycle for Sentinel-6 MF LR / Jason-3 (blue), HR / Jason-3 (red). SSH is computed using model WTC.*

## 5.4. Pseudo time tag bias

The pseudo time tag bias ($\alpha$) is found by computing at mono-mission SSH crossovers a regression between SSH and orbital altitude rate ($\dot{H}$), also called satellite radial speed: SSH = $\alpha\dot{H}$. This empirical method allows us to estimate the potential real time tag bias but it can also absorb other errors correlated with $\dot{H}$. Therefore it is called “pseudo” time tag bias. The monitoring of this coefficient estimated at each cycle is performed for Sentinel-6 LR and HR in figure 98.

Its mean is -22 $\mu$s for LR mode and -4 $\mu$s for HR mode, and never exceeds a few hundreds microseconds.

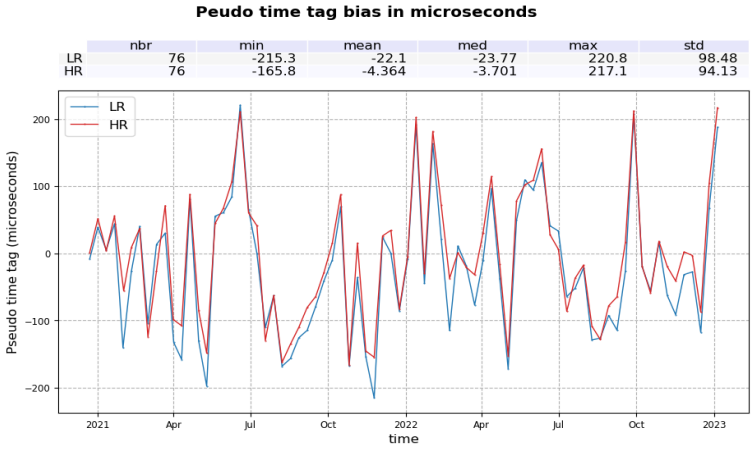


*Figure 98 – Pseudo time tag bias by cycle for LR (blue) and HR (red).*

## 5.5. Transponder analysis

An absolute calibration of the Poseidon-4 altimeter is performed over the CDN1 transponder in West Crete mountains for each descending Sentinel-6 MF pass number 18.

The range bias (cf figure 99) is calculated for each waveform seeing the CalVal site by taking the difference between the transponder-altimeter distance (accurately determined using a precise positioning of the satellite and the transponder site) and the altimeter range derived from the retracking (based on a sinc-function fit) of the transponder-generated waveform. Note that the altimeter bias is further corrected for transponder and altimeter related errors, the Doppler range shift, and delays through the atmosphere.

The datation bias is also computed and presented on figure 100.

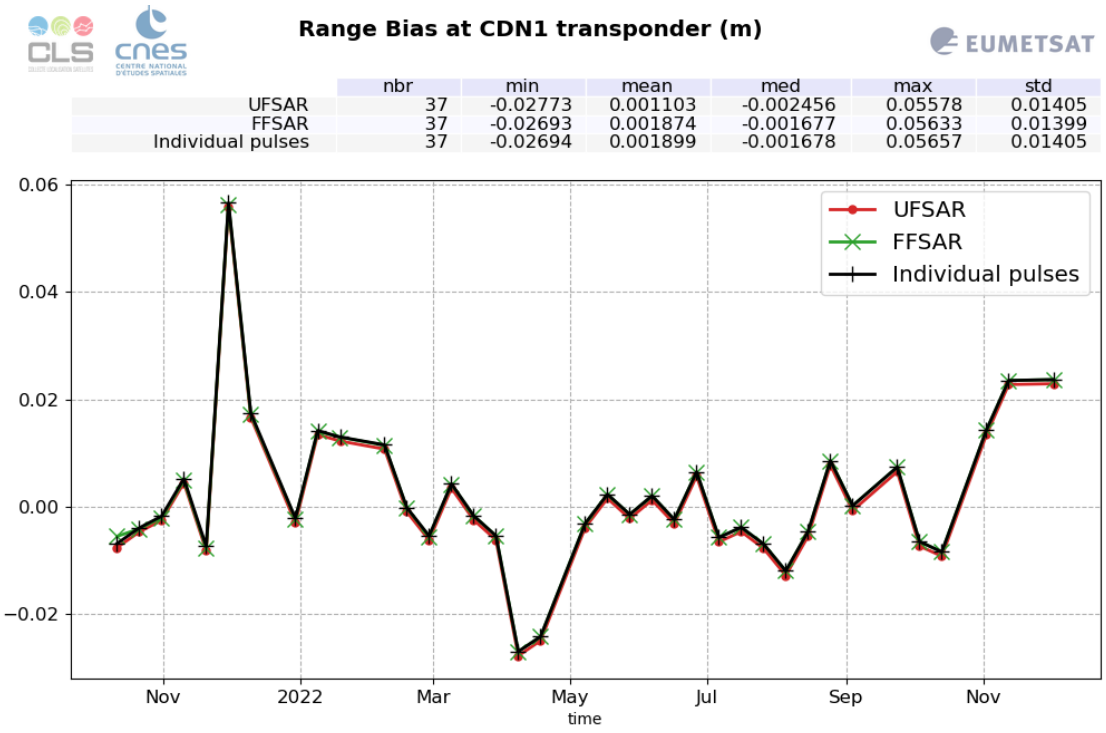


*Figure 99 – Monitoring of the range bias at CDN1 transponder, from cycle 34 to 76*

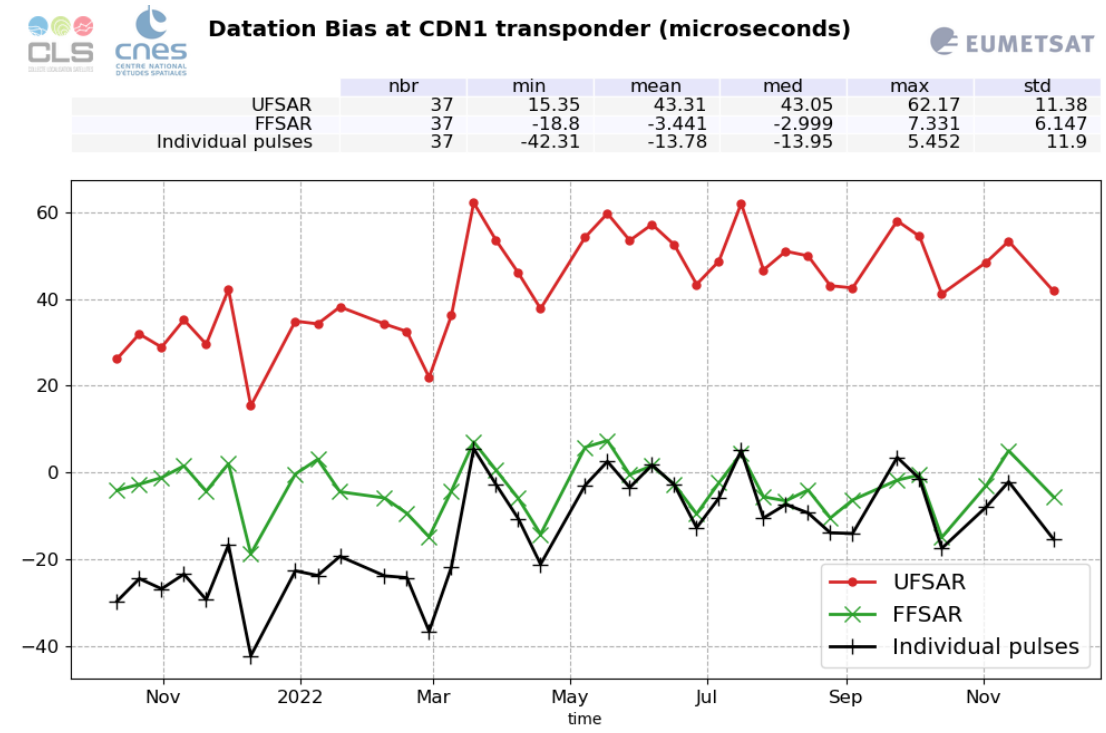


*Figure 100 – Monitoring of the datation bias at CDN1 transponder, from cycle 34 to 76*

# 6 SSHA along-track analysis

## 6.1. Overview

The Sea Surface Height Anomaly (SSHA) is the most well-known parameter estimated from altimetry. It corresponds to the elevation of sea surface, with respect to a reference called Mean Sea Surface (MSS), generated by oceanic variability and climatic phenomena (such as Gulf stream current, El Nino, ...). It is computed as follow:

$$SSHA = Orbit - AltimeterRange - \sum(GeophysicalCorrections) - MeanSeaSurface$$

The details of the geophysical corrrections can be found in Sentinel-6 ALT Level 2 Product Generation Specification [15].

SSHA analysis is a complementary indicator to estimate the altimetry system performance. It allows to study the evolution of SSHA mean (detection of jump, abnormal trend or geographical correlated biases), and also the evolution of the SSHA variance highlighting the long-term stability of the altimetry system performance.

The SSHA distributions are plotted on figure 101 for Sentinel-6 MF LR and HR as well as Jason-3. Mean values are of 4.7 cm for Sentinel-6 MF LR and 3.5 cm for Sentinel-6 MF HR. The latter is very close to Jason-3 mean value (3.4 cm). Curves for year 2022 only (solid lines) are aligned with curves for the entire timeseries (dotted lines).

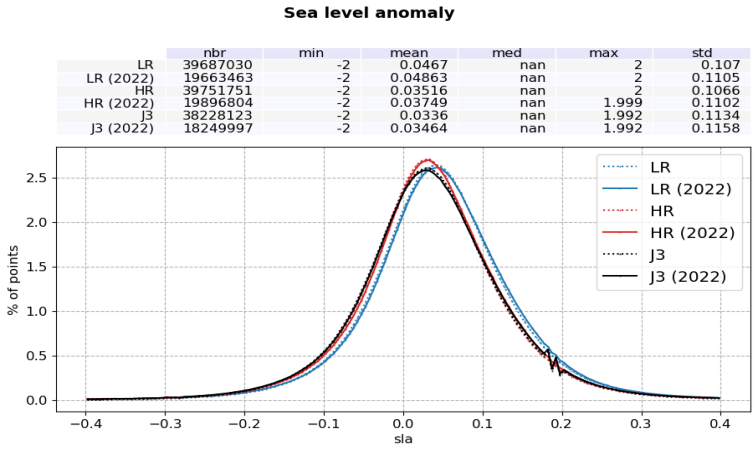


*Figure 101 – Histogram of SSHA in m for Sentinel-6 MF LR (blue), HR (red) and Jason-3 (black). Computed on the entire timeseries (dotted line) and on 2022 only (solid line).*

The mean SSHA cyclic monitoring is presented on figure 102, left panel. Sentinel-6 MF HR and Jason-3 SSHA are very close, and follow identical seasonal cycles and variations. The curves diverge between october and december 2022. This is due to the wet tropospheric correction drift discussed in section 4.9.2.. As observed on the histogram, Sentinel-6 MF LR SSHA is higher. It follows similar variations to that of HR SSHA.

On figure 102, right panel, is plotted the cyclic monitoring of the SSHA standard deviation. Curves are lower for Sentinel-6 MF LR and HR than Jason-3 by about 6mm up until the PB F07 update on 2022-08-15. With

this update, ionospheric correction was made available over the Caspian Sea, enabling SSHA computation and subsequently increasing the standard deviation of the entire dataset to levels consistent with Jason-3.

The drop in April 2022 in Jason-3 SSHA standard deviation is due to missing measurements during the orbit change after the end of the tandem phase (cf section 2.1.). Another drop at the end of the Jason-3 timeseries is caused by a switch to a defectuous Open Loop acquisition mode on December 5th 2022 with significant data loss in coastal areas due to a bug in terrain determination. A switch back to Close Loop acquisition mode was performed on January 23th 2023.

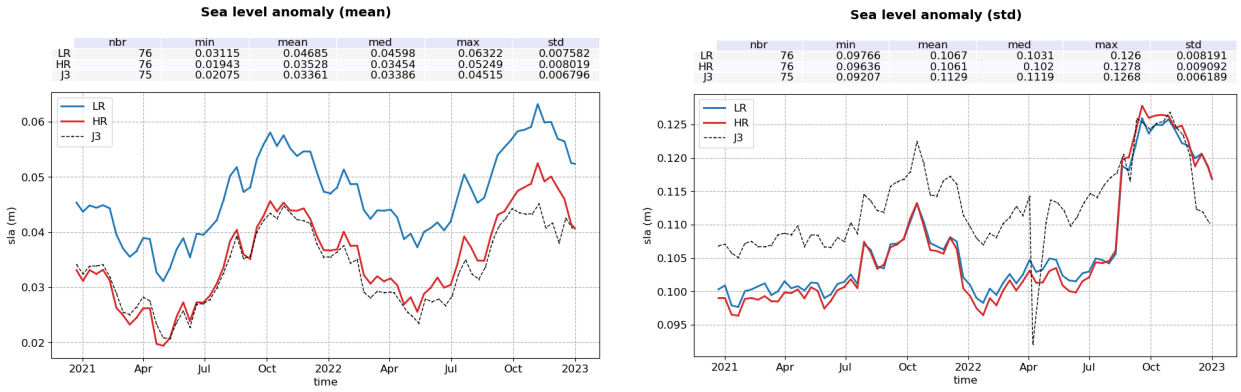


*Figure 102 – Mean (left) and standard deviation (right) SSHA by cycle for LR (red), HR (red) and Jason-3 (black).*

Figure 103 presents the monitoring of the SSHA computed with model WTC, both in mean (left panel), and standard deviation (right). The use of the model wet tropospheric correction has little impact on the SSHA mean (less than 0.5mm for both Sentinel-6 MF LR and HR and 1mm for Jason-3). As expected, the drift between Sentinel-6 MF HR and Jason-3 curves at the end of 2022 is no longer present.
The standard deviation of the SSHA is slightly impacted as well, and increases of about 0.5 mm for all datasets when using the model WTC.

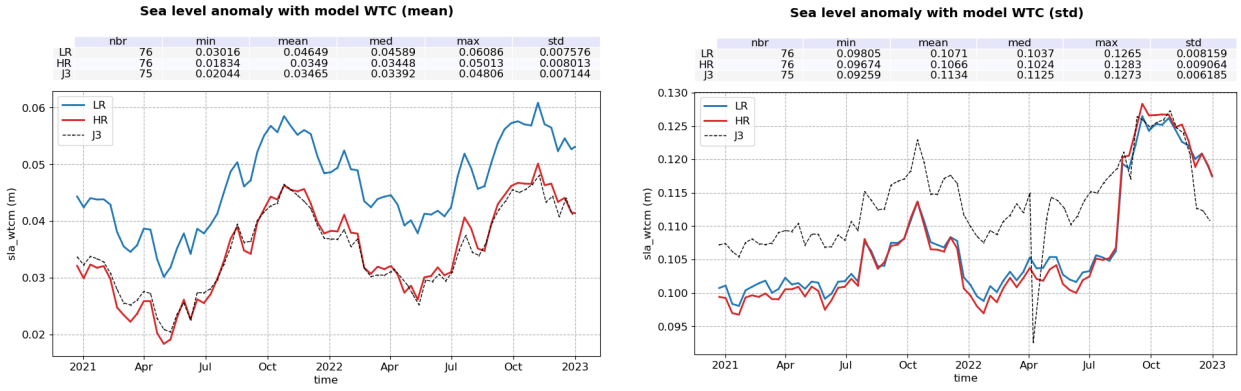


*Figure 103 – Mean (left) and standard deviation (right) SSHA with wet tropospheric correction from model by cycle for LR (red), HR (red) and Jason-3 (black).*

Over the tandem period, the average bias in SSHA between Sentinel-6 MF and Jason-3 is of 1.17 cm for LR and -0.05cm for HR. The time monitoring of this difference (figure 104) highlights two events of similar amplitudes in LR and HR:

- a jump of about +5 mm is visible after the satellite restart of 27-28 April 2021. This is partly caused by the jump in WTC (cf section 4.9.2.) of similar amplitude.
- a jump of about +2.5 mm is visible around the 20 January 2022. The origin is under investigation.

It is important to note here that we do not see any jump in the monitoring at POS4 switch to B-side on September 14th 2021. It is because the jumps visible on the SSB and the ionosphere correction are par-

tially cancelling themselves and because the SSHA difference has a standard deviation bigger than the jumps oberved. This standard deviation is stable in time and is centred around 3 cm in LR and 2.7 cm in HR (figure 105).

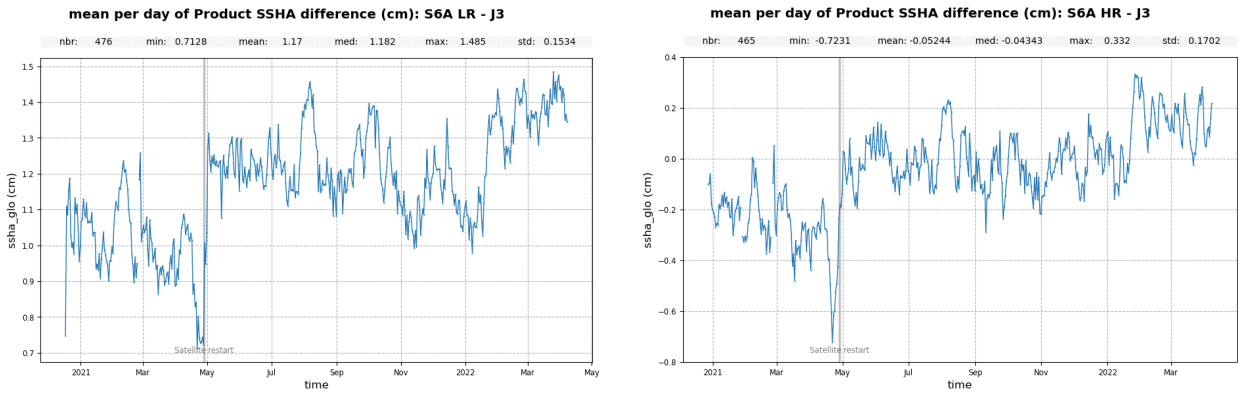


*Figure 104 – Time monitoring of product SSHA difference: Sentinel-6 MF LR (left) and HR (right) minus Jason-3. Mean per day computed over the complete tandem period.*

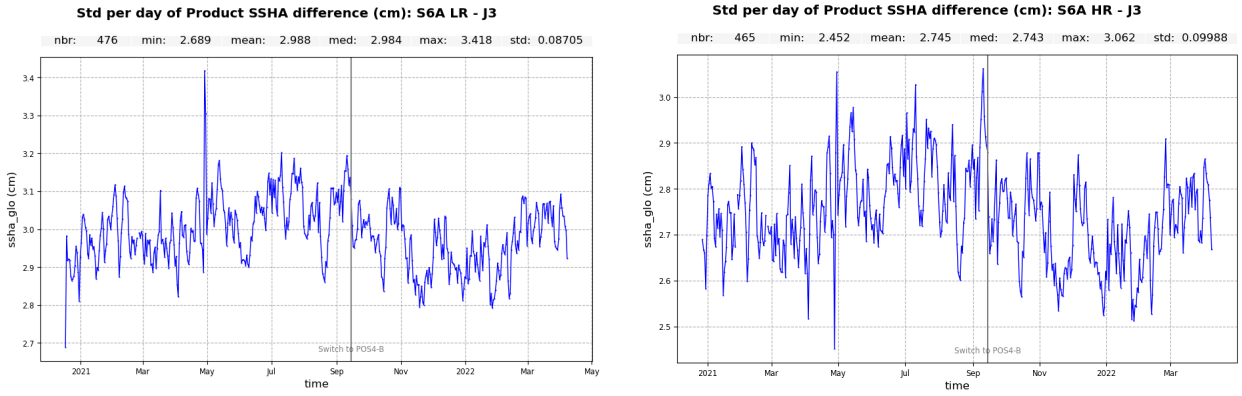


*Figure 105 – Time monitoring of product SSHA difference: Sentinel-6 MF LR (left) and HR (right) minus Jason-3. Standard deviation per day computed over the complete tandem period.*

In LR, the map of the SSHA residuals (figure 106 left panel) highlights a clear correlation to SWH. It increases by 1.3 cm between 2 and 7m wave, which is in line with the behavior observed on the orbit-range-mss and ionosphere correction bias. Future numerical retracker implemented in PB F08 should improve this behavior.
In HR (figure 106 right panel), the map of SSHA differences highlights a strong correlation to sea state condition, mainly due to the skeweness difference between Jason-3 and Sentinel-6 HR processings but also to the remaining impact of ocean vertical velocity on HR data. The later should be corrected in PB F09.
The equatorial band visible on the orbit-range-mss difference map is still observed on the SSHA difference map in both modes, with the same amplitude.

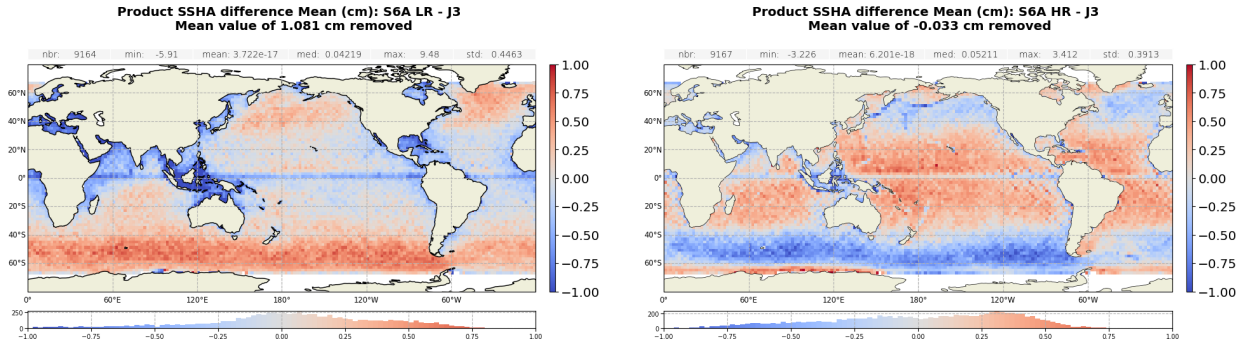


*Figure 106 – Gridded map of product SSHA difference: Sentinel-6 MF LR (left) and HR (right) minus Jason-3 computed over the complete tandem period.*

## 6.2. SSHA differences between HR and LR

Figure 107 presents the monitoring of the HR-LR SSHA differences. These differences are centred on -1.2cm, with an absolute value decrease that starts in the last quarter of 2021, after the switch to side B, with a drift of about +2mm up until the end of 2022. This drift is likely due to the absence of range walk correction in HR, discussed in section 4.3..

The standard deviation of these differences (right panel) is centred on 2.6cm with a yearly oscillation.

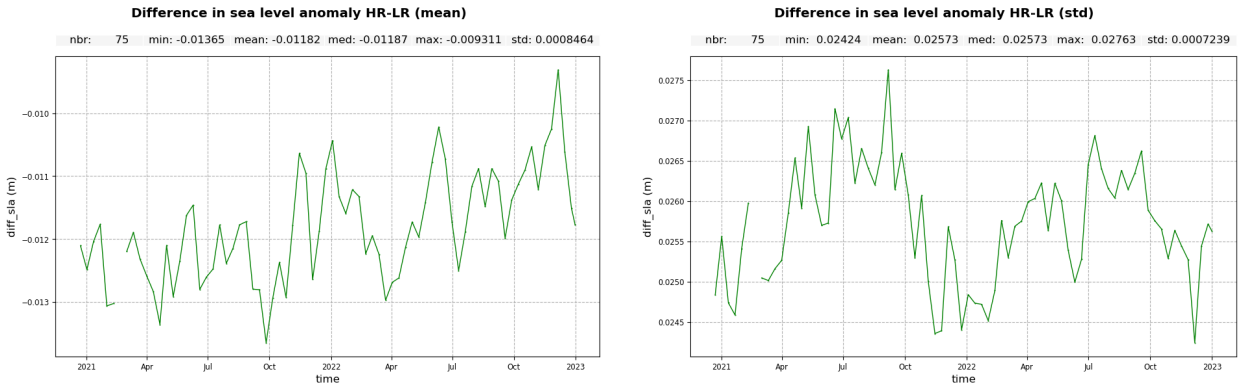


*Figure 107 – Mean (left) and standard deviation (right) SSHA HR-LR difference by cycle.*

The geographical distribution of the HR-LR SSHA differences is represented on figure 108. As expected from section 4.3., these differences are highly correlated with SWH and are due to the absence of skewness parameter in the HR processing.

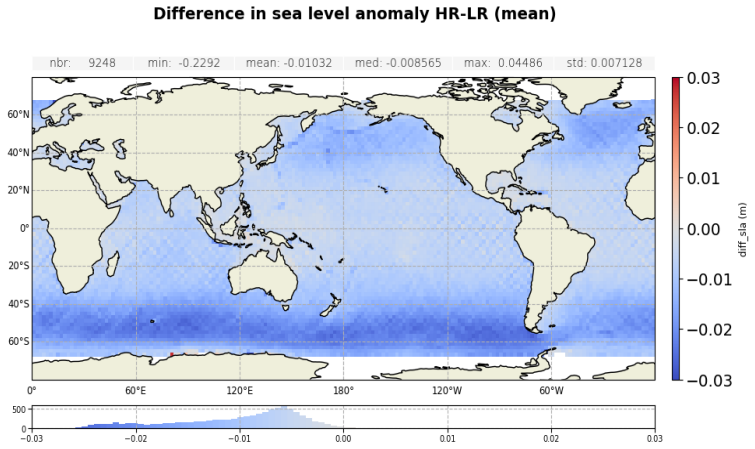


*Figure 108 – Map of mean SSHA HR-LR difference in meters. Computed on cycles 42 to 79.*

## 6.3. SSHA yearly variations

Figures 109 and 110 present the mean SSHA maps per year for 2021 and 2022 for Sentinel-6 MF LR and HR. No significant evolution is visible.

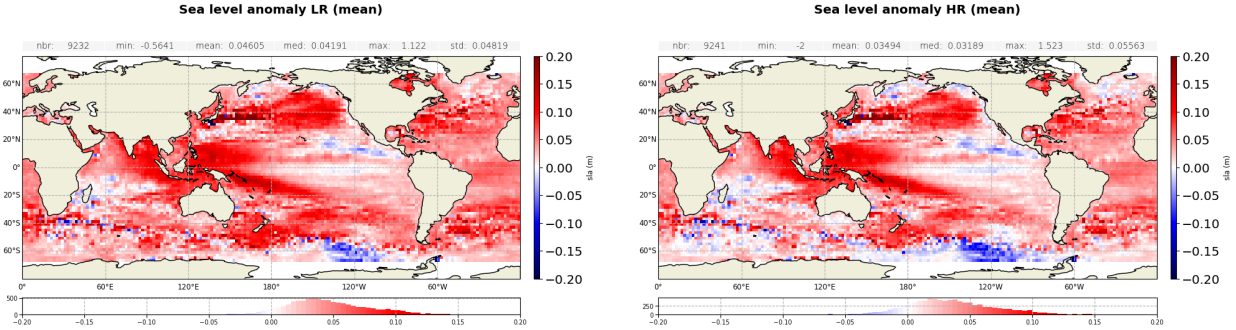


*Figure 109 – Map of mean SSHA for LR (left) and HR (right) in meters for the year 2021.*

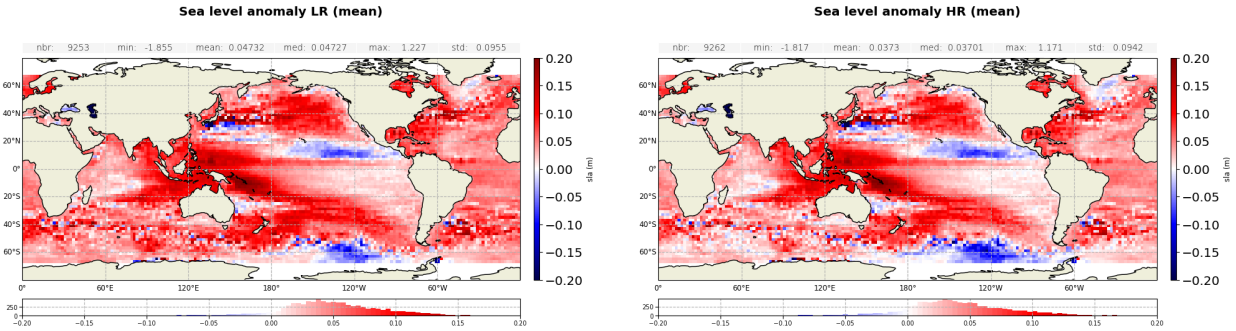


*Figure 110 – Map of mean SSHA for LR (left) and HR (right) in meters for the year 2022.*

Figures 111 and 112 present the standard deviation of SSHA maps per year for 2021 and 2022 for Sentinel-6 MF LR and HR. No significant evolution is visible.

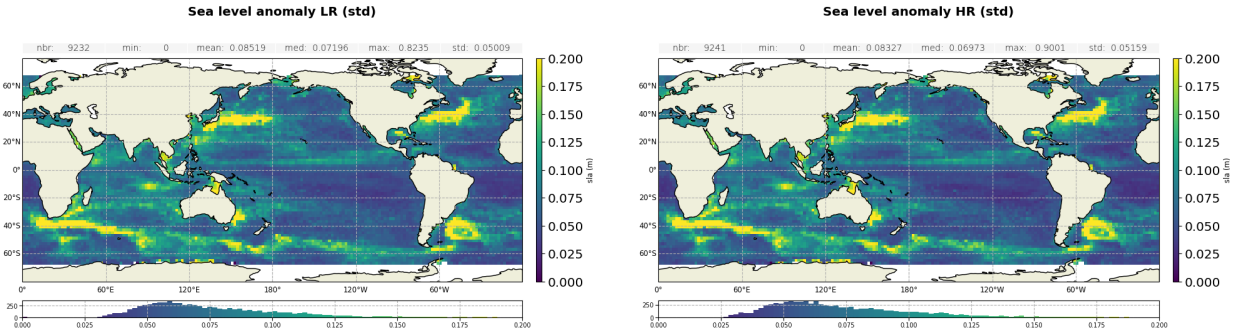


*Figure 111 – Map of SSHA standard deviation in m for LR (left) and HR (right) in meters for the year 2021.*

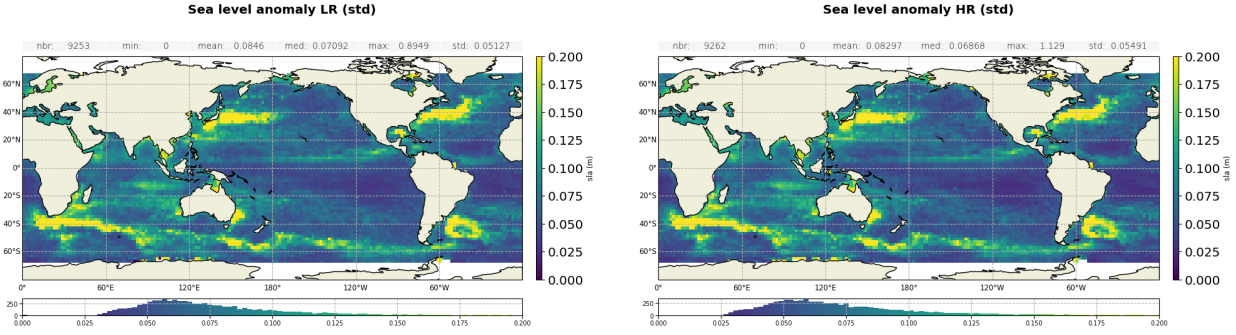


*Figure 112 – Map of SSHA standard deviation in m for LR (left) and HR (right) in meters for the year 2022.*

# 7 Mean Sea Level trends

## 7.1. Computation of the Mean Sea Level

The Global Mean Sea Level (GMSL) is one of the most important indicators of the climate change. In the past two decades, sea level has been routinely measured from space using satellite altimetry techniques. Sentinel-6 MF satellite is taking over the responsibility as the reference mission to continue the long-term record of sea-surface height measurements. The role of Copernicus Sentinel-6 Michael Freilich is not only to extend the GMSL climate record, but also to monitor the changing height of the sea surface with greater precision than before.

Over the tandem phase of Sentinel-6 MF (till cycle 051), both Jason-3 and Sentinel-6 MF satellites flew on the same ground track, only 30s apart. They therefore measured the same ocean, allowing to calibrate Sentinel-6 MF. This allowed to link precisely the MSL time series of Jason-3 and Sentinel-6 MF. The uncertainty of the bias value between the two time series is less than 1 mm. The evolution of the ocean MSL can therefore be precisely observed on a continuous basis since 1993 thanks to the 5 reference missions: TOPEX/Poseidon, Jason-1 (from may 2002 to october 2008), Jason-2 (from october 2008 to may 2016), Jason-3 (from may 2016 to april 2022) and now Sentinel-6 MF (from april 2022 onwards).
Please note that only LR mode in used in MSL computations.

Wet troposphere correction, inverse barometer correction, GIA (-0.3 mm/yr) are applied to calculate the MSL and the data series are linked together accurately thanks to the tandem flying phases. The following global bias are applied: 1.16 cm between T/P and Jason-1, 0.23 cm between Jason-1/Jason-2, -2.97 cm between Jason-2/Jason-3 and -0.21 cm for Jason-3/Sentinel-6 MF. The uncertainty relative to this Jason-3/Sentinel-6 MF global bias, which is exclusively computed on Sentinel-6 MF side B, is 0.2mm at 1 sigma.

An exhaustive overview of possible errors impacting the MSL evolution is given in [12]. Furthermore, annual and semi-annual signals are removed from the time serie and a 2-month filter is applied. For more details about Mean Sea Level (MSL) estimation method, see the dedicated report on the MSL Aviso Website: http://www.aviso.altimetry.fr/msl. This report includes the description of the Mean Sea Level indicator, the comparisons between altimetry and tide gaudes measurements, the comparisons between altimetry and ARGO+GRACE measurements and specific studies linked to MSL activities.

Though mean sea level trend is globally positive, it is inhomogeneously distributed over the ocean: locally, sea level rise or decline up to $\pm$10 mm/yr are observed as shown on the right panel of figure 113 (note that this map of regional MSL trends is estimated from multi-mission grids (Copernicus Climate Change Service products) in order to improve spatial resolution).

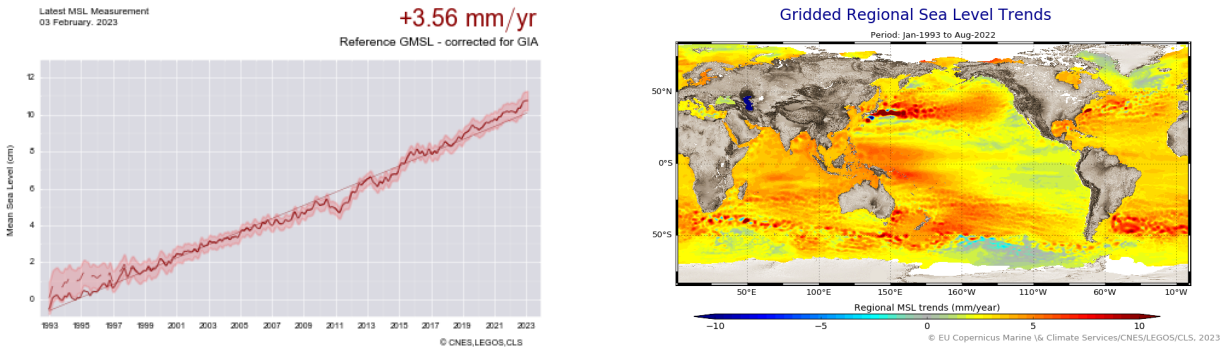


*Figure 113 – Global (left) and regional (right) MSL trends from 1993 onwards.*

## 7.2. Comparison of LR and HR GMSL

This section focusses on GMSL derived from Sentinel-6 MF from the switch to POS4-B to the end of 2022. The GMSL for LR and HR modes are plotted on figure 114, along with Jason-3 estimate over the same period. This GMSL is computed on a 2-months low-pass filtered data, after having removed the seasonal signals. Such computation is performed with an Ordinary Least Square (OLS) approach, using SSHA from L2 products as input. The details on the computation of the GMSL and its uncertainties are described in Guerou et al. (2022) [12].

Sentinel-6 MF LR and HR show trends with slopes at 4.74 $\pm$ 1.84 mm/yr and 6.03 $\pm$ 1.84 mm/yr respectively. Over the same time period, Jason-3 GMSL trend is of 0.93 $\pm$ 1.83 mm/yr. Uncertainties are given at the 1 sigma confidence level. These trends strongly change when using wet tropospheric correction from model, as shown on the dashed curves of figure 114 and in table 8. It shows the impact of the instability in the radiometer WTC on GMSL estimation (see section 4.9.).

Please note that the side B GMSL presented here are computed on a small timescale (less than 16 months) and therefore are strongly impacted by correlated noise leading to significant uncertainties.

| Mission | Trend with AMR WTC (mm/yr) | Trend with model WTC (mm/yr) |
|---|---|---|
| Sentinel-6 MF LR | 4.74 $\pm$ 1.81 | 2.57 $\pm$ 1.81 |
| Sentinel-6 MF HR | 6.03 $\pm$ 1.82 | 3.86 $\pm$ 1.82 |
| Jason-3 | 0.93 $\pm$ 1.82 | 2.09 $\pm$ 1.79 |

*Table 8 – GMSL trend values and corresponding 1 sigma uncertainties for Sentinel-6 MF LR, HR and Jason-3 (on the Sentinel-6 MF period), with AMR and model wet tropospheric corrections. Computed over POS4-B period, i.e. from cycle 32 onwards.*

Sentinel-6 MF GMSL are impacted by three known effects, **none of which are taken into account in the uncertainties computation**:

- the evolution of the PTR shape in the range direction. It impacts range (PTR dissymmetry) and SWH estimates (main lobe width) both in LR and HR. Numerical rectracker allows to account for the PTR shape evolution thanks to the use of true PTRs. Such retrackers will be implemented in the upcoming PDAP processing baseline : F08 for LR and F09 for HR.
- the evolution of the PTR shape in the azimuth direction, impacting HR range only. It is corrected thanks to the range walk correction, that will be available in PB F09 (end of 2023).

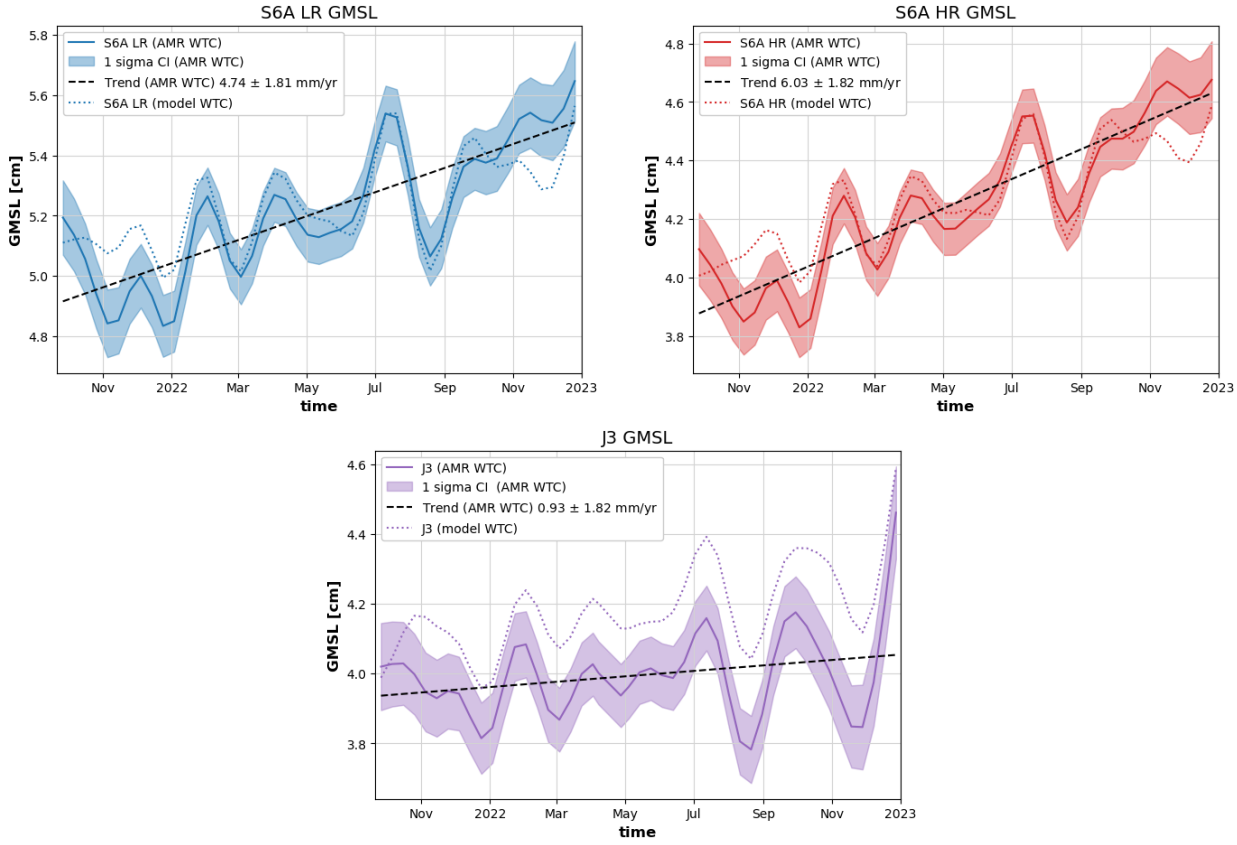


*Figure 114 – GMSL from Sentinel-6 MF LR data (top left), Sentinel-6 MF HR data (top right) and from Jason-3 GDR-F data with a 1 sigma confidence interval. Computed over Sentinel-6 MF POS4-B period, i.e. from cycle 32 onwards.*

- Additionally, the wet tropospheric correction drift presented in section 4.9.2. impact on Sentinel-6 A GMSL is very significant due to the 16 months timescale. This drift will however be corrected in the upcoming PB F08 PDAP reprocessing.

Table 9 summarizes the impact of these effects on Sentinel-6 MF POS4-B, based on Dinardo 2022 study [9]. Looking at LR data with model WTC, once the estimated error removed, the retrieved trend is of 2.27 mm/yr. This value is consistent with Jason-3 GMSL trend. Thanks to the upcoming PB F08 reprocessing and the stability improvement brought by the numerical retracker on Sentinel-6 MF LR GMSL should be more precisely computed.
In HR, the resulting GMSL trend is low (0.46 mm/yr). Please note that the Dinardo 2022 study only covers the first 9 months of side B, from September 2021 to June 2022, and that values may be different for the second half of 2022 because of an expected on-going stabilization.
Further investigations will be perfomed based on F09 reprocessed data to precisely quantify the impact of numerical retracking and range walk on Sentinel-6 MF HR data long term stability.

| | LR | HR |
|---|---|---|
| **GMSL trend with model WTC** | 2.57 $\pm$ 0.51 mm/yr | 3.86 $\pm$ 0.44 mm/yr |
| **GMSL errors estimate:** | | |
| Due to the absence of numerical rtk | 0.3 mm/yr | 0.3 mm/yr |
| Due to the absence range walk correction | N/A | 3.1 mm/yr |
| **Resulting GMSL trend** | 2.27 mm/yr | 0.46 mm/yr |

*Table 9 – GMSL errors from Dinardo 2022 [9]. Estimated using POS4-B data.*

# 8 System Requirements

In this section, the system requirements are verified for NTC data, in LR and in HR.

## 8.1. LR

### 8.1.1. R-S-00260

| Requirement | Status |
|---|---|
| For low-resolution ALT-NTC products, the standard deviation of the 1-second along-track averaged corrected low-resolution altimeter range measurements shall be less than 2.83 cm.<br>Note: This requirement is based on the apportionment given in the table of the Sentinel-6 low-resolution altimetry error budget at the end of the document.<br>Note: Like all performance requirements on the altimeter, unless specified otherwise, this specifies the maximum global RMS error over open ocean.<br>Note: A goal is 1.73 cm. | Not addressed in this report |

*Table 10 – R-S-00260*

### 8.1.2. R-S-00270

| Requirement | Status |
|---|---|
| For low-resolution ALT-NTC products, the noise of the 1-second along-track average of the low-resolution Ku-band altimeter range measurements shall be less than 1.5 cm at 2 m significant wave height.<br>Note: the requirement is applicable after ground re-tracking.<br>Note: The upper limit depends on SWH: 1.2 cm at 1 m SWH, 1.5 cm at 2 m SWH, 2.4 cm at 5 m SWH, and 3.2 cm at 8 m SWH.<br>Note: A goal is 1.0 cm at 2 m SWH | **OK** |

*Table 11 – R-S-00270*

To estimate the noise of 1-second along-track average of the LR Ku-band altimeter range, we analyse "data_01/ku/range_ocean_rms" variable from LR products. It contains the standard deviation of 20 Hz measurements used for the compression to 1hz. To retrieve 1 Hz level of noise, this value is divided by $\sqrt{20}$.

The resulting 1 Hz level of noise averaged over the complete period is plotted function of SWH on figure 115, left panel. As expected, Sentinel-6 MF LR noise level is well below Jason-3 level and below the system requirement (green curve) over almost all the SWH spectrum. For 1 m wave, the level of noise is slightly above the note in the requirement with a value of 1.24 cm and an upper limit at 1.2 cm. Please note that the requirement itself, i.e. the 2m SWH limit, is met. Table 12 reports the level of noise for the stated SWH values.

This noise level is stable in time, as shown on the cyclic monitoring of figure 115, right panel.

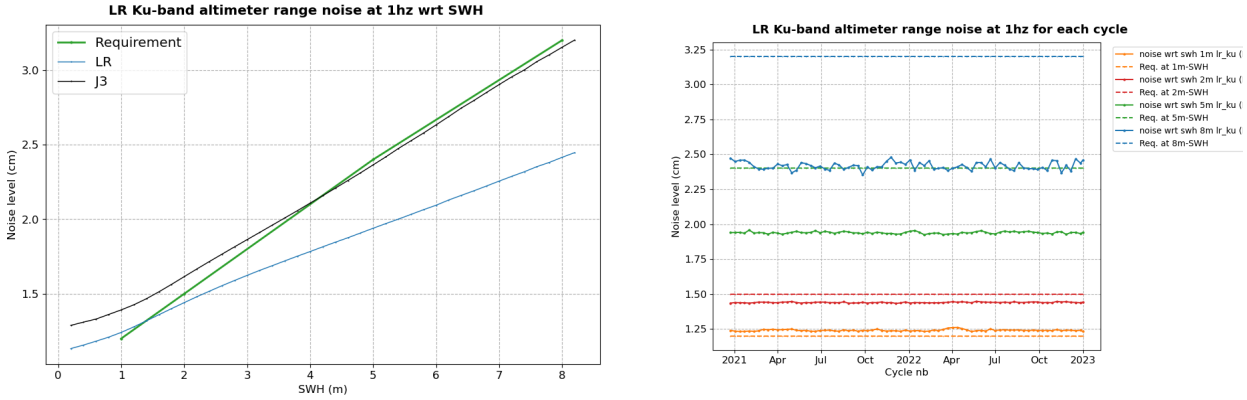


*Figure 115 – 1 Hz noise of LR Ku-band altimeter range. Left panel: noise function of SWH for Sentinel-6 MF LR and Jason-3; the green line represents the requirement thresholds. Right panel : noise level computed for each cycle and at 1, 2, 5 and 8 m-wave (solid lines) and the corresponding requirement levels (dashed lines).*

| SWH | Requirement | Noise level |
|---|---|---|
| **1 m** | **1.2 cm** | **1.24cm** |
| 2 m | 1.5 cm | 1.44 cm |
| 5 m | 2.4 cm | 1.94 cm |
| 8 m | 3.2 cm | 2.42 cm |

*Table 12 – 1 Hz noise of LR Ku-band altimeter range at 1, 2, 5 and 8 m-wave.*

### 8.1.3. R-S-00280

| Requirement | Status |
|---|---|
| For low-resolution ALT-NTC products, the noise of the 1-second along-track average of the C-band altimeter range measurements shall be less than 5.7 cm at 2 m significant wave height.<br>Note: the requirement is applicable after ground re-tracking.<br>Note: The upper limit depends on SWH: 4.5 cm at 1 m SWH, 5.7 cm at 2 m SWH, 9.1 cm at 5 m SWH, and 12.0 cm at 8 m SWH | **OK** |

*Table 13 – R-S-00280*

Similarly to Ku-band, we analyse "data_01/c/range_ocean_rms" variable from LR products to estimate the noise of 1-second along-track average of the LR C-band altimeter range.

The resulting 1 Hz level of noise averaged over the complete period is plotted as a function of SWH on figure 116, left panel. Sentinel-6 MF LR noise level is and below the system requirement (green curve) over all the SWH spectrum. Table 14 reports the level of noise for the stated SWH values.

This noise level is stable in time, as shown on the cyclic monitoring of figure 116, right panel.

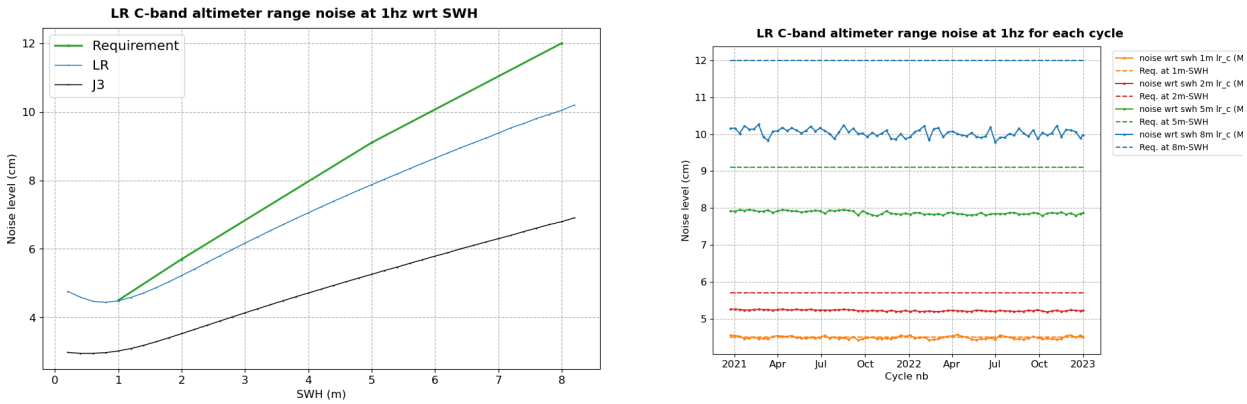


*Figure 116 – 1 Hz noise of LR C-band altimeter range. Left panel: noise function of SWH for Sentinel-6 MF LR and Jason-3; the green line represents the requirement thresholds. Right panel : noise level computed for each cycle and at 1, 2, 5 and 8 m-wave (solid lines) and the corresponding requirement levels (dashed lines).*

| SWH | Requirement | Noise level |
|---|---|---|
| 1 m | 4.5 cm | 4.5 cm |
| 2 m | 5.7 cm | 5.2 cm |
| 5 m | 9.1 cm | 7.9 cm |
| 8 m | 12 cm | 10.0 cm |

*Table 14 – 1 Hz noise of LR C-band altimeter range at 1, 2, 5 and 8 m-wave.*

### 8.1.4. R-S-00290

| Requirement | Status |
|---|---|
| For low-resolution ALT-NTC products, the contribution of the ionosphere correction error to the standard deviation of the 1-second along-track averaged corrected low-resolution altimeter range measurements shall be less than 0.5 cm.<br>Note: Derived from C and Ku band and averaged over 200 km.<br>Note: Like all performance requirements on the altimeter, unless specified otherwise, this specifies the maximum global RMS error over open ocean.<br>Note: A goal is 0.3 cm | **OK** |

*Table 15 – R-S-00290*

To quantify the contribution of the ionosphere correction error to the standard deviation of 1 Hz corrected LR range, several metrics are checked.

A first estimation of filtered ionosphere correction error is performed by checking the noise between consecutive measurements. The results shows a very low level of noise, way below the mm (figure 118), except for a single pass (cycle 15 pass 1), for which rapid ionosphere variations near the equator caused significant jumps between land masses around Indonesia. Even this extreme case is compliant with requirements.

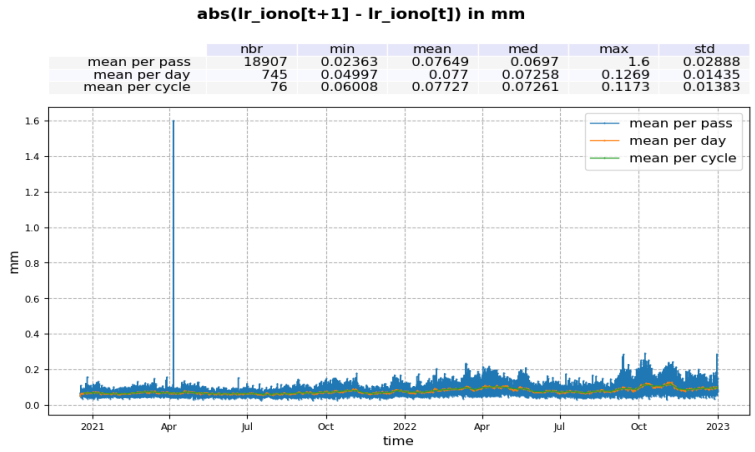


*Figure 117 – Absolute value of consecutive filtered ionosphere correction measurement. Mean per pass (blue), mean per day (orange) and mean per cycle (green).*

Comparison to Jason-3 filtered ionosphere correction highlights a standard deviation ranging between 2 and 4.5 mm (figure 118 left panel). And finally, comparison to ionosphere correction derived from GIM model shows a standard deviation ranging between 3.5 mm and 1.5 cm (figure 118 right panel). These values are all within requirement.

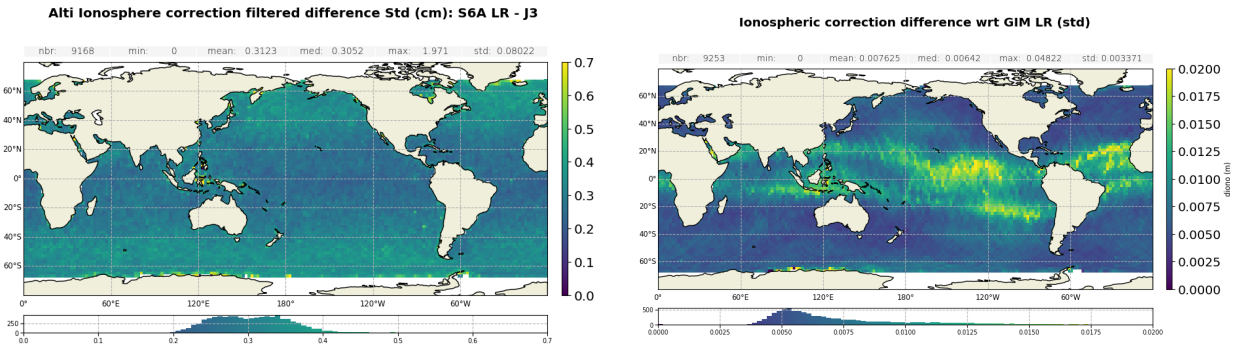


*Figure 118 – Left : Standard deviation gridded map of Altimeter Filtered Ionosphere correction Sentinel-6 MF-Jason-3 difference (cm). Computed over the tandem phase (cycles 4 to 51). Right : Standard deviation gridded map of the difference between Altimeter Filtered Ionosphere correction and GIM model (m). Computed over cycles 42 to 79.*

### 8.1.5. R-S-00300

| Requirement | Status |
|---|---|
| For low-resolution ALT-NTC products, the contribution of the sea state bias error to the standard deviation of the 1-second along-track averaged corrected low-resolution altimeter range measurements shall be less than 2.0 cm.<br><br>Note: Like all performance requirements on the altimeter, unless specified otherwise, this specifies the maximum global RMS error over open ocean.<br><br>Note: A goal is 1.0 cm | **OK** |

*Table 16 – R-S-00300*

As for ionosphere correction, a first estimation of the SSB error is performed by checking the noise between consecutive measurements. The results shows a low level of noise, below the cm (figure 119).

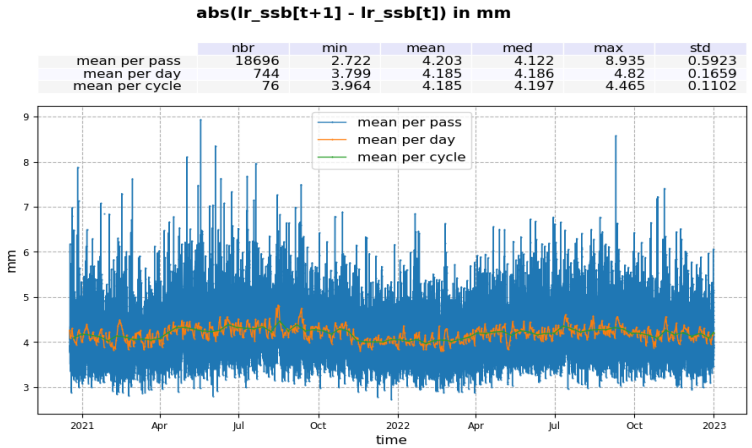


*Figure 119 – Absolute value of consecutive LR sea state bias measurement. Mean per pass (blue), mean per day (orange) and mean per cycle (green).*

Comparison to Jason-3 SSB highlights a standard deviation ranging between 4.5 and 7.5 mm (figure 120). These values are within requirement.

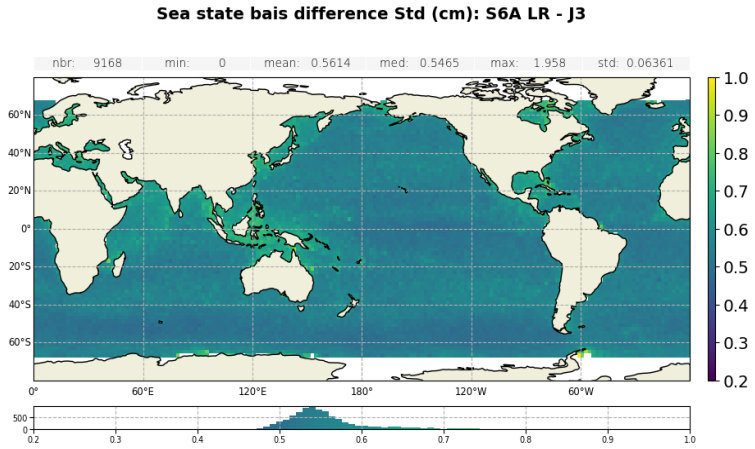


*Figure 120 – Standard deviation gridded map of Ku-band SSB difference: Sentinel-6 MF LR minus Jason-3 computed over the complete tandem period.*

### 8.1.6. R-S-00310

| Requirement | Status |
|---|---|
| For low-resolution ALT-NTC products, the contribution of the dry tropospheric correction error to the standard deviation of the 1-second along-track averaged corrected low-resolution altimeter range measurements shall be less than 0.7 cm.<br><br>Note: this requirement applies to the model to be used to calculate the dry troposphere model.<br><br>Note: Like all performance requirements on the altimeter, unless specified otherwise, this specifies the maximum global RMS error over open ocean.<br><br>Note: A goal is 0.5 cm | **OK** |

*Table 17 – R-S-00310*

The dry troposphere correction model are identical between Jason-3 and Sentinel-6 MF products: same model and same estimation from model.

Analysis have shown that the two retrievals are indeed perfectly in line (see figure 121).

System requirement for Jason-3 dry troposphere correction is the same as Sentinel-6 MF present requirement and it has been shown that Jason-3 dry troposphere correction is compliant.

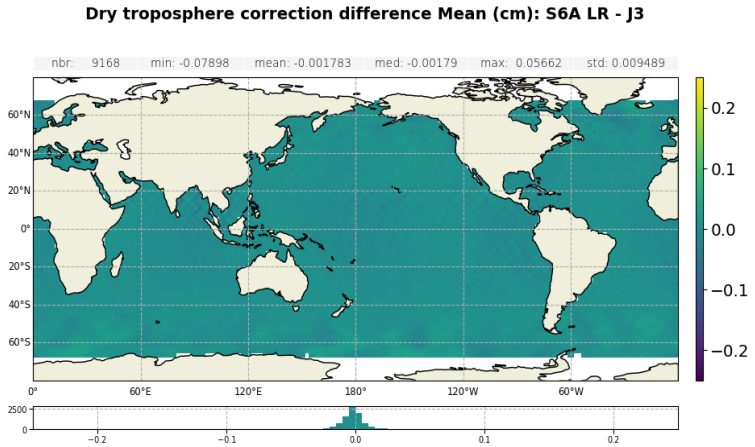


*Figure 121 – Mean gridded map of dry tropospheric correction difference: Sentinel-6 MF LR minus Jason-3. Computed over cycles 4 to 51.*

### 8.1.7. R-S-00320

| Requirement | Status |
|---|---|
| For low-resolution ALT-NTC products, the contribution of the wet tropospheric correction error to the standard deviation of the 1-second along-track averaged corrected low-resolution altimeter range measurements shall be less than 1.0 cm.<br>Note: Like all performance requirements on the altimeter, unless specified otherwise, this specifies the maximum global RMS error over open ocean.<br>Note: A goal is 0.8 cm | **OK** |

*Table 18 – R-S-00320*

A first estimation of AMR-C WTC error is performed by checking the noise between consecutive measurements. The results shows a very low level of noise, below 2 mm (figure 122).

Comparison to Jason-3 AMR WTC highlights a standard deviation below 8 mm (figure 123). These values are within requirement.

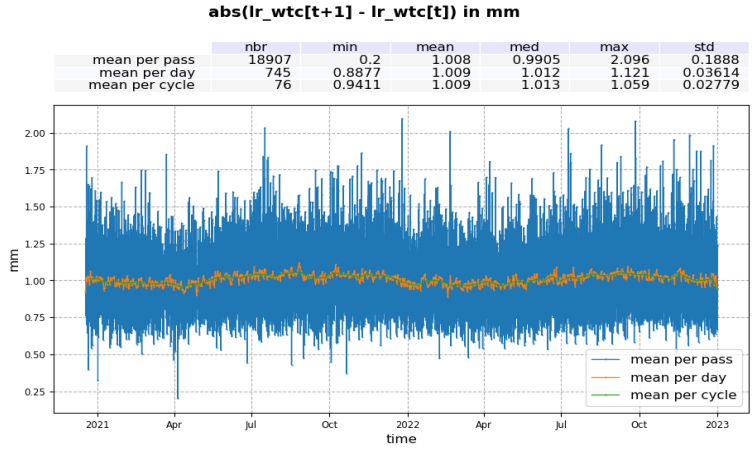


*Figure 122 – Absolute value of consecutive AMR-C WTC measurement in mm. Mean per pass (blue), mean per day (orange) and mean per cycle (green).*

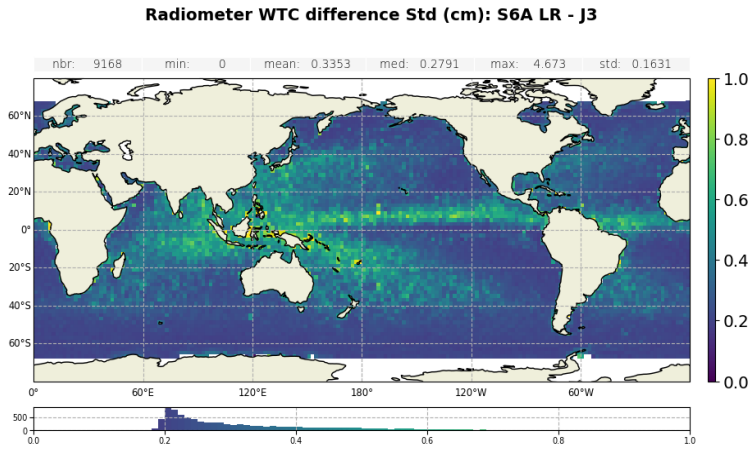


*Figure 123 – STD gridded map of AMR WTC difference: Sentinel-6 MF LR minus Jason-3, in cm. Computed over cycles 4 to 51.*

### 8.1.8. R-S-00330

| Requirement | Status |
|---|---|
| For low-resolution ALT-NTC products, the standard deviation of the determination of the radial component of the orbit shall be less than 1.5 cm.<br><br>Note: This requirement is applicable to the orbital solution derived from the combined set of data from DORIS, GNSS-POD and LRA.<br><br>Note: Orbit errors have a larger than 1000 km length scale, significantly different from the 1 Hz altimetry noise. Nevertheless the orbit error is added in a RSS sense, presuming that the error is uncorrelated from cycle to cycle at the same location.<br><br>Note: a goal is 1.0 cm | Not addressed in this report |

*Table 19 – R-S-00330*

### 8.1.9. R-S-00340

| Requirement | Status |
|---|---|
| For low-resolution ALT-NTC products, the standard deviation of the 1-second along-track averaged corrected low-resolution measurements of sea surface height shall be less than 3.20 cm.<br><br>Note: This requirement is based on the apportionment given in the table of the Sentinel-6 low-resolution altimetry error budget at the end of the document.<br><br>Note: Like all performance requirements on the altimeter, unless specified otherwise, this specifies the maximum global RMS error over open ocean.<br><br>Note: A goal is 1.99 cm | **OK** |

*Table 20 – R-S-00340*

To verify this requirement, the crossover analysis presented in section 5.2. is used. The standard deviation of corrected LR SSH difference is centred around 4.7 cm (see figure 92). It means that the error is of 3.3 cm (standard deviation divided by $\sqrt{2}$). This value is slightly above requirement. However looking at a region with low variability, for example the pacific patch, the error is of 2.25 cm in average. On a cyclic basis, this error is always below the requirement limit of 3.2 cm as shown on figure 124.

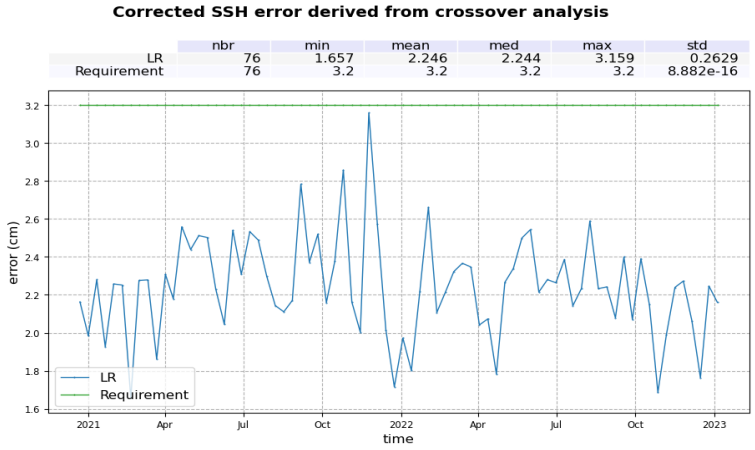


*Figure 124 – Corrected LR SSH error derived from crossover analysis with a selection over Pacific patch (latitude in [-24.5 °N; -3 °N] and longitude in [220 °E; 246 °E]), in cm. The error equals to the standard deviation of the SSH difference divided by $\sqrt{2}$. Computed on a cyclic basis.*

### 8.1.10. R-S-00350

| Requirement | Status |
|---|---|
| For low-resolution ALT-NTC products, the uncertainty of 1-second along-track averaged low-resolution measurements of significant wave height in the range 0.5 to 8 m shall be less than 15 cm plus 5% of significant wave height.<br>Note: This is based on the combination of noise and systematic error.<br>Note: A goal is 10 cm plus 5% of significant wave height | **OK** |

*Table 21 – R-S-00350*

LR Ku-band SWH are compared to SWH derived from ERA-5 model on figure 125. It shows a good consistancy between the two datasets, the difference being below requirement limit over the complete SWH spectrum.

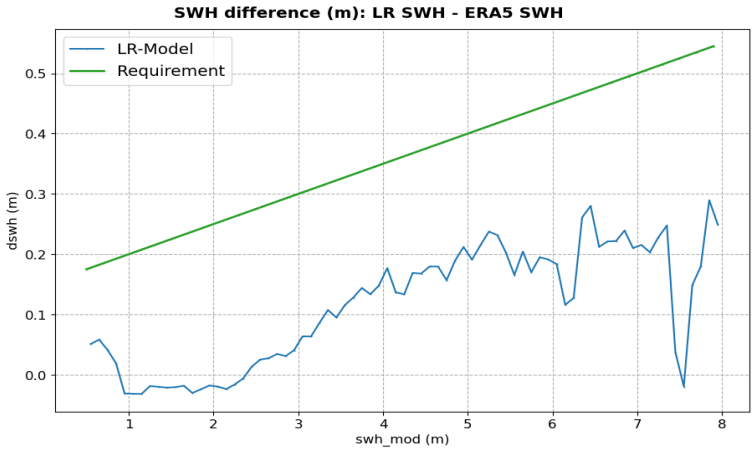


*Figure 125 – SWH difference between Sentinel-6 MF LR data and ERA-5 SWH, plotted function of ERA-5 SWH. Computed over Sentinel-6 MF cycle 70. Green lines represent requirement limits. Results are identical for all cycles.*

### 8.1.11. R-S-00355

| Requirement | Status |
|---|---|
| For low-resolution ALT-NTC products, significant wave heights shall be provided up to at least 20 m.<br>Note: The measurement performance under high sea state conditions will be determined during commissioning | **OK** |

*Table 22 – R-S-00355*

Figure 126 shows the maximum value per cycle of Sentinel-6 MF LR SWH. The values are above 20 m, as

expected.

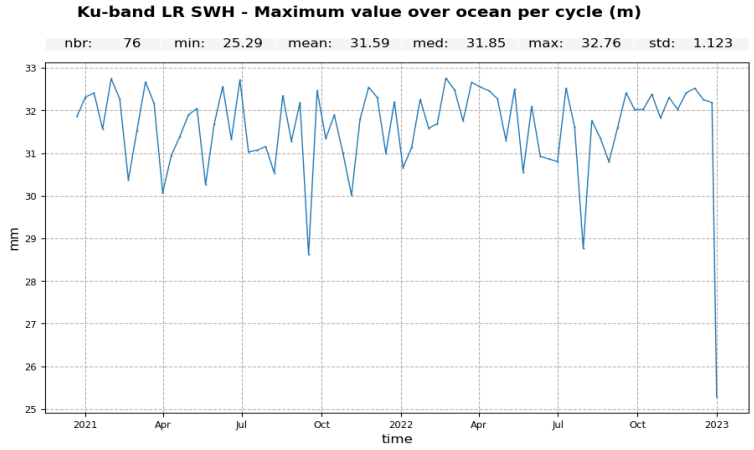


*Figure 126 – Maximum value of Sentinel-6 MF LR SWH per cycle.*

### 8.1.12. R-S-00360

| Requirement | Status |
|---|---|
| For low-resolution ALT-NTC products, the uncertainty of 1-second along-track averages of 10 meter wind speed over ocean surfaces, derived from low-resolution altimeter measurements, shall be better than 1.5 m/s for wind speeds in the range 3 m/s to 20 m/s.<br>Note: Wind speed refers to the wind (not neutral wind) speed at a reference height of 10 meters above the sea surface.<br>Note: This wind speed accuracy requirement translates to an accuracy requirement on the backscatter.<br>Note: A goal is 1.0 m/s | **OK** |

*Table 23 – R-S-00360*

To verify the uncertainty of Sentinel-6 MF LR altimeter wind-speed, a comparison to model is performed. The model wind speed used is derived from U and V components provided in L2 product ("data_01/wind_speed_mod_ and "data_01/wind_speed_mod_v"). Difference between altimeter and model wind speed is plotted on figure 127 function of model wind speed. Values are within requirement.

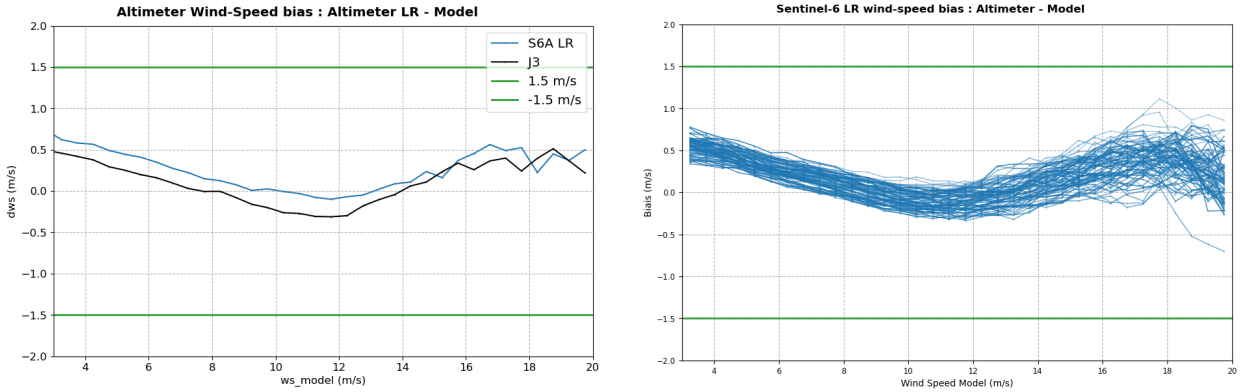


*Figure 127 – Difference between Altimeter LR wind speed and model wind speed function of model wind speed, in m/s. Computed over Sentinel-6 MF cycle 70 (left) and for all cycles (right, darker curves correspond to more recent cycles). Green lines represent requirement limits.*

### 8.1.13. R-S-00370

| Requirement | Status |
|---|---|
| For low-resolution ALT-NTC products, the absolute accuracy of 1-second along-track averaged low-resolution measurements of normalised radar cross-section at Ku-band and vertical incidence, in the range 7 to 16 dB, shall be better than 0.3 dB.<br><br>Note: This value (0.3 dB) is not the value at satellite level (1 dB), but it is achieved after external in-flight calibration to ensure coherence with other missions. In other words, 0.3 dB is the global value, what allows 1 dB at satellite level, to be compensated by the ground processing.<br><br>Note: This requirement also sets limits on the accuracy of sigma0 attenuation correction to be supplied by the radiometer | Not addressed in this report |

*Table 24 – R-S-00370*

The absolute accuracy of the LR sigma0 is not addressed in this report as there is currently no facility available to measure it.

## 8.2. HR

### 8.2.1. R-S-00680

| Requirement | Status |
|---|---|
| For high-resolution ALT-NTC products, the standard deviation of the 1-second along-track averaged corrected high-resolution altimeter range measurements shall be less than 2.53 cm.<br>Note: This requirement is based on the apportionment given in the table of the Sentinel-6 high-resolution altimetry error budget at the end of the document.<br>Note: Note: Like all performance requirements on the altimeter, unless specified otherwise, this specifies the maximum global RMS error over open ocean.<br>Note: Note: A goal is 1.49 cm. | Not addressed in this report |

*Table 25 – R-S-00680*

### 8.2.2. R-S-00690

| Requirement | Status |
|---|---|
| For high-resolution ALT-NTC products, the noise of the 1-second along-track average of the high-resolution Ku-band altimeter range measurements shall be less than 0.8 cm at 2 m significant wave height.<br>Note: the requirement is applicable after ground re-tracking.<br>Note: The upper limit depends on SWH: 0.7 cm at 1 m SWH, 0.8 cm at 2 m SWH, 1.3 cm at 5 m SWH, and 2.0 cm at 8 m SWH.<br>Note: A goal is 0.5 cm at 2m SWH | **OK** |

*Table 26 – R-S-00690*

Similarly to LR, we analyse "data_01/ku/range_ocean_rms" variable from HR products to estimate the noise of 1-second along-track average of the HR Ku-band altimeter range.

The resulting 1 Hz level of noise averaged over the complete period is plotted function of SWH on figure 128, left panel. As expected, Sentinel-6 MF HR noise level is well below Jason-3 and Sentinel-3A levels. However, Sentinel-6 MF HR noise level is above the additional note in the requirement (green curve) for 5 m and 8 m wave upper limits. Please note that the requirement itself, i.e. the 2m SWH limit, is met. Table 27 reports the level of noise for the stated SWH values.

Please note that the use of a numerical retracking for HR will improve noise levels and will be implemented in the coming PB F09 update.

This noise level is stable in time, as shown on the cyclic monitoring of figure 128, right panel.

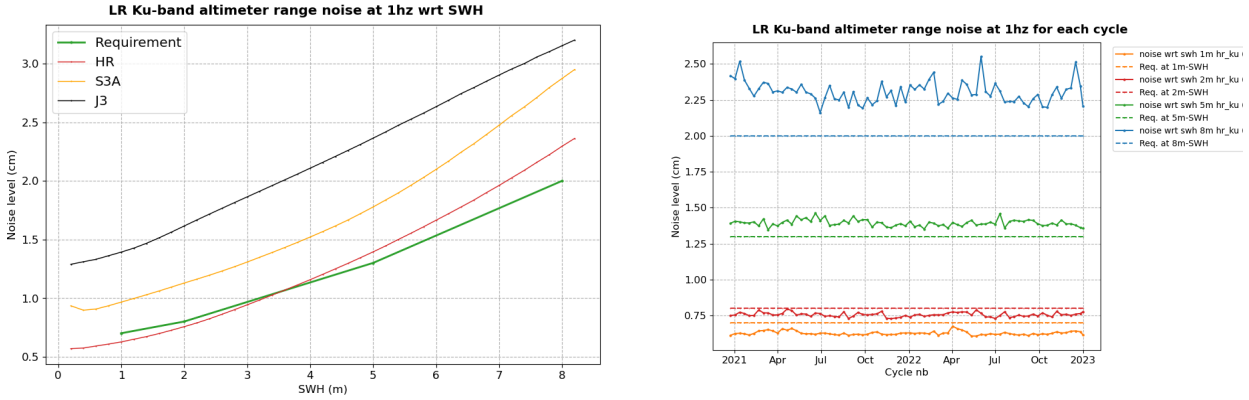


*Figure 128 – 1 Hz noise of HR Ku-band altimeter range, in cm. Left panel: noise function of SWH in m for Sentinel-6 MF HR and Jason-3; the green line represents the requirement thresholds. Right panel : noise level computed for each cycle and at 1, 2, 5 and 8 m-wave (solid lines) and the corresponding requirement levels (dashed lines).*

| SWH | Requirement | Noise level |
|---|---|---|
| 1 m | 0.7 cm | 0.63 cm |
| 2 m | 0.8 cm | 0.76 cm |
| **5 m** | **1.3 cm** | **1.39 cm** |
| **8 m** | **2.0 cm** | **2.30 cm** |

*Table 27 – 1 Hz noise of HR Ku-band altimeter range at 1, 2, 5 and 8 m-wave.*

### 8.2.3. R-S-00700

| Requirement | Status |
|---|---|
| For high-resolution ALT-NTC products, the contribution of the ionospheric correction error to the standard deviation of the 1-second along-track averaged corrected high-resolution altimeter range measurements shall be less than 0.5 cm.<br>Note: Derived from C and Ku band and averaged over 200 km.<br>Note: Like all performance requirements on the altimeter, unless specified otherwise, this specifies the maximum global RMS error over open ocean.<br>Note: A goal is 0.3 cm | **OK, see section 8.1.4.** |

*Table 28 – R-S-00700*

### 8.2.4. R-S-00710

| Requirement | Status |
|---|---|
| For high-resolution ALT-NTC products, the contribution of the sea state bias error to the standard deviation of the 1-second along-track averaged corrected high-resolution altimeter range measurements shall be less than 2.0 cm.<br><br>Note: Since the sea state bias model will have to be determined for the altimeter data itself, the error can only be evaluated based on day-2 processing.<br><br>Note: Like all performance requirements on the altimeter, unless specified otherwise, this specifies the maximum global RMS error over open ocean.<br><br>Note: A goal is 1.0 cm | **OK** |

*Table 29 – R-S-00710*

As for LR data, a first estimation of HR SSB error is performed by checking the noise between consecutive measurements. The results shows a low level of noise, below the cm (figure 129).

Comparison to Jason-3 SSB highlights a standard deviation ranging between 4.5 and 8.5 mm (figure 130). These values are within requirement.

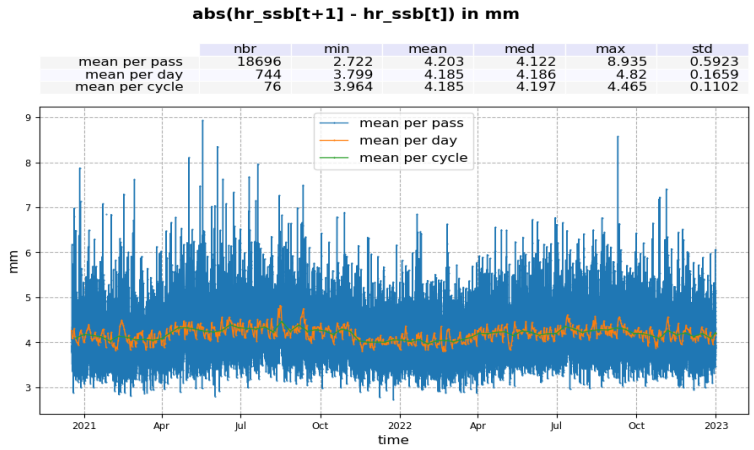


*Figure 129 – Absolute value of consecutive HR sea state bias measurement. Mean per pass (blue), mean per day (orange) and mean per cycle (green).*

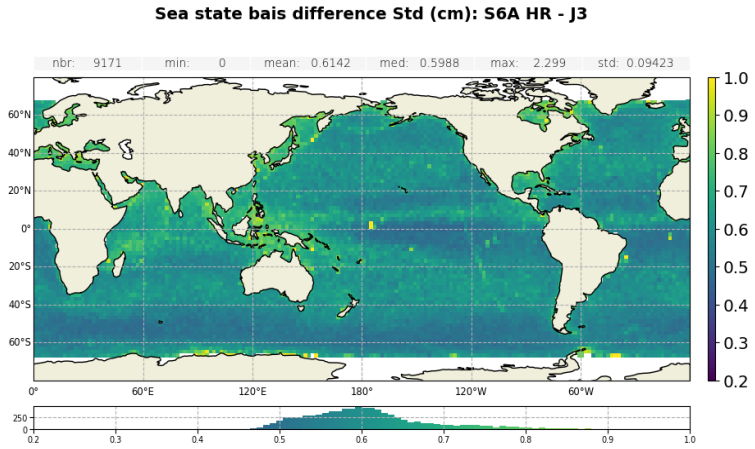


*Figure 130 – Standard deviation gridded map of Ku-band SSB difference: Sentinel-6 MF HR minus Jason-3 computed over the complete tandem period.*

### 8.2.5. R-S-00720

| Requirement | Status |
|---|---|
| For high-resolution ALT-NTC products, the contribution of the dry tropospheric correction error to the standard deviation of the 1-second along-track averaged corrected high-resolution altimeter range measurements shall be less than 0.7 cm.<br><br>Note: this requirement applies to the model to be used to calculate the dry troposphere model.<br><br>Note: Like all performance requirements on the altimeter, unless specified otherwise, this specifies the maximum global RMS error over open ocean.<br><br>Note: A goal is 0.5 cm | **OK, see section 8.1.6.** |

*Table 30 – R-S-00720*

### 8.2.6. R-S-00730

| Requirement | Status |
|---|---|
| For high-resolution ALT-NTC products, the contribution of the wet tropospheric correction error to the standard deviation of the 1-second along-track averaged corrected high-resolution altimeter range measurements shall be less than 1.0 cm.<br><br>Note: Like all performance requirements on the altimeter, unless specified otherwise, this specifies the maximum global RMS error over open ocean.<br><br>Note: A goal is 0.8 cm | **OK, see section 8.1.7.** |

*Table 31 – R-S-00730*

### 8.2.7. R-S-00740

| Requirement | Status |
|---|---|
| For high-resolution ALT-NTC products, the standard deviation of the determination of the radial component of the orbit shall be less than 1.5 cm.<br>Note: This requirement is applicable to the orbital solution derived from the combined set of data from DORIS, GNSS-POD and LRA.<br>Note: Orbit errors have a larger than 1000 km length scale, significantly different from the 1 Hz altimetry noise. Nevertheless the orbit error is added in a RSS sense, presuming that the error is uncorrelated from cycle to cycle at the same location.<br>Note: A goal is 1.0 cm | Not addressed in this report |

*Table 32 – R-S-00740*

### 8.2.8. R-S-00750

| Requirement | Status |
|---|---|
| For high-resolution ALT-NTC products, the standard deviation of the 1-second along-track averaged corrected high-resolution measurements of sea surface height shall be less than 2.94 cm.<br>Note: This requirement is based on the apportionment given in the table of the Sentinel-6 high-resolution altimetry error budget at the end of the document.<br>Note: Like all performance requirements on the altimeter, unless specified otherwise, this specifies the maximum global RMS error over open ocean.<br>Note: A goal is 1.80 cm | **OK** |

*Table 33 – R-S-00750*

To verify this requirement, the crossover analysis presented in section 5.2. is used. The standard deviation of corrected HR SSH difference is centred around 4.5 cm (see figure 92). It means that the error is of 3.2 cm (standard deviation divided by $\sqrt{2}$). This value is slightly above requirement. However looking at a region with low variability, for example the pacific patch, the error is of 2.03 cm in average. On a cyclic basis, this error is always below the requirement limit of 3.2 cm as shown on figure 124, except for two cycles (19 and 24).

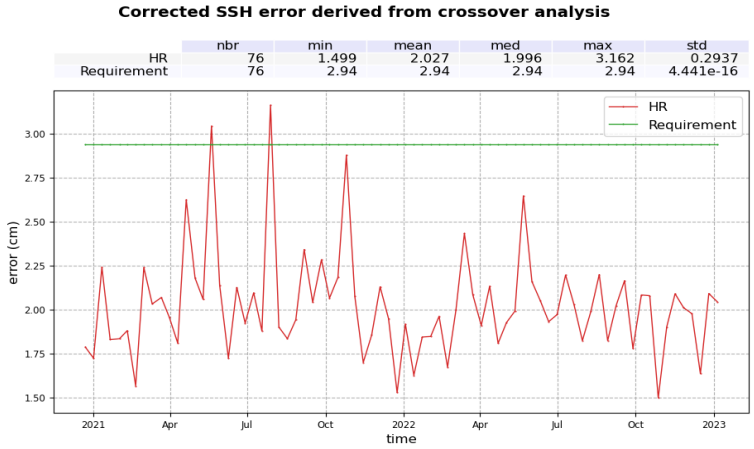


*Figure 131 – Corrected HR SSH error derived from crossover analysis with a selection over Pacific patch (latitude in [-24.5 °N; -3 °N] and longitude in [220 °E; 246 °E]), in cm. The error equals to the standard deviation of the SSH difference divided by $\sqrt{(2)}$. Computed on a cyclic basis.*

### 8.2.9. R-S-00760

| Requirement | Status |
|---|---|
| For high-resolution ALT-NTC products, the uncertainty of 1-second along-track averaged high-resolution measurements of significant wave height in the range 0.5 to 8 m shall be less than 15 cm plus 5% of significant wave height.<br>Note: This is based on the combination of noise and systematic error.<br>Note: A goal is 10 cm plus 5% of significant wave height | **NOK** |

*Table 34 – R-S-00760*

HR Ku-band SWH are compared to SWH derived from ERA-5 model on figure 132. Sentinel-6 MF HR SWH are not compliant with requirement. Please note that the use of a numerical retracking for HR will improve the uncertainties and will be implemented in the coming PB F09 update.

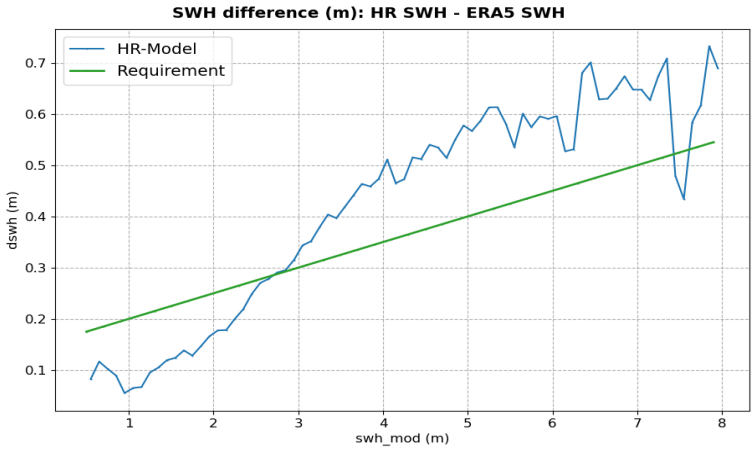


*Figure 132 – SWH difference between Sentinel-6 MF HR data and ERA-5 SWH, plotted function of ERA-5 SWH. Computed over Sentinel-6 MF cycle 70. Green lines represent requirement limits. Results are identical for all cycles.*

### 8.2.10. R-S-00765

| Requirement | Status |
|---|---|
| For high-resolution ALT-NTC products, significant wave heights shall be provided up to at least 20 m.<br>Note: The measurement performance under high sea state conditions will be determined during commissioning | **OK** |

*Table 35 – R-S-00765*

Figure 133 shows the maximum value per cycle of Sentinel-6 MF HR SWH. It equals to 20 m for all cycles, which is consistant with the requirement.

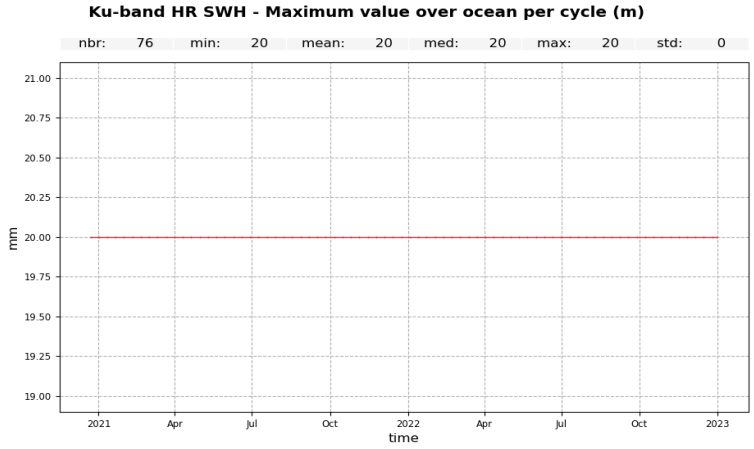


*Figure 133 – Maximum value of Sentinel-6 MF HR SWH per cycle.*

### 8.2.11. R-S-00770

| Requirement | Status |
|---|---|
| For high-resolution ALT-NTC products, the uncertainty of 1-second along-track averages of 10 meter wind speed over ocean surfaces, derived from high-resolution altimeter measurements, shall be better than 1.5 m/s for wind speeds in the range 3 m/s to 20 m/s.<br>Note: Wind speed refers to the wind (not neutral wind) speed at a reference height of 10 meters above the sea surface.<br>Note: This wind speed accuracy requirement translates to an accuracy requirement on the backscatter<br>Note: A goal is 1.0 m/s | **OK** |

*Table 36 – R-S-00770*

As for LR, a comparison to model is performed to verify the uncertainty of Sentinel-6 MF HR altimeter wind-speed. Difference between altimeter and model wind speed is plotted on figure 134 function of model wind speed. Values are within requirement.

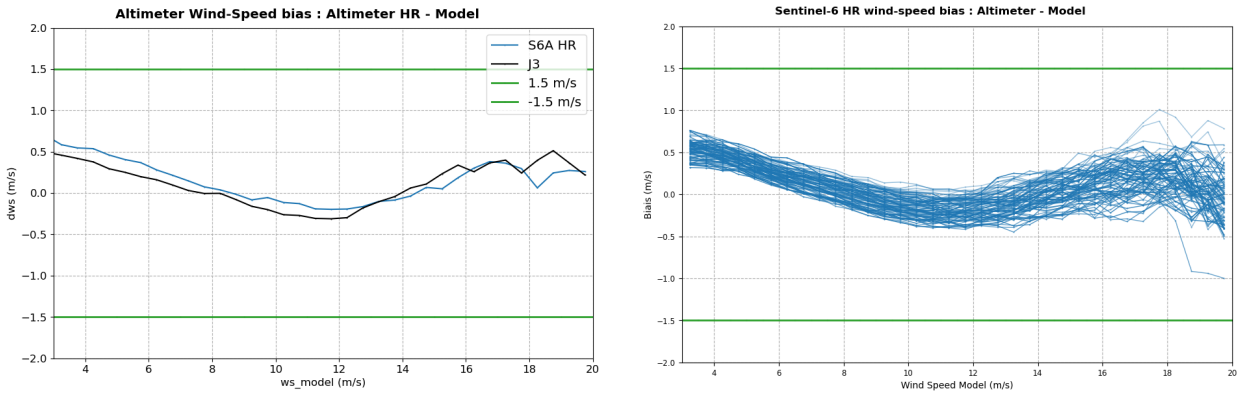


*Figure 134 – Difference between Altimeter HR wind speed and model wind speed function of model wind speed, in m/s. Computed over Sentinel-6 MF cycle 70 (left) and for all cycles (right, darker curves correspond to more recent cycles). Green lines represent requirement limits.*

### 8.2.12. R-S-00780

| Requirement | Status |
|---|---|
| For high-resolution ALT-NTC products, the absolute accuracy of 1-second along-track averaged high-resolution measurements of normalised radar cross-section at Ku-band and vertical incidence, in the range 7 to 16 dB, shall be better than 0.3 dB.<br><br>Note: This value (0.3 dB) is not the value at satellite level (1 dB), but it is achieved after external in-flight calibration to ensure coherence with other missions. In other words, 0.3 dB is the global value, what allows 1 dB at satellite level, to be compensated by the ground processing.<br><br>Note: This requirement also sets limits on the accuracy of sigma0 attenuation correction to be supplied by the radiometer | Not addressed in this report |

*Table 37 – R-S-00780*

The absolute accuracy of the HR sigma0 is not addressed in this report as there is currently no facility available to measure it.

# 9 Conclusions

Sentinel-6 MF was launched on November 21th 2020 and reaches its operational orbit on December 17th 2020. From this date until April 7th 2022, Jason-3 and Sentinel-6 MF were flying in tandem formation, with only 30 seconds delay, before Jason-3 was moved to the interleaved orbit. On April 7th 2022, Sentinel-6 MF became the reference mission in DUACS mission, taking on the responsiblility to extend the global sea level record on the reference ground track started in 1992 by Topex/Poseidon and continued by the Jason's series.

The tandem flight phase between Jason-3 and Sentinel-6 MF has shown that the excellent quality of Sentinel-6 MF data, at least of the same order as the Jason-3 one.

In 2022, Sentinel-6 MF data have been fully reprocessed using the Processing Baseline F06. It was the first opportunity to assess Sentinel-6 MF performance with an homogenuous processing.

The main points of the performance assessment are summarized below:

- Ocean data availability is excellent with a percentage of 99% in LR mode and 98% HR mode (in LMRC only mode) due to the Fairbanks Ground Station key hole effect.
- Data quality is also very good with 6.6% and 5.2% of measurements not consistent with altimeter and radiometer parameters threshold criterion in LR and HR respectively.
- LR data are in line with Jason-3 with a SWH bias below the centimeter and of only 0.8 cm in range. The total SSHA bias with respect to Jason-3 is also excellent, only 1.3 cm. The correlation to SWH in range should be improved thanks to the upcoming numerical retracker (PB F08).
- HR mode is impacted by the remaining effect of ocean vertical velocity. The future processing baseline F09 will provide a correction for this effect. The absence of skewness parameter in the HR processing does not allow to properly compare HR range derived parameter to LR data or to Jason-3. Please note that in the future F09 processing baseline, the HR numerical retracker will use the same skewness coefficient as in LR.
- The Sentinel-6 MF - Jason-3 sigma0 biases are not identical between the two sides of the altimeter: -1.24 dB for side A and -1.21 dB for side B in LR ; and 4.4 dB for side A and 4.43 for side B in HR. These biases should be taken into account for the calibration bias applied on sigma0 for the wind speed computation.
- At crossovers, Sentinel-6 MF shows very good performance with standard deviations of 5.1 cm and 4.7 cm for LR and HR respectively. Jason-3 standard deviation is similar to LR.
- At crossovers between Sentinel-6 MF and Jason-3, SSH performance presents excellent results with an SLA bias of about -1.2 cm and 0.1 cm for HR and LR respectively.
- MSL estimations are impacted by the absence of numerical retracker. It is available in the PB F08 for LR and will be available in the PB F09 for HR. In HR, the range walk correction will also be implemented in the PB F09, improving event more GMSL estimation.

Despite the excellent performance of Sentinel-6 MF, three events reduce their stability over time, all linked to the radiometer wet tropospheric correction:

- A loss of stability in the SSHA difference with respect to Jason-3 is observed at the satellite restart occuring on 27-28 April 2021. It is concomitant with an event on AMR-C WTC (- 4 mm) following a calibration.

- Another event more spread over time, occuring beginning of 2022, impacts also the SSHA and GMSL stability. The origin of such behavior is under investigation (Sentinel-6 MF AMR-C, Jason-3 AMR, other).
- A calibration error in the microwave radiometer caused a drift of -2 mm per month of the radiometer WTC from 2022-10-01 to 2022-12-14. This event will be corrected in the 2023 F08 reprocessing.

The compliance status to system requirements shows once again the excellent quality of Sentinel-6 MF data, especially for LR dataset. The only exception is due to the remaining impact of ocean vertical velocity on HR data, with HR SWH uncertainty above requirement (R-S-00760).

# 10 References

## References


[1] Sentinel-6A user handbook available at https://eumetsatspace.atlassian.net/wiki/spaces/SEN6/overview

[2] Product notice for Sentinel-6A Processing Baseline F06 available at : https://www.eumetsat.int/media/48237

[3] Sentinel-6A F06 Reprocessing Calval Assesment available at : https://www-cdn.eumetsat.int/files/2022-10/S6A_F06_Reprocessing_Calval_Assesment_v2_draft4.pdf

[4] Product notice for Sentinel-6A Processing Baseline F07 available at : https://www.eumetsat.int/media/50079

[5] Raynal et al, Lessons learned from Sentinel SARM missions in preparation of Jason-CS. Oral Presentation, Ocean Surface Topography Science Team Meeting 2019, Chicago

[6] Jason-3 product handbook available at https://www.aviso.altimetry.fr/fileadmin/documents/data/tools/hdbk_j3.pdf

[7] Brown G.S., "The average impulse response of a rough surface and its application", IEEE Transactions on Antenna and Propagation, Vol. AP 25, N1, pp. 67-74, Jan. 1977.

[8] Thibaut, P. O.Z. Zanif´e, J.P. Dumont, J. Dorandeu, N. Picot, and P. Vincent, 2002. Data editing: The MQE criterion. Paper presented at the Jason-1 and TOPEX/Poseidon Science Working Team Meeting, NewOrleans (USA), 21-23 October.

[9] Dinardo S. poster, Sentinel 6 MF Poseidon 4 main results from the first year of mission from the S6PP LRM and UF SAR chain , OSTST 2022

[10] Changes in ECMWF model, web page: https://www.ecmwf.int/en/forecasts/documentation-and-support/changes-ecmwf-model

[11] Boy F., Callahan P., Desjonqueres J. D., Egido A., Smith W. H. F., Fornari M., Martin-Puig C. (2022): High-Level Instrument Processing Summary for Jason 3 and Sentinel-6 Michael Freilich Tandem Phase. Oral Presentation, Ocean Surface Topography Science Team Meeting(Virtual). Available on-line at https://ostst.aviso.altimetry.fr/fileadmin/user_upload/OSTST2022/presentations/01-Jason3andSentinel-6MFTandemPhaseInstrumentProcessing_20220321.pdf

[12] Guérou, A., Meyssignac, B., Prandi, P., Ablain, M., Ribes, A., and Bignalet-Cazalet, F.: Current observed global mean sea level rise and acceleration estimated from satellite altimetry and the associated uncertainty, EGUsphere [preprint], https://doi.org/10.5194/egusphere-2022-330, 2022.

[13] Nencioli Francesco, Roinard Hélène, Bignalet-Cazalet Francois. 2021. Filtering ionospheric correction from altimetry dual-frequencies solutions. DOI 10.24400/527896/a02- 2021.001. Availableathttps://www.aviso.altimetry.fr/fileadmin/documents/data/tools/NT-Nencioli_FilteredIonosphericCorrection.pdf

[14] Obligis, E., L. Eymard, M. Ablain, B. Picard, J.F. Legeais, Y. Faugere and N. Picot, 2010. The wet tropospheric correction for altimetry missions: A mean sea level issue. Oral presentation at OSTST meeting, Lisbon, Portugal. Available at http://www.aviso.oceanobs.com/fileadmin/documents/OSTST/2010/oral/19_Tuesday/OBLIGIS.pdf.

[15] Sentinel-6 ALT Level 2 Product Generation Specification available at https://www.eumetsat.int/media/48266

[16] Michaël Ablain, Benoît Meyssignac, Lionel Zawadzki, Rémi Jugier, Aurélien Ribes, Giorgio Spada, Jerôme Benveniste, Anny Cazenave, and Nicolas Picot : Uncertainty in satellite estimates of global mean sea-level changes, trend and acceleration ESSD, 11, 1189–1202, 2019